CHALMERS

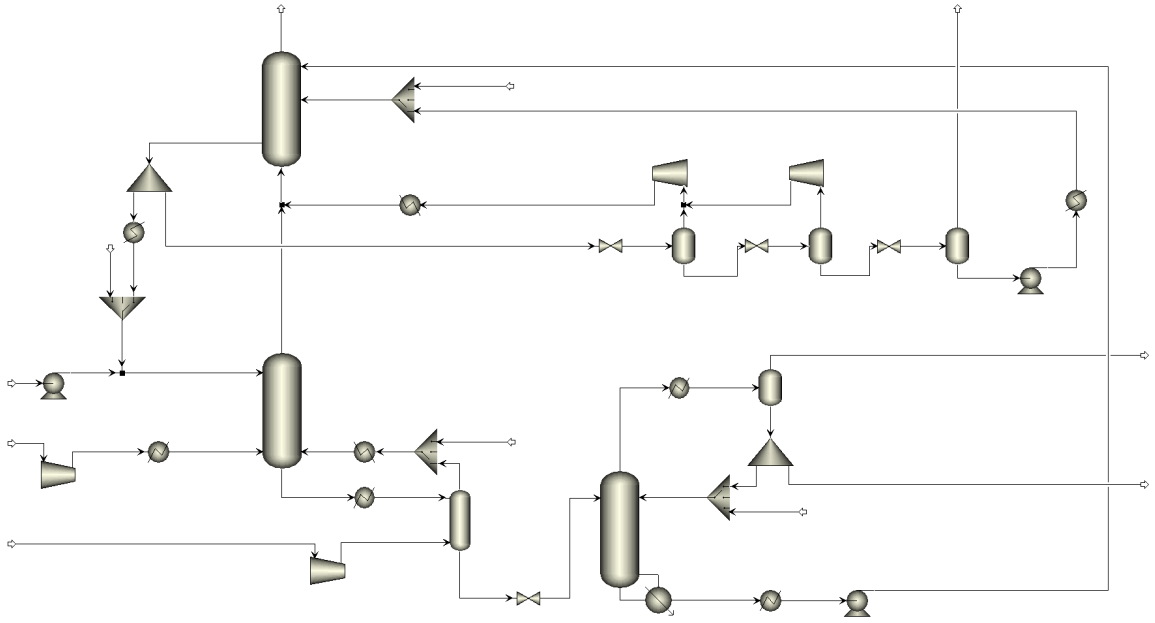

Simulation and Assessment of Carbon Capture Processes Applied to a Pulp Mill

Master of Science Thesis in the Master Degree Programme, Innovative and Sustainable Chemical Engineering

JOAKIM HEDSTRÖM

Department of Energy and Environment
Division of Energy Technology
Chalmers University of Technology
Gothenburg, Sweden 2014

Master of Science Thesis

Simulation and Assessment of Carbon Capture Processes Applied to a Pulp Mill

JOAKIM HEDSTRÖM

Supervisors: M.Sc. Stefanìa Òsk Gardarsdòttir
Ph.D. Fredrik Normann
Examiner: Assoc. Prof. Klas Andersson

Division of Energy Technology
Department of Energy and Environment
Chalmers University of Technology
Gothenburg, Sweden 2014

Simulation and Assessment of Carbon Capture Processes Applied to a Pulp Mill

JOAKIM HEDSTRÖM

Master of Science Thesis
Division of Energy Technology
Department of Energy and Environment
Chalmers University of Technology
SE-412 96 Gothenburg
Sweden
Telephone +46 (0)31 772 1000

Cover: Aspen Plus flowsheet of the Selexol process.

Reposervice
Gothenburg, Sweden 2014

Acknowledgement

I would like to express my sincere gratitude to my supervisor Stefanìa Òsk Gardarsdòttir, for always making time for me and my never-ending questions. Stefanìas support and guidance throughout the whole project has been invaluable, whether it was help with the simulations in Aspen Plus or feedback on the report.

I am also particularly grateful for the assistance given by my supervisor Fredrik Normann, who helped me bounce ideas and always provided valuable input. Fredrik has been a guiding light, steering me in the right direction in the decision making process regarding the content of the thesis.

Many thanks to Henrik Jilvero for sharing his knowledge regarding dimensioning of process equipment. I also would like to thank Karin Pettersson for helping me understand the overall balance of the pulp mill and providing essential process data required in the project. Ragnhild Skagestad and Nils Henrik Eldrup are acknowledged for their fast and well executed investment cost analysis.

Lastly, I wish to acknowledge the much appreciated feedback on the report provided by my examiner Klas Andersson and my opponent Simon Lindqvist.

Göteborg, June 2014
Joakim Hedström

Abstract

Global warming is a serious threat that could have catastrophic effects if emissions of greenhouse gases are not reduced drastically. This thesis evaluates the suitability for pulp mills to help in reducing these emissions with focus on carbon capture and storage (CCS) technologies. This industry is based on a renewable feedstock that can be used to reduce greenhouse gas emissions by replacing fossil fuels in transportation or heat and power generation. Furthermore, capturing CO_2 from pulp mills would result in a "negative" net emission that would reduce the global CO_2 emissions.

Three future scenarios of the pulp mill are considered. The first scenario assumes the pulp mill is run as the present day situation and that post-combustion capture of CO_2 using the MEA processes is applied to the stack gas emissions from the recovery boiler. In the second scenario the recovery boiler is substituted with black liquor gasification technology and the produced syngas is used for electricity production. Pre-combustion capture of CO_2 using the Selexol process is applied in this scenario. The third scenario also utilizes black liquor gasification technology for recovery but the syngas is used to produce DME instead of electricity. Pre-combustion capture of CO_2 with the Rectisol process is used in this scenario.

Each scenario is divided into two cases; one with capture and one without capture. The cases are simulated using Aspen Plus and the utility consumption of the processes is determined. Pinch analysis is used to reduce the utility demand. All process equipment is dimensioned to provide a basis for an investment cost analysis which is performed by an external partner. The results from the simulations are used in an overall energy and mass balance of the pulp mill which determines the additional resource consumption associated with carbon capture. The resource consumption together with the investment cost is used to calculate a total cost for carbon capture.

The scenario utilizing the MEA process shows the highest potential to offset global CO2 emissions with a net reduction of $715\,ktCO_2$/year at a capture cost of $431\,SEK/tCO_2$. The scenario with black liquor gasification for electricity production has the lowest net reduction with only $318\,ktCO_2$/year and also the highest capture cost of $453\,SEK/tCO_2$. The scenario with co-production of DME at the pulp mill has the potential to reduce global emissions with $393\,ktCO_2$/year and a low capture cost of $88\,SEK/tCO_2$.

Today there exists an over-abundance of low price emission certificates, in Mars 2014 an emission certificate costed 5.0 €. Hence, in none of the studied scenarios carbon capture was profitable. However, if the emission certificate market recovers then the pulp mill would be a suitable candidate for CCS.

Keywords: CO_2 capture, MEA, Rectisol, Selexol, pulp mill, pre-combustion, post-combustion, Aspen Plus, process simulation, BECCS

Contents

List of Figures

List of Tables

Abbreviations and symbols

Abbreviations

ADt	Air-Dry Tonne
ASME	American Society of Mechanical Engineers
BECCS	Bio-Energy with Carbon Capture and Storage
BLGCC	Black Liquor Gasification Combined Cycle
BLGMF	Black Liquor Gasification with Motor Fuel production
C	Chlorine
CCS	Carbon Capture and Storage
CLC	Chemical Looping Combustion
COP	Coefficient Of Performance
CTMP	Chemithermomechanical pulping
D	Chlorine dioxide
DEA	Diethanolamine
DEPG	Dimethyl Ethers of Polyethylene Glycol
DME	Dimethyl Ether
FT	Fischer-Tropsch
HP	High Pressure
HRSG	Heat Recovery Steam Generator
IEA	International Energy Agency
IMTP	Intalox Metal Tower Packing
IPCC	Intergovermental Panel on Climate Change
LP	Low Pressure
M	The MEA capture process
MEA	Monoethanolamine
MDEA	N-methyldiethanolamine
MP	Medium Pressure
NC	No Capture
NRTL	Non-Random Two-Liquid
O	Oxygen
P	Hydrogen peroxide
PR-BM	Peng Robinson equation of state with Boston-Mathias alpha function
PC-SAFT	Perturbed-Chain Statistical Associating Fluid Theory
Pz	Piperazine
Q	Chelating agent
R	The Rectisol capture process
RB	Recovery Boiler
S	The Selexol capture process
SCA	Svenska Cellulosa Aktiebolaget
SCOT	Shell Claus Off-Gas Treating
TRI	ThermoChem Recovery International

Symbols

COP_{Ideal}	Ideal coefficient of performance	[-]
F	Volume flow	[$\text{m}^3\,\text{s}^{-1}$]
T_{COND}	Condensation temperature	[K]
T_{EVAP}	Evaporation temperature	[K]
Q_{COND}	Heat rejected in the condenser	[W]
Q_{EVAP}	Heat absorbed in the evaporator	[W]
W	Work supplied by the compressor	[W]
η	Efficincy	[-]

1 Introduction

This thesis investigates the possibilities of applying carbon capture and storage to the pulp and paper industry. A brief introduction to this subject is presented in this chapter, along with the aim and scope of the work.

1.1 Background

There is little doubt among climate scientists that industrial emissions of CO_2, and other greenhouse gases, are causing global warming and our emissions needs to rapidly decline, or else the global temperature increase will surpass 2 °C. This rise in temperature, compared to the pre-industrial average temperature, has long been considered the limit for which the most serious consequences of global warming can be avoided (European Council, 1996). However, recent research suggests that even an increase of only 1 °C may have dangerous effects (J. B. Smith et al., 2009).

Most CO_2 emissions originate from combustion of fossil fuel which today's energy system is highly dependent on. The global emissions of CO_2 from fossil fuels in 2011 were 31 $GtCO_2$, this corresponds to an increase by 49 % compared to the levels in 1990 and emissions are steadily rising (IEA, 2013). A complete substitution to renewable energy sources cannot be realized overnight and therefore transitions technologies are needed; Carbon Capture and Storage (CCS) is one example. By capturing the CO_2 formed in, for example coal-based power production, the environmental impact of such a facility would be greatly reduced. This would buy mankind some well needed time to find alternative ways to satisfy the ever growing energy demand. However, everything comes at a price. The capture processes are energy consumers as well. Hence, the heat or electricity that can be sold is reduced and inevitably, so are profits. For CSS to be widely implemented, policies that provide incentive for capturing CO_2 needs to be in place. The IPCC (Intergovernmental Panel on Climate Change) states that such policies can be in the form of economic instruments, government funding or regulation (IPCC, 2007). One example is the EU's emissions trading scheme which aims to reduce CO_2 emissions by gradually decreasing the number of available certificates. A certificate grants the holder the right to emit one tonne of CO_2, thus large emitters such as power plants needs to purchase a considerable number of certificates. Consequently, this policy has the potential of making CCS economically viable. However, the price of a certificate has steadily decreased during the past years, reaching an all-time low of 2.8 € in April 2013 (Swedish Energy Agency, 2013). Low prices means that the focus of CCS projects may need to change from aiming to capture bulk amounts of CO_2 to smaller but more easily available CO_2 with less costs associated. Hence, opportunities to capture CO_2 in industries which previously have not been associated with CCS should be examined.

An industry branch that has received increased attention with respect to CCS in the past years is the pulp and paper sector. In a Swedish perspective this industry is

of great importance. The total CO_2 emissions from fossil fuel in Sweden in 2011 were 49 $MtCO_2$, as a comparison the pulp and paper industry emitted 22 $MtCO_2$ originating from biofuel combustion (Swedish Environmental Protection Agency (2013); European Environment Agency (2011)). Hektor (2008) has evaluated the implications of applying post combustion capture onto pulp and paper mills whereas Pettersson (2011) examined the pre-combustion alternative. An interesting aspect of the pulp and paper industry is that it is based on a renewable feedstock, i.e. forest resources. That implies that a pulp mill can be considered a zero net contributor to global CO_2 emission, since the trees will reabsorb the CO_2 through photosynthesis as they grow. This reasoning is only valid if a sustainable management of the forest resources with sufficient replantation is practised. However, if this is the case then capturing the CO_2 would actually result in a negative net contribution to the global CO_2 emissions. If CCS technology is applied to emissions originating from biomass it is called BECSS, abbreviation for Bio-Energy with Carbon Capture and Storage. By implementing BECSS it is possible to compensate for emissions from other sources, such as transport, since CO_2 actually is removed from the atmosphere. This also gives the means to recover from an "over-shoot" of the 2 °C target. Applying BECCS to the pulp and paper industry is not only important in a Swedish perspective. The pulp and paper industry is responsible for 5.7 % of the global industry energy usage and the industry is in turn accountable for 21 % of global CO_2 emissions (IEA (2007); IEA (2013)).

1.2 Aim and scope

The aim of this thesis is to evaluate the possibility for implementing CO_2 capture at a pulp mill given three future scenarios. The first scenario uses the conventional recovery boiler to regenerate the cooking chemicals. The second scenario replaces the recovery boiler with black liquor gasification technology to produce additional electricity. The third scenario also utilizes the black liquor gasification technology but DME is produced instead. The study investigates if pulp mills have any easily available CO_2 sources that can be captured at a low cost. Specifically, the study estimates the potential net reduction in global CO_2 emissions, the cost for the reduction and the different sellable products produced in the pulp mill for the three scenarios.

Models of the capture processes are built using the simulation tool Aspen Plus. A rate-based approach in the simulations enables the possibility to design and size all equipment and thereby perform an investment cost analysis. However, cost calculations are beyond the scope of this thesis and are instead performed by an external partner. The results from the simulations are used to calculate the overall energy and mass balance of the pulp mill. By combining the results from the overall balances and the investment cost analysis a total cost for carbon capture is obtained.

2 Carbon capture and storage

CCS can be divided into three consecutive steps. Naturally the first step is to capture the CO_2. Three different approaches can be adopted for this task: post-, pre- or oxy-fuel combustion. The second step is to compress and transport the CO_2 to a suitable storage site. Lastly the CO_2 is pumped down into the carefully selected underground storage site.

2.1 Post-combustion

The concept of post-combustion imply separation of CO_2 from the flue gases after combustion, see Figure 1. This technology has a large advantage due to the fact that it can be retrofitted to any existing plant.

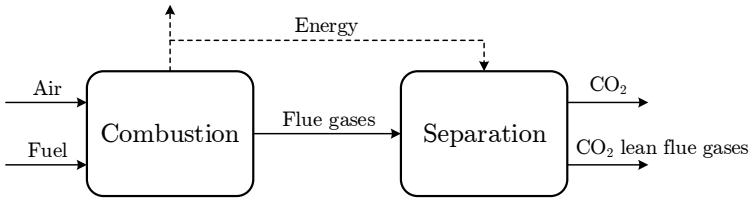

Figure 1: Schematic representation of the post-combustion process.

Chemical absorption is the most commonly used separation method in post-combustion applications. However other methods such as membranes, adsorption or cryogenic technology exist as well. In chemical absorption the solvent forms weak bounds to the CO_2 in an absorber at low temperatures, around 50 °C. These bounds are broken in a stripper at higher temperatures (around 120 °C, the exact temperature depends on the solvent used) and the CO_2 is released. The solvent is then recycled back to the absorber, see Figure 2. The main disadvantage is that the regeneration of the absorbent is energy consuming.

Both organic and inorganic absorbents can be used in the process. The most frequently used organic solvent is monoethanolamine (MEA). Piperazine (Pz), diethanolamine (DEA) and N-methyldiethanolamine (MDEA) are other examples of amines used. Some separation processes use a mixture of several different absorbents (Bougie & Iliuta, 2012). Examples of inorganic solvents are potassium carbonate, sodium carbonate and ammonia. (Hektor, 2008)

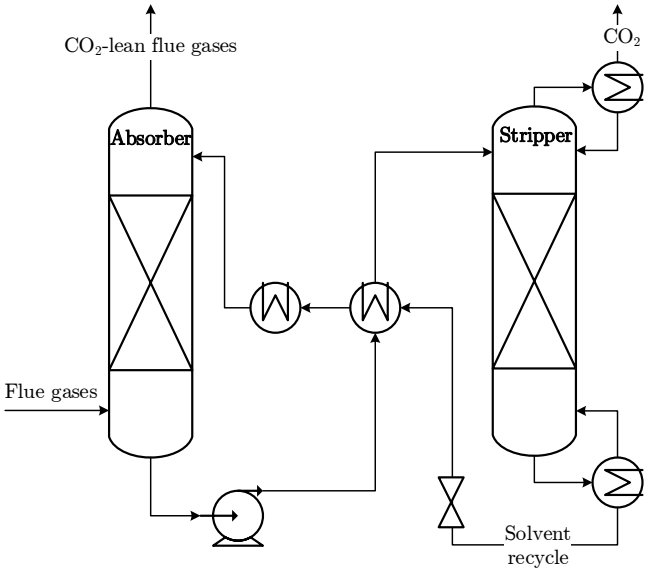

Figure 2: Simplified flowsheet of the post-combustion process.

2.2 Pre-combustion

The principle of pre-combustion capture is shown in Figure 3. In this approach the fuel is gasified, i.e. partially combusted. The gasification is carried out in a pressure range of 30-70 bar using a deficient supply of oxygen resulting in a gas mixture consisting mostly of CO, CO_2 and H_2 (Gibbins & Chalmers, 2008). Depending on the application of the formed syngas (synthesis gas), it is sometimes desirable to adjust the ratio between CO and H_2. This is carried out by adding water and passing the mixture through a number of reactors containing catalyst beds. Inside the reactors the water-gas shift reaction occurs. The addition of water displaces the equilibrium towards the right hand side of the reaction:

$$CO + H_2O \longleftrightarrow CO_2 + H_2 \tag{1}$$

The CO_2 is then separated from the syngas and thereafter the syngas is either combusted or used for other purposes such as fuel synthesis. The separation of CO_2 is most often carried out using physical absorption e.g. the Rectisol or Selexol processes. Physical absorption is used when higher concentration of CO_2 is present, compared to the levels present in post-combustion where chemical absorption has to be used instead. An advantage with physical absorption is that CO_2 is absorbed at high pressures and released at low pressures which reduces the energy consumption for regeneration of the absorbent. However, there will be a loss of efficiency due to the shift reaction since less CO reaches the combustion chamber and consequently a reduced mass flow of CO_2 pass through the turbine. Hence, less power is generated. (Gibbins & Chalmers, 2008)

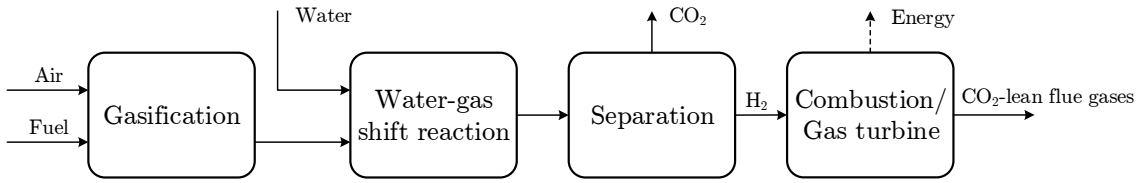

Figure 3: Schematic layout of the pre-combustion process.

2.3 Oxy-fuel combustion

Oxy-fuel combustion differs from the other technologies in the aspect that oxygen is used instead of air in the combustion process, see Figure 4. Oxygen is separated from the air in an initial step, the dominating method is cryogenic air separation. The pure oxygen stream is then used in the combustion of the fuel. However, using pure oxygen results in high peak-flame temperatures and therefore a part of the flue gases are recycled to meet material constraints. The flue gases have a high concentration of CO_2, over 80 %, and the remaining part is mostly water which can easily be removed by condensation. An advantage with this process is that the gas volume is heavily reduced in the absence of nitrogen which makes flue gas treatment cheaper. A disadvantage with oxy-fuel combustion is that the separation process to obtain the oxygen is energy demanding. (Davison & Thambimuthu, 2005)

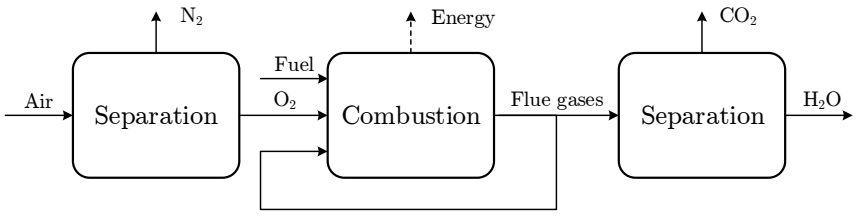

Figure 4: Schematic overview illustrating the oxy-fuel combustion process.

Chemical looping combustion (CLC) is another version of the oxy-fuel combustion concept. This method uses metal particles as oxygen carriers between two fluidized bed reactors. In the first reactor the oxygen carriers are exposed to air and are oxidized, they are then transported to the second reactor. In this reactor fuel is injected and the oxygen carriers are reduced by the fuel to form water and CO_2. The oxygen carriers are transferred back to the first reactor to close the loop. (Moldenhauer et al., 2012)

2.4 Transportation and storage

Once the CO_2 is captured it needs to be transported to a suitable storage site, this can be carried out by either ships or pipelines. If the CO_2 is to be transported using the latter alternative, it needs to be compressed to a supercritical state, i.e. to a pressure above 80 bar. This increases the density of the fluid and thereby facilitates the pumping, which is less energy demanding than transportation in a gaseous state. If instead ships are used, the pressure is only raised to 7 bar which transforms the CO_2 into liquid state. (IPCC, 2005)

The storage of CO_2 can either be on- or off-shore and three types of geological formations are suggested to be suitable: oil and gas reservoirs, unminable coal beds or deep saline formations. Storing CO_2 in oil and gas reservoirs would be beneficial since this increases or maintains the pressure inside the reservoirs and thereby enhances the oil recovery. Storage in coal beds, where mining is unlikely, would give methane as a byproduct, since it is displaced when CO_2 is injected. Deep saline formations storage does not facilitates extraction of natural resources, however global storage capacity in these formations is estimated to be far more extensive than the previous alternatives. (IPCC, 2005)

3 The pulp mill

The purpose of a pulp mill is to process wood logs into pulp which can be used to produce various paper products. Mechanical and chemical pulping are two approaches used to produce pulp. The former method accomplish this by mechanically grinding the wood logs. The latter method uses chemicals instead. Consequently, the two processes produce pulps with greatly differing properties. There is also hybrid processes such as CTMP (chemithermomechanical pulping) which uses chemicals to soften the wood before it is mechanically grounded into pulp. However, the demand for chemical pulp is larger and is thus the dominating technique. There exist a few chemical pulping methods using different chemicals e.g. kraft cooking, sulphite cooking and soda cooking. SCA Östrands pulp mill uses the kraft process which is described in the following three sections. For more information about the pulping process, see Ek et al. (2009a) and Ek et al. (2009b).

3.1 Wood as raw material

A tree mainly consists of four compounds: cellulose, lignin, hemicelluloses and extractives. Pine is commonly used as raw-material in the pulping process and typically has the composition shown in Figure 5.

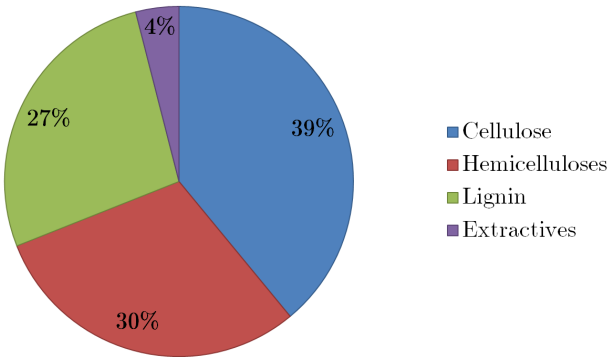

Figure 5: Approximate composition of pine wood.

Cellulose is the main building block of the wood and is long linear polysaccharides. Several cellulose chains can aggregate and form microfibrils which are the building blocks of the fibres. These fibres are main component of the produced pulp.

Lignin is a polymer consisting of a branched network of different aromatic alcohols. However the exact structure of this complex molecule is not yet known. The lignin is present to some extent in the fibres and gives stiffness. The space between the fibres is mainly occupied by lignin which acts as a glue. The lignin is the compound which is degraded in chemical pulping to free the fibres.

Hemicelluloses are, just like cellulose, polysacchariedes but they are branched and have shorter chains. Their most important function is to give strength to the cell walls in cooperation with lignin. Hemicelluloses are to some degree degraded in

chemical pulping. However, this degradation should be minimized as the pulp yield increases if hemicelluloses are kept intact.

Extractives are various compounds with low molecular mass and they constitute a small percentage of the wood. They have various functions such as protecting the tree against fungus and some are important for the metabolism of the cells. Extractives are undesired in the pulp as they can cause stains and discolouration of the paper products.

3.2 The kraft pulping process

A basic flowsheet describing the kraft pulping process, including the recovery system for the cooking chemicals, is presented in Figure 6.

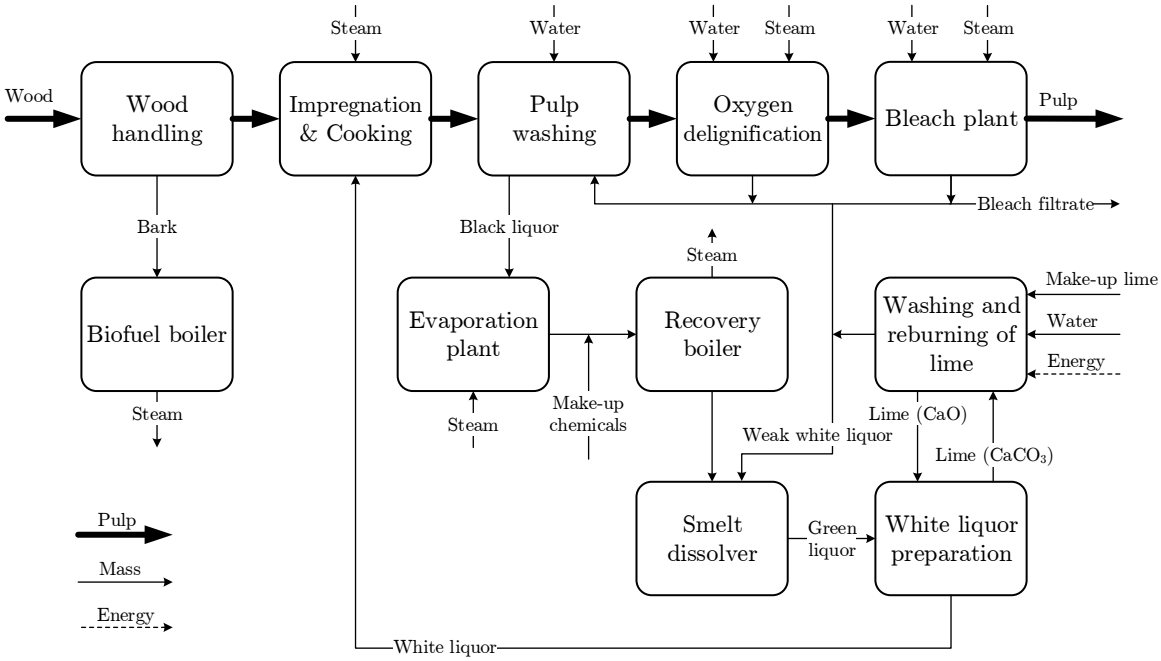

Figure 6: A schematic overview illustrating the kraft pulping process. The bold arrows represent the flow of the wood or pulp through the process.

The first step in the process is the *wood handling*, of which the two most important steps are debarking and chipping. The bark of the tree has a high content of extractives and a low amount of fibers, it may also contain sand. Thus, the bark is removed in the first step of the process. The discarded bark is often used as fuel by producing steam in a *biofuel boiler*. The debarked logs are then cut into small chips, typically with dimensions in the following range: (20-30)x(15-30)x(3-8) mm. By chipping the wood into small pieces of approximately equal size, the cooking chemicals are distributed more evenly and faster into the wood.

The wood chips pass a steaming vessel where air inside the chips is replaced by steam. They are then transported to the *impregnation* vessel where warm impregnation liquid is applied with the purpose of raising temperature and to evenly distribute the cooking chemicals. The impregnation liquid is a mixture of white liquor containing the cooking chemicals i.e. sodium sulfide (Na_2S) and sodium hydroxide (NaOH), but also black liquor containing used cooking chemicals. After the impregnation the chips enter the digester and the temperature is raised to 160-170 °C and consequently the cooking chemicals start to react. Sodium sulfide reacts with water to form hydrogen sulfide ions and hydroxide ions. Hydrogen sulfide ions are responsible for degrading the lignin whereas the hydroxide ions neutralize acidic groups and keep the degraded lignin in solution. The cooking chemicals are consumed during cooking to form sodium carbonate (Na_2CO_3) and sodium sulfate ($NaSO_4$). The mixture of degraded lignin and cooking chemicals is called black liquor.

After the cooking is terminated the pulp proceeds to the *washing* step. The black liquor is displaced by washing water. Several different types of equipment can be used for the washing step e.g. drum filters and pressurized diffusers.

Oxygen delignification is applied after cooking to further reduce the amount of lignin present in the pulp. This operation has several benefits compared to prolonging the cooking. The greatest one being that the pulp is bleached, resulting in a decreased demand of other bleaching chemicals and thereby reduced pollution. In addition this increases the strength of the pulp compared to prolonging the cooking.

Before the pulp can be shipped to the paper mill it needs to be *bleached* further to a desirable brightness. This is conducted using several stages which utilizes a variety of bleaching chemicals e.g. chlorine (C), chlorine dioxide (D), oxygen (O), hydrogen peroxide (P) and chelating agent (Q). Bleaching with compounds containing chlorine was common but has gradually declined since the 1970s and today many mills uses bleaching sequences without chlorine due to environmental concerns, OQP(OP)Q(PO) is an example of a chlorine free sequence. At this stage, the pulp can be dewatered and transported to a paper mill.

3.3 The recovery system for cooking chemicals

The black liquor containing dissolved lignin and used cooking chemicals is removed in the washing step and pumped to the *evaporation plant*. By evaporating a major part of the water, the dry content is increased from 15-20 % to 70-80 %. This raises the heat value of the black liquor substantially. The evaporation plant consists of six or seven separate evaporators, which are coupled in such a way that the steam formed in an evaporator is used to heat the next one. This reduces the energy demand.

To regenerate the cooking chemicals and also utilize the latent heat of the organic components, the strong black liquor from the evaporation plant is combusted. This is performed in a *recovery boiler* which is a large furnace with a height of 60-70 m, see Figure 7.

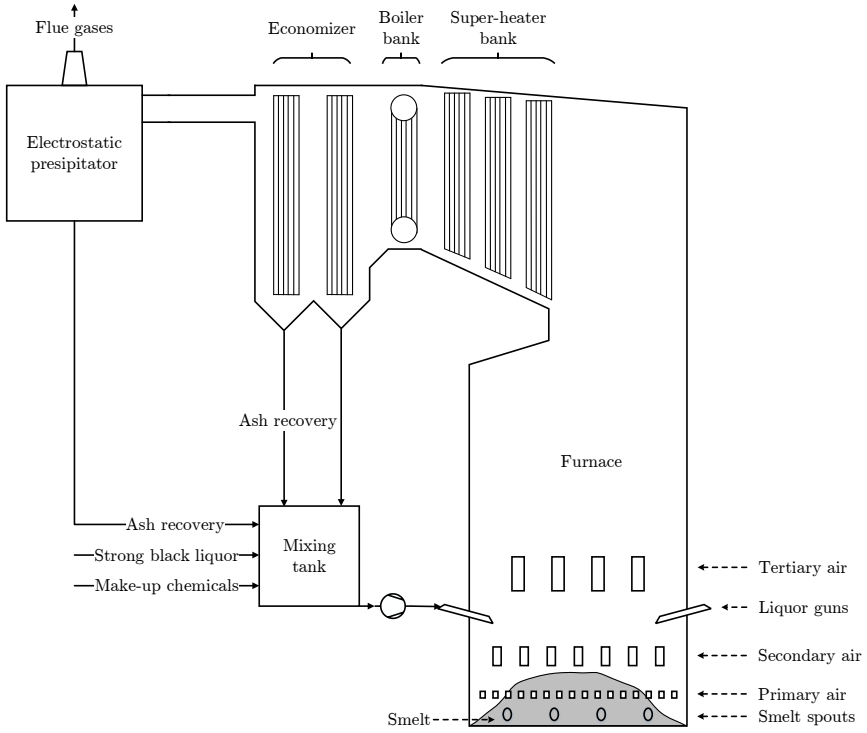

Figure 7: Cross-sectional view of the recovery boiler and its components.

The strong black liquor is sprayed into the furnace along with air. The air is injected at several different heights which make it possible to form an reductive environment close to the bottom where the combustion is incomplete, while higher up in the furnace the atmosphere is oxidizing. After the strong black liquor is injected it forms small drops which undergo drying, pyrolysis and char combustion before reaching the bottom of the recovery boiler where a smelt is formed. In the top layer of the smelt carbon reacts with sodium sulfate to regenerate the sodium sulfide, see Reaction 2.

$$4\mathrm{C(s)} + \mathrm{Na_2SO_4(l)} \longrightarrow \mathrm{Na_2S(l)} + 4\,\mathrm{CO(g)} \tag{2}$$

The heat released by combustion is absorbed by the walls, consisting of boiler tubes. Heat is also extracted from the flue gases as they pass a super-heater bank, boiler bank and economizer before being treated in a electrostatic precipitator to remove fly ash. The steam produced in the recovery boiler is of high pressure (over 100 bar) and is expanded in a back pressure steam turbine to produce electricity. MP-steam (approximately 12 bar) and LP-steam (approximately 4 bar) is extracted from the turbine to cover the need of the pulping process. The steam generation efficiency, based on lower heating value, is usually around 75 % for a recovery boiler (Anderberg (2010); Vakkilainen & Ahtila (2011)). If a steam surplus is present, which often is the case for a modern pulp mill with a high degree of heat integration,

the steam is further expanded in a condensing turbine. In such cases the pulp mill can be a major net exporter of electricity (Pettersson & Harvey, 2012). The recovery boiler typically have an electrical efficiency around 12 % (Pettersson, 2014). In addition, the pulp mill also has a potential of providing district heating as there often exist low temperature waste heat suitable for this purpose (Hektor, 2008).

The smelt is drained through smelt spouts into a *smelt dissolver*, basically a large tank filled with weak white wash, which is a water solution containing a small amount of cooking chemicals from other parts of the process. This results in a solution called green liquor. In the *white liquor preparation plant* the green liquor enters a slaker where reburned lime (CaO) is added which leads to the formation of calcium hydroxide ($Ca(OH)_2$), see Reaction 3. The solution then proceeds to the causticization vessels where sodium hydroxide is formed by Reaction 4. Now that all cooking chemicals are regenerated, the white liquor is filtrated and recycled back to the cooking step. Calcium carbonate ($CaCO_3$) is separated by the filtration and washed before it enters the lime kiln. Here it is dried and heated to over 850° which results in Reaction 5. The reburned lime can once again be used in the slaker and the cycle is complete.

$$CaO(s) + H_2O \longrightarrow Ca(OH)_2(s) \tag{3}$$

$$Ca(OH)_2(s) + Na_2CO_3(aq) \longleftrightarrow 2NaOH(aq) + CaCO_3(s) \tag{4}$$

$$CaCO_3(s) \longleftrightarrow CaO(s) + CO_2(g) \tag{5}$$

4 Black liquor gasification

The recovery boiler suffers from several drawbacks such as corrosion, fouling and smelt-water explosions (Pettersson, 2011). The latter occurs when water comes in contact with the molten smelt and thereby instantaneously evaporates, causing a pressure wave due to the increased volume. These explosions have been costly with respect to both production losses and human lives (Anderson (1969); Grace (2008)). Improvements have been made over the years but the recovery boiler and its Rankine steam cycle have some inherent limitations such as low thermal efficiency and low power-to-heat ratio. In addition, modern pulp mills have a steam surplus which motivates a better use of the energy contained in the black liquor, such as electricity generation or biofuel production. All the facts stated above have been incentives for examining other alternatives to recover the cooking chemicals. (Stigsson & Berglin, 1999)

Black liquor gasification is an alternative technology that has the potential to solve many of the stated problems. Gasification of spent cooking liquor was examined as early as in the 1950s and 1960s. Since then, a number of research projects and pilot plants have examined this process. However, most were discontinued since they did not show any significant improvement compared to the conventional Tomlinson recovery boiler or other reasons such as shifting development priorities by companies. (Gebart et al. (2005); Consonni et al. (1998); Bajpai (2014))

Today two gasification technologies are competing; fluidized bed technology developed by ThermoChem Recovery International (TRI) and entrained flow technology supplied by Chemrec. The former process operates at a relatively low temperature around 600 °C and near atmospheric pressure. The black liquor is injected in the bottom of a fluidized bed and steam is used as gasifying agent. Part of the produced syngas is combusted in heat tubes integrated in the fluidized bed to ensure that high enough temperatures are reached (Dahlquist, 2013). TRI has built two facilities using their technology, whereas Chemrec has installed one plant using their air-blown atmospheric-pressure version and one demonstration plant utilizing their oxygen-blown pressurized gasification technology (TRI (2012); Chemrec (2011)). However, the Chemrec technology is considered to be the most commercially advanced alternative as the TRI technology has had problems reaching the needed operating temperature to obtain a sufficient conversion (Dahlquist (2013); Bajpai (2014)). Hence, only the Chemrec technology will be considered from here on and a detailed description is provided in the following section.

4.1 Chemrec black liquor gasification

As previously mentioned Chemrec has developed two different technologies for black liquor gasification: air-blown atmospheric-pressure gasification and oxygen-blown pressurized gasification. The former technology is used as a booster to relieve overloaded recovery boilers by providing additional capacity. The latter technology is

designed to fully replace the recovery boiler. A schematic description of the oxygen-blown pressurized gasification is presented in Figure 8. Here follows a brief description of the gasification process, for a more detailed description, see Ekbom et al. (2005).

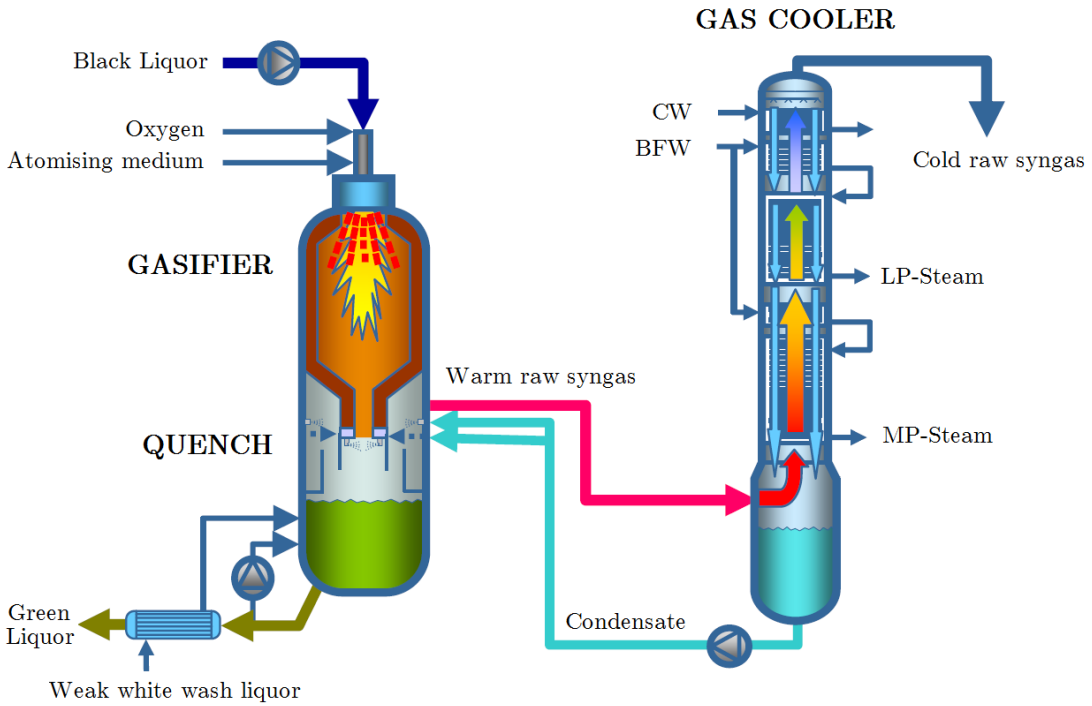

Figure 8: The pressurized, oxygen-blown, high-temperature black liquor gasification technology developed by Chemrec. Adapted from Lindblom & Landälv (2007).

Before the black liquor enters the gasification process it is filtered to remove solid impurities and the pressure is elevated to 32 bar. After the pressure increase, the black liquor is preheated to 120 °C to adjust the viscosity so that a good atomization is achieved in the burner i.e. disintegration into a spray of fine droplets. Black liquor and oxygen is injected into the entrained flow reactor through the burner where it is atomized. The diameter of the droplets and the size distribution is adjusted so that a high conversion of carbon is achieved, but equally important is the regeneration of the cooking chemicals; therefore a high reduction rate of inorganic salts is needed as well. An important design feature is the use of oxygen instead of air, as oxidant. This requires an on-site air separation unit such as a cryogenic air fractionation process. Because of the use of oxygen as gasifying agent the temperature in the reactor reaches values of 950-1000 °C, which is well above the melting point of the inorganic salts. The melted inorganic salts flow downward into the quenching section, where condensate from the gas cooling unit is injected and as a result the smelt droplets are cooled and solidified. The droplets fall down into the condensate in the lower section of the vessel where they are dissolved to form green liquor. To increase the

dissolution rate, part of the exiting green liquor is recycled back to the quench vessel. The exiting green liquor enters two parallel heat exchangers where the temperature is reduced from 220 °C to 90 °C. The heat exchangers are used to preheat weak white wash liquor and evaporator condensate to 205 °C, which then enters the quench vessel and the bottom section of the gas cooler, respectively. The produced green liquor will contain some dissolved gases that will be released when the pressure is reduced. This gas is rejoined with the gas out of the gas cooler.

The gas formed in the gasification process is a mixture mainly composed of CO, H_2, CO_2, H_2O and H_2S but it also contains minor amounts of N_2, CH_4 and COS. After the quench section the produced gas enters the counter-current gas cooler which is a cylindrical pressure vessel with four cooling sections. In the first, second and third section the gas releases heat to generate MP-steam and LP-steam. To achieve the final cooling in the top section cooling water is utilized. As the temperature is reduced thorough the cooler, water will condensate and fall down to the bottom. This serves as a cleaning step as particulate material is removed from the produced syngas by the falling condensate.

The syngas produced is primarily used in two different applications. One alternative is to combust the syngas in a gas turbine to produce electricity and steam, which is denoted black liquor gasification combined cycle (BLGCC). The other alternative uses syngas as a feedstock for production of fuel and is denoted black liquor gasification with motor fuel production (BLGMF). The concepts are further explained in the following two sections.

4.2 Black liquor gasification combined cycle

The process schematics for the black liquor gasification combined cycle (BLGCC) is illustrated in Figure 9. The first three operations; air separation, gasification and gas cooling are explained in section 4.1.

The syngas produced in the gasification contains a considerable amount of H_2S, since approximately half of the sulfur leaves with the gas phase, resulting in a concentration of around 2 mole-% on a dry basis (Ekbom et al., 2005). All sodium leaves the gasification dissolved in the green liquor. Hence, a split between sodium and sulfur is achieved. This split of the cooking chemicals is one of the benefits with the gasification process, since this presents opportunities to produce polysulfide cooking liquors. The pulp yield can be increased by a few percent by using polysulfide cooking liquors and consequently less wood is needed to produce a certain amount of pulp. However, the split of sodium and sulphur comes at the price of an increase in the causticizing load which leads to increased fuel consumption in the lime kiln. The reason is that less sulphur is present in the green liquor and therefore the sodium will form more Na_2CO_3 instead of Na_2S, consequently a larger causticizing load follows, see Reaction 4. (Lindström et al., 2006)

To produce the alternative cooking liquors the H_2S needs to be captured from the syngas. Another reason to capture the H_2S is due to emission regulations for SO_x,

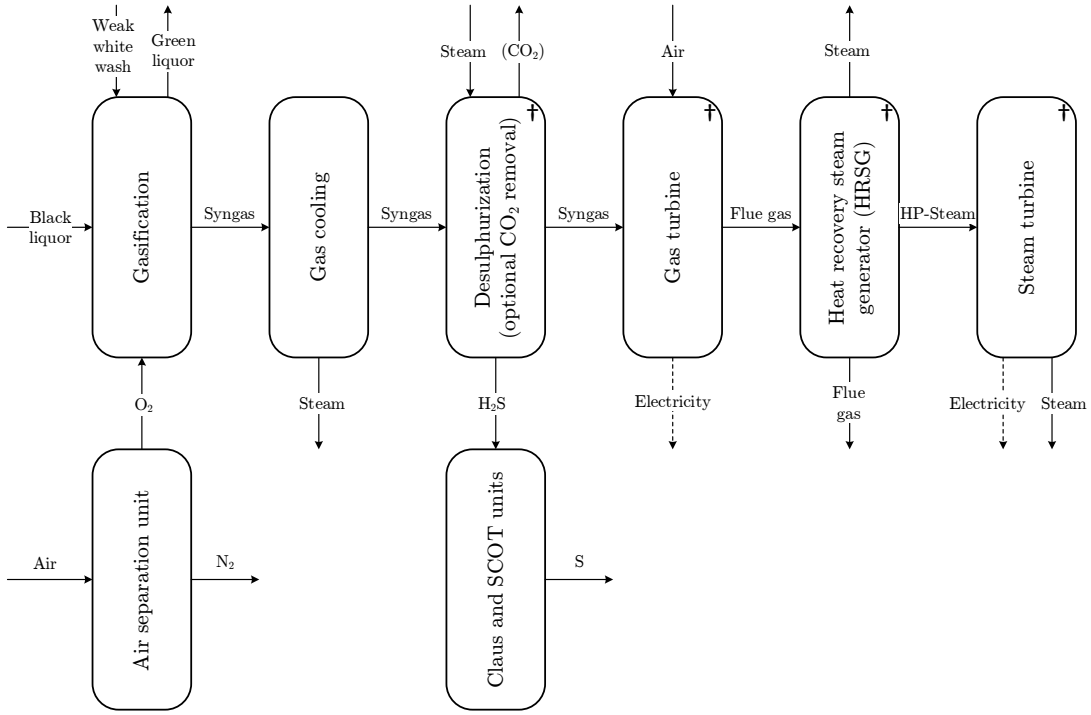

Figure 9: Process schematic illustrating the black liquor gasification combined cycle. † These processes are simulated in this work.

which are formed from H_2S in the combustion zone of the gas turbine. To avoid such problems the sulphur levels in the syngas need to be reduced below 20 ppmv before entering the gas turbine (Korens et al., 2002). A commercial process that can reduce sulphur levels to meet the requirements is the Selexol process. The solvent used in this process is a mixture of dimethyl ethers of polyethylene glycol. The chemical formula is $CH_3O(CH_2CH_2O)_nCH_3$, where n is between 2 and 9. The Selexol solvent utilizes physical absorption to remove acid gases. Hence, no chemical reaction occurs which is an advantage compared to chemical solvents, such as MEA, which degrades over time due to formation of heat-stable salts (Breckenridge et al., 2000). The Selexol process also has a high selectivity of H_2S over CO_2, which makes is suitable for gas turbine applications, since the co-absorption of CO_2 can be minimized. One downside with the Selexol solvent is its limited ability to absorb COS. A solution is to add a COS hydrolysis unit before the Selexol process. By addition of steam, COS reacts and forms CO_2 and H_2S in the hydrolysis unit, and consequently the concentration of COS is reduced from over hundred ppmv down to 10 ppmv. (Kubek et al., 2000)

In the Selexol process (Figure 10) the solvent and the syngas are contacted in a counter-current packed absorber operating at high pressures, 20-140 bar (Maxwell, 2004). The sulfur compounds are absorbed and some CO_2 is inevitably also co-absorbed. The H_2S-rich solvent is then passed through a second column where N_2 is

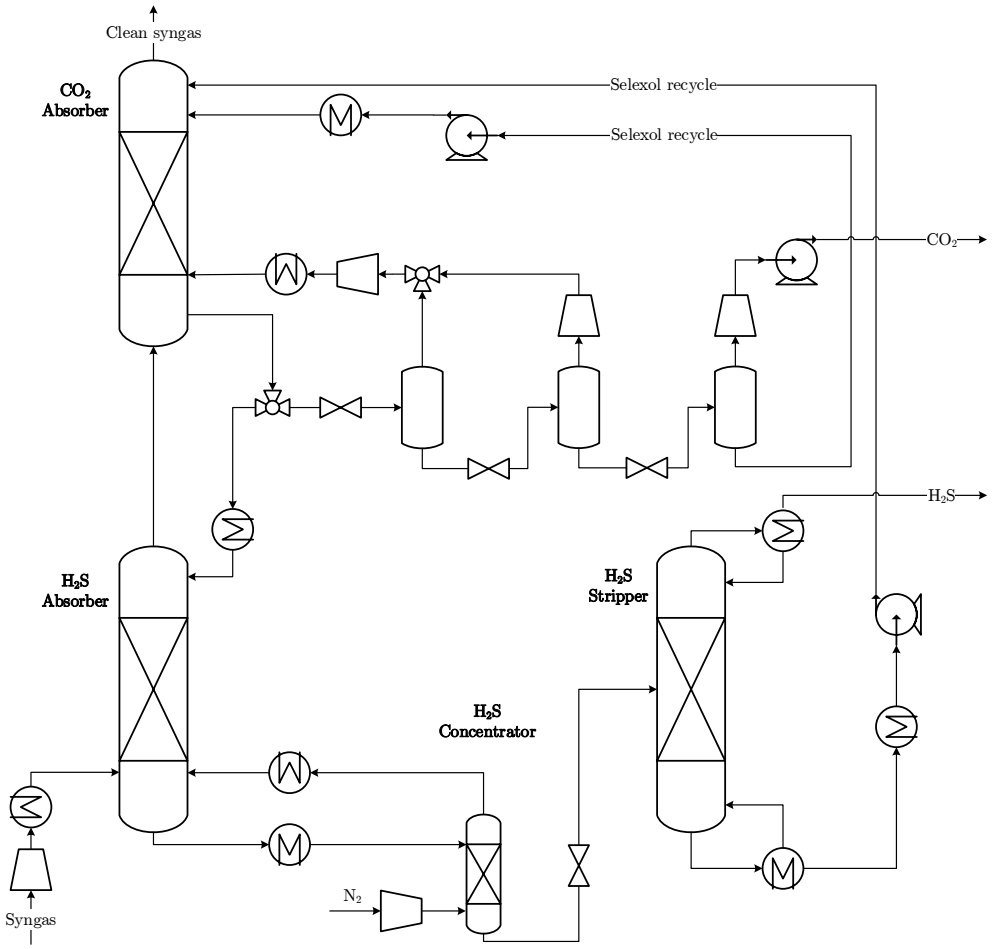

Figure 10: Simplified flowsheet of the Selexol process with CO_2 capture, based on the work of Field & Brasington (2011a).

added as stripping gas. Most of the absorbed CO_2 is stripped from the solvent and recycled back to the absorber, whereas the H_2S-rich solvent enters a second stripper. In this packed stripper heat is applied in the reboiler to regenerate the solvent and to produce a gas stream rich in H_2S. The solvent is recycled back to the absorber and the H_2S-rich gas stream is sent to a Claus unit for further processing. If CO_2 capture is desired the Selexol process can be modified to meet such requirements as well. By letting the sulfur free syngas pass a second absorber the CO_2 is absorbed. The solvent is regenerated by lowering the pressure and the flashed CO_2 can be compressed and transported to storage. (Field & Brasington, 2011a)

The H_2S-stream sent to the Claus unit should have a concentration of at least 40 mole-%. If this is fulfilled the straight-through Claus process can be used, which is the least complex alternative. Otherwise alternatives such as direct oxidation can be used for lower concentrations. In the Claus process the H_2S gas stream is introduced in a reaction furnace together with air. The reaction occurring in the combustion zone converts a large portion of the H_2S into elemental sulphur. To convert the

remaining part of the H_2S, the gas is passed over a number of catalytic beds. To recover essentially all sulphur, which is important to reduce raw material costs, a Shell Claus Off-Gas Treating (SCOT) unit can be added after the Claus unit. With this unit over 99.7 % of the sulphur is recovered (Linde Process Plants Inc., 2012). As previously mentioned the elemental sulphur can be used to prepare polysulphide cooking liquor by dissolving it in the green liquor formed in the gasifier:

$$3S(aq) + Na_2S(aq) \longrightarrow Na_2{-}S_3{-}S(aq) \tag{6}$$

The clean syngas is combusted in a gas turbine to produce electricity. The flue gases then pass through a heat recovery steam generator where HP-, MP-, and LP-steam is produced. The MP- and LP-steam is used where it is needed in the pulping process. The HP-steam is passed through a steam turbine to produce additional electricity. If a steam surplus is present in the pulp mill, the steam can be expanded further in a condensing turbine to increase electricity production.

4.3 Black liquor gasification with motor fuel production

The process schematic for motor fuel production is shown in Figure 11. DME has been chosen as a product but several other alternatives exist, such as methanol, hydrogen or FT-diesel. DME is chosen since this fuel can be used in modified diesel engines and is considered a fairly realistic alternative to be implemented in the years before 2020 (Pettersson & Harvey, 2012). This perception was further strengthened by the European BioDME project which was successfully concluded in 2012. In this project DME produced in Chemrecs pilot plant showed a great well to wheel efficiency, compared to other biofuels, after a driving distance of 450 000 km by the test fleet of Volvo trucks. The energy consumption was 270 MJ/100 km compared to e.g. 440 MJ/100 km for ethanol from wheat straws (Salomonsson, 2013).

The gasification process is identical to that of the BLGCC alternative. However, the gas cleaning process differs substantially as the DME production has a more stringent requirement of the sulphur level in the syngas. To avoid deactivation of the catalyst in the DME synthesis a sulphur concentration below 0.1 ppmv is required. The Selexol process is unable to meet this specification and hence another gas cleaning process must be used (Korens et al., 2002). The DME production is also inhibited by the presence of CO_2. The reason is that CO_2 is a reaction product in the formation of DME and therefore shifts the equilibrium towards the reactants. Hence, the CO_2 concentration should be reduced to below 3 mole-%. The Rectisol process is capable of producing a clean synthesis gas with the requirements specified above. (Ju et al., 2009)

The Rectisol process was developed in the 1950s and is today widely used in sour gas treatment. Methanol is utilized as solvent in this process and it separates the unwanted species, i.e. CO_2, H_2S and COS from the remaining gas by physical absorption (Sun & Smith, 2013). Unlike the Selexol process, the Rectisol process is capable of removing COS to satisfying levels and hence a COS hydrolysis unit is

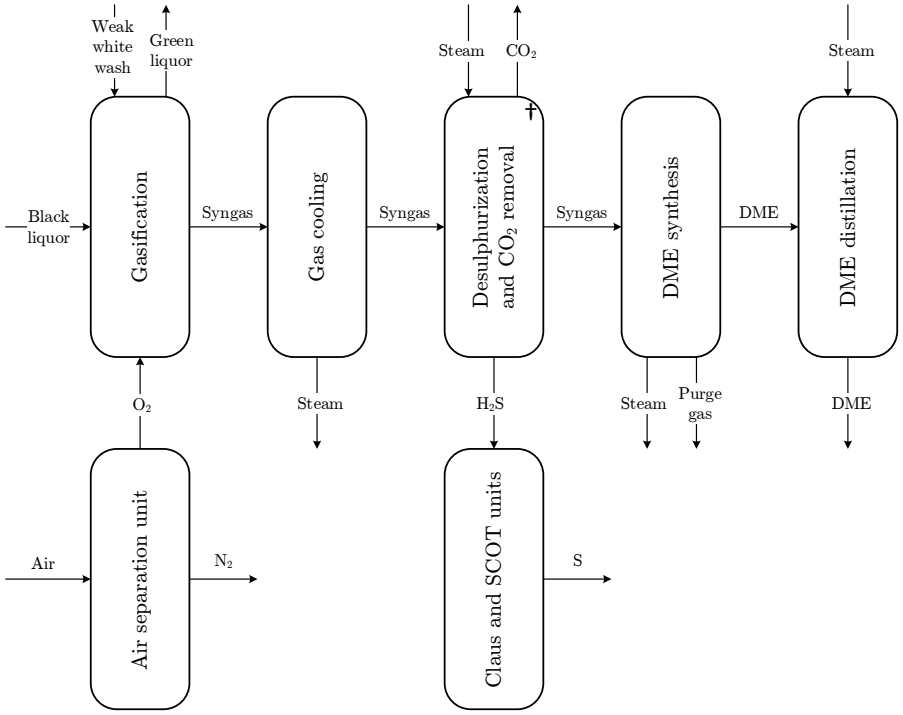

Figure 11: Process schematic of black liquor gasification with DME production. † These processes are simulated in this work.

redundant. The solubility of CO_2 and H_2S differs to such an extent that selective removal is possible. Also the solubility of sour gases, and thereby the absorption rate, is enhanced at high pressures and low temperatures. Hence, Rectisol processes are operated at temperatures between -20 to $-60\,°C$ and pressures in the range of 30-80 bar (Weiss, 1988).

A modified version of the Rectisol process, provided by Gatti et al. (2013), is presented in Figure 12. The syngas produced in the gasifier enters the bottom of a packed absorber divided into two sections. Refrigerated methanol enters the absorber and after passing through the top section, about 45 % of the methanol, containing almost exclusively absorbed CO_2, is withdrawn. The remaining solvent flows through the bottom section and exits the absorber, rich in both CO_2 and H_2S. Both streams are flashed to recirculate co-absorbed CO and H_2. After further pressure reduction the streams enters two stripper columns to desorb the CO_2. The CO_2 rich stream enters the top of the strippers whereas the stream containing H_2S enters in the bottom, this is to ensure that only a small amount of H_2S ends up in the CO_2 stream for sequestration. A stripper, equipped with a reboiler and partial condenser, regenerates the methanol which is recycled to the absorber. The top product from the stripper is a gas stream with high H_2S-concentration which is to be further processed in the Claus unit.

The Claus and the SCOT unit is identical to those in the BLGCC case, for

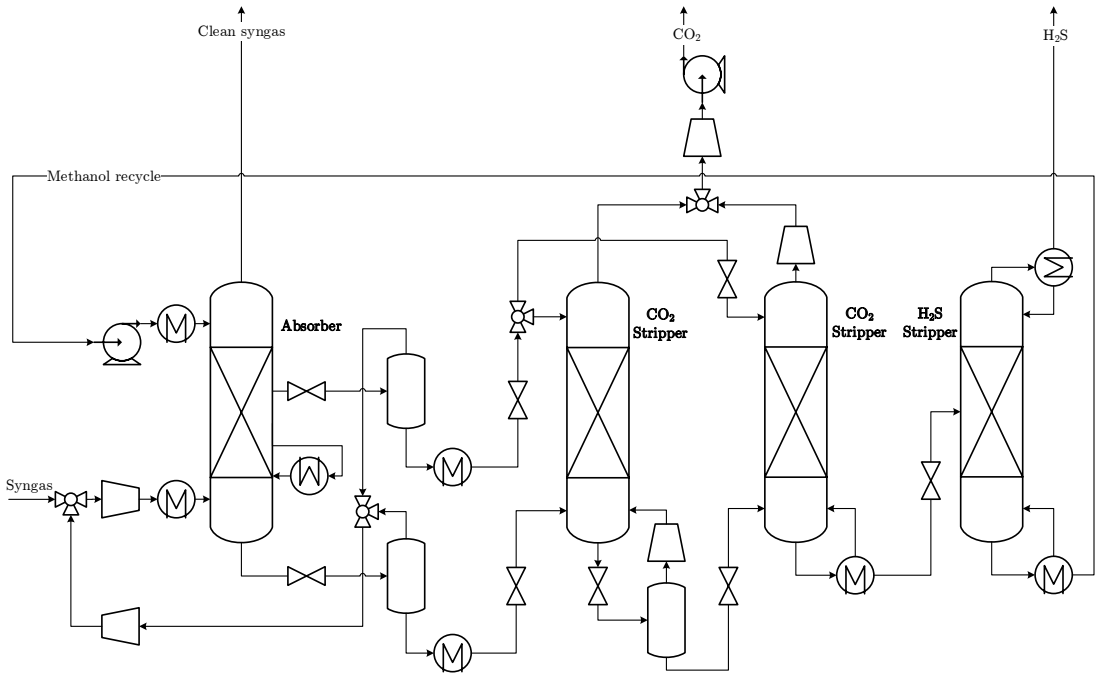

Figure 12: Simplified flowsheet of the Rectisol process, based on Gatti et al. (2013).

more information see Section 4.2. The clean syngas out from the Rectisol process enters the DME synthesis. The conventional manufacturing process of DME is an indirect two step synthesis route, where methanol is produced via methanol synthesis and then converted to DME by dehydration. A new technology has recently been developed by Ohno et al. (2006). The new process is a direct synthesis where DME is produced from the syngas according to this overall reaction:

$$3\,\mathrm{CO} + 3\,\mathrm{H_2} \longrightarrow \mathrm{CH_3OCH_3} + \mathrm{CO_2} \tag{7}$$

The new process is operated at 50 bar and 260 °C in a slurry bed reactor containing a catalyst (Ohno et al., 2006). A syngas composition of 1:1 molar ratio of H_2 and CO gives highest conversion. The conventional process requires a molar ratio of 2:1 (Ju et al., 2009). The syngas out of the gasifier has a molar ratio of 1.03 which means that the new process eliminates the need of a water-gas shift reactor to adjust the ratio (Ekbom et al., 2005). However, the major advantage with this new process is that it overcomes the equilibrium limitations of the methanol synthesis and thereby gives higher conversion (Marchionna et al., 2008). The gas mixture produced in the DME reactor is separated in a series of distillation columns. Unreacted gas and formed methanol are recycled back to the reactor. As can be seen in Reaction 7, CO_2 is formed in the DME production. However, the possibility to capture this carbon dioxide has not been considered in this work.

5 Method

In an initial literature review the pulp mill was studied to determine the most probable development of the pulping process in the nearest future. Three scenarios were identified. The first one is the "business as usual" case where the conventional recovery boiler continues to be the technique used for regeneration of the cooking chemicals. In the second scenario the recovery boiler is replaced with a gasifier which generates syngas that is used to produce electricity in a gas turbine. The third scenario also utilizes a gasifier but instead of producing electricity the syngas is used as raw material for DME production. In this work the possibility of capturing CO_2 in these three scenario are examined, see Table 1. In the first scenario post-combustion capture using the MEA process is examined. For the second scenario pre-combustion capture with the Selexol process has been determined to be the most suitable. Pre-combustion capture using the Rectisol process is applied to the third scenario.

Table 1: Three possible scenarios for the future development of the pulp mill. The last letter in the abbreviation indicates which capture process is applied to that scenario.

Scenario	**Recovery system**	**Additional product**	**Capture technology**	**Capture process**
RB-M	Recovery boiler	N/A	Post-combustion	MEA
BLGCC-S	Black liquor gasification	Electricity	Pre-combustion	Selexol
BLGMF-R	Black liquor gasification	DME	Pre-combustion	Rectisol

5.1 Process simulation

To evaluate the suitability and the specific cost of capturing CO_2, process simulations of the capture processes are performed. The software used is Aspen Plus 8.0, section 5.5 gives a brief account of the capabilities of this modelling tool.

The cost of capturing CO_2 can be estimated if each of the scenarios is divided into one case with CO_2-capture and one without capture. These cases will henceforth be denoted "CCS" and "NC", respectively. For the RB-M-scenario, the NC-case is simply the present day situation where the flue gases are vented to the atmosphere and hence will not need any modelling. A remark worth noticing is that only the flue gases from the recovery boiler have been considered, but it is also possible to capture CO_2 from the biofuel boiler. Due to lack of process data regarding the biofuel boiler and its flue gases, this possibility has been omitted in this work. However,

the recovery boiler produces the major part of the pulp mills emissions. In the BLGCC-S-scenario, models for both the CCS-case and the NC-case is needed, since even if CO_2 is not to be captured the Selexol process is still present to remove H_2S from the gases entering the gas turbine. For the BLGMF-R-scenario, two cases are modelled as well. Since, as explained in section 4.3, CO_2 has to be removed also for the NC-case to maximize DME yield.

For each of the five modelled cases, all required process equipment is included, with the exception of maintenance pumps. These are needed to overcome pressure drops occurring in the process equipment, pipes and difference in elevation. This is a necessary simplification as exact knowledge regarding the relative placement of the process equipment is not obtained at a preliminary design stage and thus, the calculation of these pressure drops is not possible. Chemical reactions are taken into account in the models and where applicable, a rate-based approach is employed. All process equipment in the models are adjusted to suitable sizes to ensure that the outgoing streams meet the requirements, see Appendix A.

In addition to the capture processes, modelling of the gas turbine, HRSG and the steam cycle has been carried out as well. Figure 9 and 11 indicates which processes that have been simulated.

5.2 Pinch analysis

A vital part of reducing the cost for carbon capture is to design processes with low utility demands and heat exchanging should therefore be applied. Pinch analysis can be used to construct a heat exchanger network that achieves a high degree of heat integration and thereby reduces utility demand. In this work Pro-Pi2, see section 5.5 for a brief description of the software, is used to design the heat exchanger network.

Stream data such as temperatures and cooling or heating demand is extracted from Aspen Plus and inserted into Pro-Pi2. From the given data, Pro-Pi2 calculates the pinch point and creates a graphical stream representation displaying each stream and its heating or cooling need. To this graphical interface heat exchangers, coolers and heaters are added to construct a heat exchanger network for maximum heat recovery. However, to avoid a design with inconveniently many heat exchangers the network can be simplified, if needed, by removing the units with smallest impact on heat recovery. See Appendix B for further information and assumptions regarding the pinch analysis.

5.3 Dimensioning

The last step in the design of the process is to add buffer tanks and maintenance pumps to the process flowsheet. The buffer tanks are located in-between large process equipment such as absorbers and strippers and are needed in case of variations in production and greatly increase the ease of process control. Maintenance pumps are also added to the process flowsheet before the design is complete. As stated in

section 5.1, these pumps are not modelled in Aspen Plus as information of exact pressure drops is not available.

Each component in the complete flowsheet is sized and when possible Aspen Plus provides the characteristic design variable such as power requirements for pumps. Other equipment, e.g. flashes are sized using correlations provided in chemical literature. See Appendix C for assumptions regarding the dimensioning of the equipment. The characteristic size and operating range of all units are summarized, thus providing a basis for an investment cost estimation. Using this data Skagestad & Eldrup (2014) conducts an analysis for each of the five cases and provides a total investment cost which also includes installation costs. In addition, operating costs which cannot be extracted from the simulations i.e. maintenance cost and salaries are provided as well.

5.4 Overall energy and mass balance

The simulations result in an estimation of utility demand. However, directly comparing the value of MP-steam, LP-steam and electricity is tedious. Hence, to make a fair comparison, an overall balance of the pulp mill, including the major in and outflows of energy and mass, is constructed for all six cases. For detailed information of the calculation procedure see Appendix D, here follows a short summary of the procedure. As explained in section 4.2 and 4.3 the BLGCC-S- and BLGMF-R-scenarios include several additional processes compared to today's market pulp mill. To determine the utility consumption or production of these processes various sources are consulted and the obtained information is scaled to match the pulp production rate of SCA Östrand. However, some of these processes are simulated in Aspen Plus, namely the gas turbine, the HRSG and the steam cycle, see Figure 9 and 11. For details about the simulations see Appendix, E, F and G. The steam cycle is modelled to determine the amount of external fuel needed to balance the energy demand of the complete pulp mill. The information obtained about the additional processes is combined with data on SCAs pulp mill in Östrand and the results are presented in the form of a graphical representation of input and output streams to the process. From the results of the overall balance, in combination with the investment cost analysis, it is possible to determine the specific cost of capturing CO_2, by comparing the difference in electricity, solid wood fuel and cooling water demand for the two cases in each scenario.

During the calculation of the overall energy and mass balance it was noticed that the process data obtained from SCA must have been extracted when the pulp mill was running on part load. Hence, all results from the simulations are scaled to compensate for this. This also affects the size of the equipment, instead of redoing the entire dimensioning the investment cost was also scaled.

5.5 Modelling tools

The software used for the process simulations is Aspen Plus 8.0, developed by Aspen Technology Inc.. This software is a process simulation tool that can be used for conceptual design, optimization and performance monitoring of various processes. Aspen Plus handles mass and energy balances and performs rigorous calculations of process equipment. A large databank of pure component and equilibrium data also enables Aspen Plus to handle chemical reactions and equilibrium. Transport phenomena can also be included, thus making sizing of process equipment such as absorbers possible.

The pinch analysis software used to aid in the design of the heat exchanger network is the Excel add-in Pro-Pi2, developed by the department of Energy and Environment at Chalmers University of Technology. Pro-Pi2 has several functions including pinch-point calculation, construction of grand composite curves and a graphic interface for design of a heat exchanger network.

6 Modelling

This chapter presents the input data used in the modelling work and then gives a thorough review of the modelling approach. Assumptions regarding the modelled components and their design specifications are also presented.

6.1 Input data

This thesis is a case study on SCAs pulp mill in Östrand, hence the simulations are based on data obtained from their engineering department. However, only the most essential data has been provided, i.e. the mass flow of black liquor and the oxygen concentration and volume flow of flue gases. Remaining data has been extracted from other sources and where applicable scaled to match the pulp production rate of SCAs pulp mill. The flue gas stream entering the RB-M-scenario is based on Hektor (2008) in addition to the process data provided by SCA. The specifications for the syngas stream entering both the BLGCC-S- and BLGMF-R-scenarios has been determined from Gebart et al. (2011), Ekbom et al. (2005) and Kubek et al. (2000), as well as process data from SCA. From the aforementioned sources, the composition, temperature, pressure and mole-flow of the streams entering the capture process have been determined, see Table 2. For all three scenarios, the simulated processes are adapted to capture 85 % of the ingoing CO_2.

Table 2: Process stream data used in the simulations. The composition is specified as mole-% except the COS-concentration where ppmv is used.

Scenario	$\dot{n}$ [mol/s]	P [bar]	T [°C]	H_2	CO	CO_2	H_2S	CH_4	O_2	N_2	H_2O	COS
RB-M	5014	1.0	110	0	0	13.3	0	0	4.4	63.3	19.0	0
BLGCC-S	865	31.5	30	39.2	38.1	19.0	1.9	1.3	0	0.2	0.2	10
BLGMF-R	865	31.5	30	39.2	38.1	19.0	1.9	1.3	0	0.2	0.2	122

6.2 RB-M-scenario

For the RB-M-scenario where post combustion capture with MEA is applied, the property method Electrolyte NRTL is used for the simulations in Aspen Plus. This method can handle aqueous and mixed solvent systems for a wide range of concentrations and hence should give an accurate representation of the behaviour of the compounds involved in this process. The physical property data is provided in the Aspen Plus rate-based MEA template, which has been used as a starting point for the simulations. This data contains reaction kinetics which has been validated

against industrial applications. A number of reactions occur in the system at hand but the seven reactions defined below are considered to be most influential. Reaction 8-10 are assumed to be in equilibrium, whereas Reaction 11-14 are rate-controlled reactions (Aspen Technology, 2012b).

$$H_2O + MEAH^+ \longleftrightarrow MEA + H_3O^+ \tag{8}$$

$$2\,H_2O \longleftrightarrow H_3O^+ + OH^- \tag{9}$$

$$HCO_3^- + H_2O \longleftrightarrow CO_3^{2-} + H_3O^+ \tag{10}$$

$$CO_2 + OH^- \longrightarrow HCO_3^- \tag{11}$$

$$HCO_3^- \longrightarrow CO_2 + OH^- \tag{12}$$

$$MEA + CO_2 + H_2O \longrightarrow MEACOO^- + H_3O^+ \tag{13}$$

$$MEACOO^- + H_3O^+ \longrightarrow MEA + CO_2 + H_2O \tag{14}$$

6.2.1 RB-M-CCS-case

The flowsheet from Aspen Plus is presented in Figure 13 in which all components and streams are named. This section will explain the general assumptions and design parameters chosen for the simulation. All auxiliary equipment such as coolers, heaters, pumps, flashes etc. are explained in more detail regarding modelling approach and assumptions in Section 6.5, as they are identical for the three different scenarios. However the modelling of columns will be explained in detail for each process as they differ from case to case.

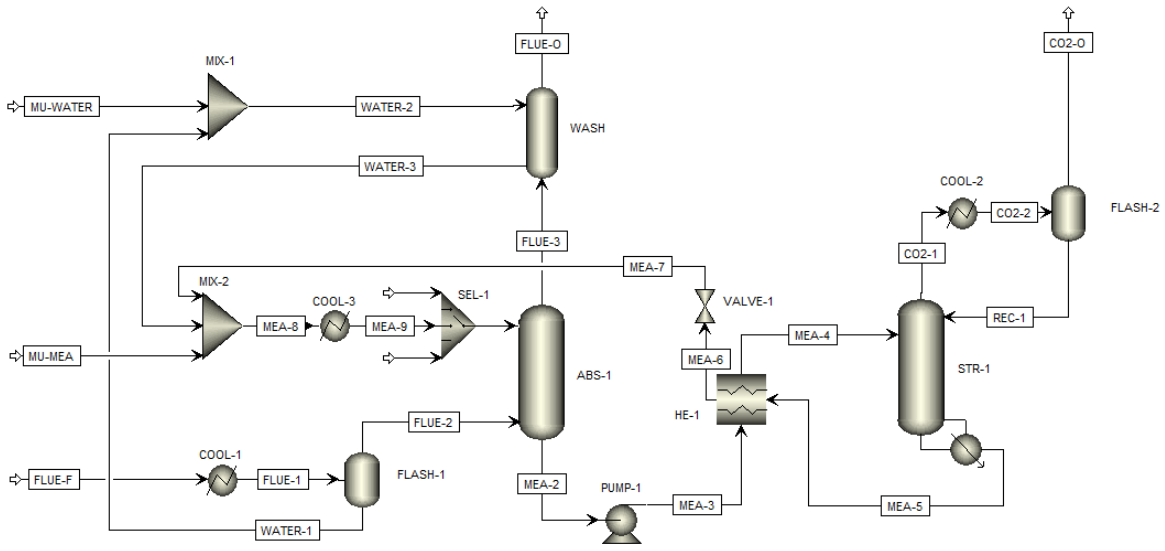

Figure 13: Aspen Plus flowsheet of the MEA capture process for the RB-M-CCS-case.

The flue gases from the recovery boiler enters the capture process at ambient pressure and a temperature of 110 °C. Before the flue gases is fed to the absorber the temperature is reduced to 40 °C in COOL-1, but since a considerable amount of water is present some of it will condensate. FLASH-1 separates the condensed water and the remaining flue gases, which leaves in the top of the flash and enters the bottom stage of the absorber, ABS-1. In the top a solution of MEA and water enters the absorber at 40 °C. A weight ratio of 30 % MEA is commonly used and this corresponds to a mole ratio of 0.126. The mole ratio is used as a measurement to maintain the specified proportions between water and MEA. Since the solution entering the absorber is a recycle stream it will contain a certain amount of CO_2 bound by MEA in the form of $MEACOO^-$. Therefore the weight ratio between all MEA species and water would give an incorrect value as the molar weight of $MEACOO^-$ is higher than that of MEA.

The absorber is modelled as a packed column filled with Mellapak 250Y, which is a structured packing. A rate-based approach using the "RadFrac" block has been applied for the simulations meaning that transport resistance is included in the model. For the liquid phase, diffusional film resistance is assumed with reactions occurring in the film. The film is discretized using 10 points, see Table 3. The reactions are fast and most CO_2 will react with MEA as soon as it enters the liquid (Kothandaraman, 2010). The discretization points are therefore concentrated towards the liquid-vapour interface, where the gradients will be the largest. No reactions are assumed to take place in the vapour phase and therefore only diffusional resistance is taken into account in the vapour film.

Table 3: Locations of the discretization points in the liquid film. The liquid-vapour interface is located at 0 and 1 corresponds to the bulk liquid. (Kothandaraman, 2010)

Point	1	2	3	4	5	6	7	8	9	10
Distance	0	0.001	0.005	0.010	0.050	0.100	0.150	0.200	0.300	1

The absorber is divided into 20 stages. In contrast to equilibrium calculations, an increased number of stages do not increase the separation performance of a column, instead more accurate calculations are obtained as the column is divided into more calculation steps. However, using more stages increases the number of equations solved and hence there is a trade-off between accuracy and computational time. The height of the column is set manually to achieve a certain capture rate. The diameter on the other hand is calculated using the flooding approach in Aspen Plus. In this approach the stage with the highest vapour and liquid flows are chosen as a base stage. The column diameter is then adjusted so that fluxes on this stage are 70 % of that corresponding to flooding, a state where a too high vapour flux prevents the liquid from flowing downwards. The most important design parameters and results from the absorber is presented in Table 4.

Table 4: Design parameters and dimensions of ABS-1.

Name	Packing material	Stages	Pressure [bar]	Diameter [m]	Height [m]
ABS-1	Mellapak-250Y	20	1	9.8	15

Two product streams exits the absorber. The top product is the flue gases now CO_2 lean. A fraction of the stream is MEA-slip which has to be recovered from the flue gas to reduce the cost of make-up MEA. A packed wash column, with the dimensions presented in Table 5, is added to accomplish this task. In the column, water from FLASH-1 and some make-up water flows counter-current to the flue gas flow and removes MEA. The clean flue gases leaving the wash column contains 2.2 mol-% CO_2.

Table 5: Design parameters and dimensions of WASH.

Name	Packing material	Stages	Pressure [bar]	Diameter [m]	Height [m]
WASH	Mellapak-250Y	10	1	6.3	3

The CO_2 absorbed in the liquid solvent exits the absorber at the bottom stage mainly as $MEACOO^-$. The amount of CO_2 in a stream is expressed in the form of loading, i.e. the ratio of all species containing CO_2 and all MEA-species. In this study the optimal loading for the rich solvent exiting the absorber was found to be 0.536. PUMP-1 elevates the pressure of the bottom product to 1.8 bar before it enters a heat exchanger (HE-1) which raises the temperature to 101 °C. To model HE-1, the "MHeatX" block is used as this block is suitable when recycle streams is involved, since this block tears the energy stream thus facilitating easier convergence. The heated stream enters the stripper (STR-1) on the second stage out of 20 in total. The stripper is modelled with the same assumptions regarding mass transfer and discretization of the liquid film. In contrast to the absorber the stripper is equipped with both a partial condenser and a reboiler. However, the partial condenser is modelled as a cooler and a flash to ease convergence. Table 6 summarizes the design parameters of the stripper.

Table 6: Design parameters and dimensions of STR-1.

Name	Packing material	Stages	Pressure [bar]	Diameter [m]	Height [m]
STR-1	Mellapak-250Y	20	1.8	6.4	15

The bottom stream from the reboiler exits STR-1 with a lean loading of 0.284 and a temperature of 118 °C. This lean loading was found to be the optimal value to obtain a low reboiler duty. To minimize the utility demand of the process this stream is heat exchanged in HE-1 with the inlet stream to the stripper. VALVE-1

then lowers the pressure to 1 bar. Small amounts of MEA are lost in both the flue gases and the CO_2-stream and hence a make-up stream is added. In addition, the water from the wash column is added to adjust the ratio between MEA and water. The amount of make-up MEA added is determined by a balance block in Aspen Plus, which performs a component balance over all inlet and outlet streams. Before the regenerated absorbent is fed to the absorber once again, the temperature is reduced to 40 °C by COOL-3.

The gas stream leaving the partial condenser of STR-1 has a CO_2-concentration of 99.0 mol-% and is compressed to 80 bar in a multistage compressor consisting of 4-stages with intermediate cooling to 25 °C. At such high pressures the gas mixture will be in a supercritical state and therefore a pump can be used to increase the pressure to the 150 bar required for transportation and storage (Field & Brasington, 2011b). However, the Electrolyte NRTL model only gives accurate results up to medium pressures i.e. tens of atmospheres. Hence, this section of the flowsheet is modelled separately using a model more suitable for high pressures namely, the PSRK property method which is based on the Predictive Soave-Redlich-Kwong equation-of-state model (Aspen Technology, 2010). Figure 14 shows the flowsheet of the compression section. The streams out from the multistage compressor labelled L1, L2 and L3 are condensed water.

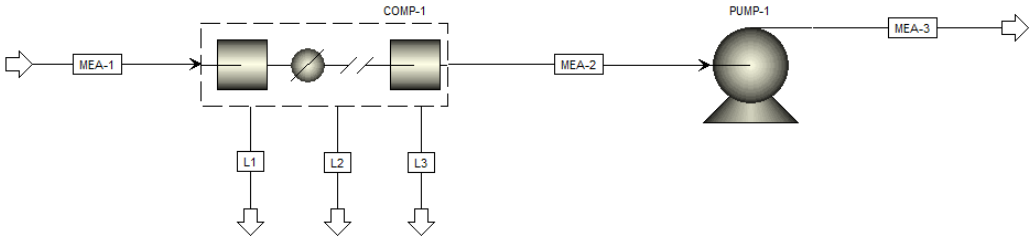

Figure 14: Aspen Plus flowsheet of the CO_2 compression section.

6.2.2 RB-M-NC-case

The RB-M-NC-case is equivalent to the present situation at a market pulp mill. Hence, no modelling in Aspen Plus is necessary. This case is however important for the study as it will be compared with the previously described capture case.

6.3 BLGCC-S-scenario

For the BLGCC-S-scenario, the Selexol process will be used to capture CO_2. The Aspen Plus rate-based DEPG template is used as a starting point for the simulations (Aspen Technology, 2012a). The solvent trademarked under the name Selexol is, as explained in Section 4.2, a mixture of dimethyl ethers of polyethylene

glycol (DEPG) with a chemical formula of $CH_3O(CH_2CH_2O)_nCH_3$. The weight-distribution between DPEG of varying chain length is provided by the template and is presented in Table 7.

Table 7: Weight-distribution of DEPG-compounds.

Chain length (n)	2	3	4	5	6	7	8	9
Weight-%	0	6	23	26	21	14	7	3

The Perturbed-Chain Statistical Associating Fluid Theory (PC-SAFT) is used as property method. This method determines the intermolecular forces by dividing them into repulsive and attractive forces and calculate contributions from different segments of the molecules (Field & Brasington, 2011b). Hence, this model is suitable for polymers or other compounds with repeating units such as DEPG. Physical data used in the template has been regressed against vapour-liquid equilibrium data (Aspen Technology, 2012a).

6.3.1 BLGCC-S-CCS-case

The model of the Selexol process for carbon capture is based on the model constructed by Field & Brasington (2011a). Figure 15 presents a flowsheet of the process, including numbering of units and streams.

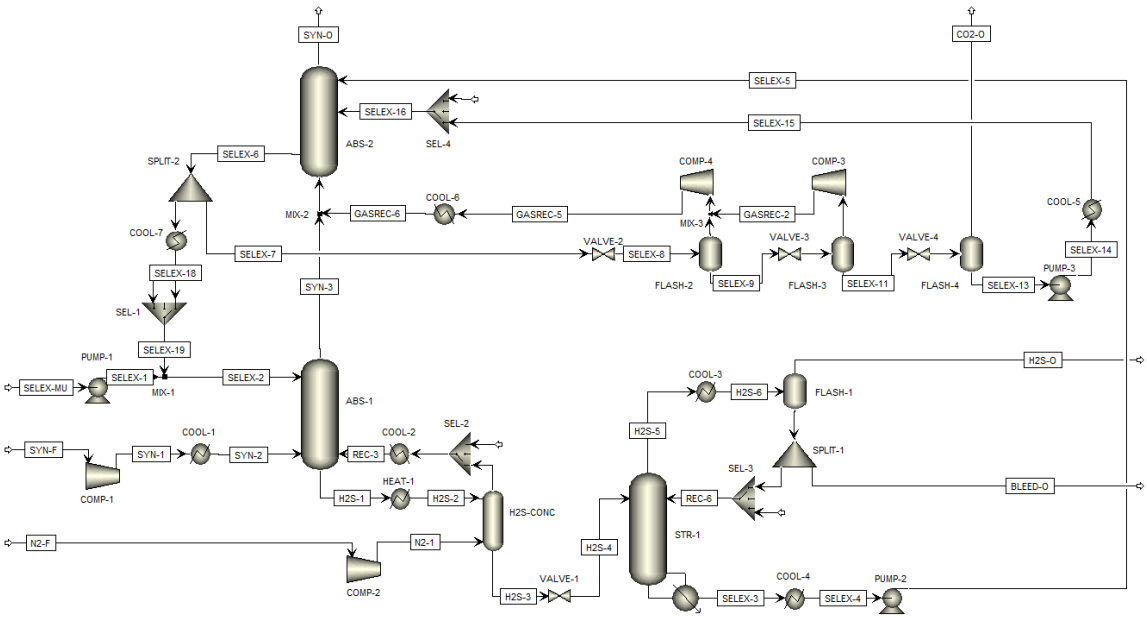

Figure 15: Aspen Plus flowsheet of the Selexol capture process for the BLGCC-S-CCS-case.

The gasifier produces syngas at a pressure of 31.5 bar. Before entering the bottom stage of the absorber (ABS-1), the syngas is compressed and cooled to 52 bar and

35 °C. At the top stage a Selexol stream enters, which is partially loaded with CO_2. The purpose of ABS-1 is to absorb essentially all H_2S and COS. A rate-based modelling approach using the "RadFrac" block is applied for all columns in this simulation. Film diffusion resistance has been applied, however no reactions are modelled since it is a physical absorption process. To ease convergence of all columns in this simulation the convergence method is set to Sum-Rates which is recommended for wide-boiling mixtures. The design parameters for ABS-1 are presented in Table 8.

Table 8: Design parameters and dimensions of ABS-1.

Name	Packing material	Stages	Pressure [bar]	Diameter [m]	Height [m]
ABS-1	IMTP 50 mm	20	52	1.9	20

The H_2S rich solvent stream exits the absorber below the bottom stage and is heated to 105 °C before entering the H2S-concentrator column (H2S-CONC). The column uses nitrogen as stripping gas with the purpose of releasing most of the absorbed CO_2 and recycle it to ABS-1. See Table 9 for design specifications of H2S-CONC.

Table 9: Design parameters and dimensions of H2S-CONC.

Name	Packing material	Stages	Pressure [bar]	Diameter [m]	Height [m]
H2S-C.	IMTP 50 mm	20	52	1.3	26

The bottom stream from H2S-CONC is expanded in VALVE-1 to the operating pressure of the H_2S-stripper (STR-1) which is 2 bar. STR-1 is equipped with both a reboiler and a partial condenser. However the partial condenser is modelled as a cooler and a flash for two reasons. Firstly to ease convergence and secondly to enable the possibility to extract a bleed stream, mostly consisting of water, from the recycle stream entering the top stage of the stripper. The simulations predicts the temperature in the reboiler to be 206 °C which is an unreasonably high value. Field & Brasington (2011b) states that the Selexol process can be modelled accurately in Aspen Plus with the exception of the stripper, where the actual temperature should be around 130 °C. One possible reason for this deviation could be that the vapour-liquid equilibrium data used in the regression of physical properties was inadequate for DEPG6, DEPG7, DEPG8 and DEPG9 (Aspen Technology, 2012a). Consequently the model predicts a too high temperature for evaporating the mixture present in the reboiler. Since the temperature is over 186 °C, MP-steam cannot be used to provide the needed energy, but MP-steam has been assumed anyway as this would be used in reality. Another consequence of the high temperature is that the cooler (COOL-4) after the reboiler will have a larger duty. Otherwise this should not affect any other results.

Table 10: Design parameters and dimensions of STR-1.

Name	Packing material	Stages	Pressure [bar]	Diameter [m]	Height [m]
STR-1	IMTP 50 mm	20	2	1.7	5

The top product from STR-1 has a H_2S-concentration well above the required 40 mol-%, see Section 4.2. The lean solvent exits the bottom of the reboiler and is cooled to a temperature of 15 °C by COOL-4. After an pressure increase to 52 bar by PUMP-2, the lean solvent enters the top stage of the second absorber (ABS-2). The purpose of this absorber is to reduce the CO_2-concentration of the syngas below 3 mol-%. See Table 11 for design specifications.

Table 11: Design parameters and dimensions of ABS-2.

Name	Packing material	Stages	Pressure [bar]	Diameter [m]	Height [m]
ABS-2	IMTP 50 mm	30	52	3.4	32

A Selexol stream, loaded with CO_2 and some co-absorbed H_2 and CO, is extracted from the bottom of ABS-2. This stream is divided into two by SPLIT-2, where a fraction of 0.91 enters the flash section of the process and the remaining part is recycled back to ABS-1. FLASH-2 and FLASH-3 operates at 14 bar and 6.2 bar respectively, and by lowering the pressure the co-absorbed H_2 and CO is desorbed along with some CO_2. After re-compression and cooling to 52 bar and 15 °C this gas recycle is joined with the flue gases entering ABS-2. The bottom product from FLASH-3 is further expanded to 1.5 bar in FLASH-4, where almost all CO_2 is released. From FLASH-4 the lean solvent is recycled back to ABS-2 and enters stage 8 at 52 bar and 15 °C. Small amount of solvent is present in all of the outlet streams and to compensate for this, a balance block calculates the component balance for each DEPG fraction and add the correct amount to the "SELEX-MU"-stream.

A CO_2-concentration of 95 mol-% is obtained in the stream sent to the compression section which is modelled in a separate flowsheet, as the "PC-SAFT" model is not accurate for critical conditions. The compression section is identical to the one presented for the RB-M-CCS-case, see Section 6.2.1 for details. The only difference is that the stream that is to be compressed contains essentially no water, hence no water is condensed during compression.

6.3.2 BLGCC-S-NC-case

As explained in Section 4.2 the Selexol process is still needed even if carbon capture is not applied since the H_2S has to be removed from the syngas. However, if CO_2 removal is not required the process can be greatly simplified as the second absorber and the associated flash section is redundant. Figure 16 presents the flowsheet of the Selexol process without carbon capture.

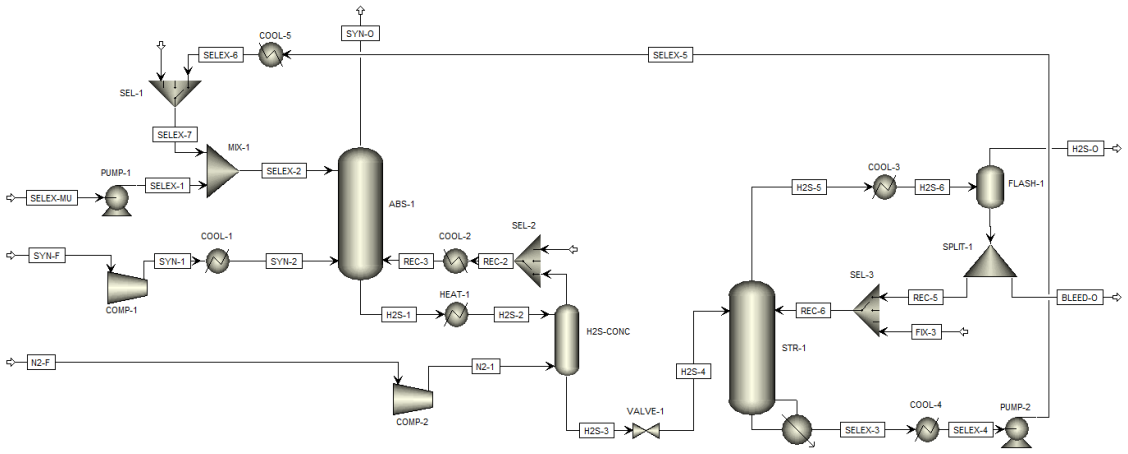

Figure 16: Aspen Plus flowsheet of the Selexol process for the BLGCC-S-NC-case.

From the flowsheet it can be observed that the layout of the bottom section is identical to the case with capture, the only exception being that the recycle of lean solvent from the stripper now enters ABS-1 instead of ABS-2. However sizes of the equipment will vary, see Table 12.

Table 12: Design parameters and dimensions of columns.

Name	Packing material	Stages	Pressure [bar]	Diameter [m]	Height [m]
ABS-1	IMTP 50 mm	30	52	2.0	30
H2S-C.	IMTP 50 mm	20	52	1.2	12
STR-1	IMTP 50 mm	20	2	1.7	5

6.4 BLGMF-R-scenario

For the BLGMF-R-scenario the Rectisol process is used to capture CO_2 and H_2S. The Aspen Plus rate-based MEOH template is used as a starting point since the Rectisol process utilizes methanol as solvent (Aspen Technology, 2012c). This template also uses the PC-SAFT as property method. Physical properties in the template have been regressed against experimental data.

6.4.1 BLGMF-R-CCS-case

The design of the process is based on the single stage Rectisol process found in Gatti et al. (2013) and Munder et al. (2010). Figure 17 shows the finalized Aspen Plus flowsheet of the process.

The syngas produced in the gasifier contains a considerable amount of water. It has to be removed or else it will freeze and block the pipes. Water removal can be achieved by cooling the gas and thereby condensing the water. Hence, is it possible to

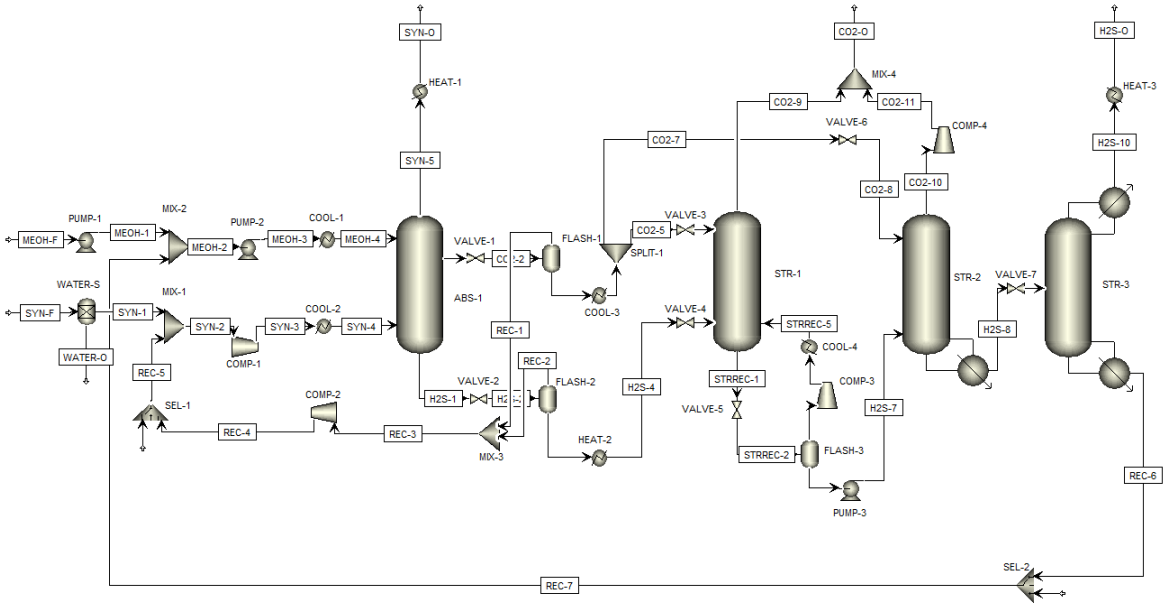

Figure 17: Aspen Plus flowsheet of the Rectisol capture process for the BLGMF-R-CCS-case.

perform this in the gas cooler in the gasification section of the process and therefore, this operation is considered to be outside the boundary of this simulation. Because of this, the water is removed by a "Sep" block that has no utility consumption. This component separator is an artificial unit, without a real counterpart, that separates the flow by specified component split fractions.

The absorber (ABS-1) operates at a pressure of 60 bar and therefore the syngas is compressed and subsequently cooled to a temperature of $-34\,°C$ before entering the column at the bottom stage. All columns in this case are modelled using a rate-based approach with a "RadFrac" block. Diffusional resistances are assumed for both liquid and vapor phase. See Table 13 for design specifications of ABS-1. The purpose of the column is to absorb CO_2 and H_2S to such an extent that the syngas exiting the column fulfils the requirements to be used as feedstock for DME production, see Section 4.3. The syngas leaving the column has a CO_2 concentration of 0.2 mole-% and contains 0.092 ppmv of total H_2S and COS. Methanol enters the top stage of the column at 60 bar and $-50\,°C$. The low temperatures present in the column favours the absorption of CO_2 and H_2S over the other gases present. Since this physical absorption into methanol is an exothermic process the produced heat needs to be removed, so that the benefits of a low absorption temperature can be utilized throughout the whole column. This is achieved by adding cooling loops inside the absorber. In the flowsheet the cooling loops are modelled by specifying side duties which extract heat from certain stages of the column, namely 14 and 18.

Two liquid product streams exits the absorber. At stage 18, about 45 % of the methanol is withdrawn. This methanol stream is loaded with CO_2 but essentially free of H_2S. As H_2S has a higher solubility than CO_2 in methanol, almost all H_2S

Table 13: Design parameters and dimensions of ABS-1.

Name	Packing material	Stages	Pressure [bar]	Diameter [m]	Height [m]
ABS-1	IMTP 75 mm	30	60	1.4	21.7

will leave the column in the bottom product. Both of these streams enters a flash (FLASH-1 and FLASH-2) where the pressure is reduced to release co-absorbed CO and H_2 which is then recycled to the syngas inlet. From the bottom of FLASH-1 the methanol stream loaded with CO_2 exits and is thereafter cooled to $-50\,°C$. This stream is then split into two streams, 90 % enters the first stripper (STR-1) and the remaining part enters the second stripper (STR-2). The bottom product of FLASH-2 is heated and then also enters STR-1 but on the bottom stage. STR-1 is a packed column operating at 6 bar, see Table 14. The lower operating pressure of STR-1 results in that absorbed gases will be released. Since the methanol stream only loaded with CO_2 enters the top of the column, a very pure top product, consisting of CO_2 and almost no H_2S, is obtained. The bottom product still contains a considerable amount of CO_2, some of which is released and recycled by FLASH-3 that operates at 2 bar.

Table 14: Design parameters and dimensions of STR-1.

Name	Packing material	Stages	Pressure [bar]	Diameter [m]	Height [m]
STR-1	IMTP 75 mm	30	6	1.5	15

The liquid stream from FLASH-3 containing both CO_2 and H_2S enters the second stripper (STR-2) at the bottom stage, see Table 15 for specifications. In the top of STR-2 the remaining 10 % of the absorbent only containing CO_2 enters. A 1-stage Rectisol process normally uses N_2 as stripping gas in the second absorber. However, that is unsatisfactory in this application since an diluted CO_2-product would be obtained. To reach the same amount of recovered CO_2 a reboiler is added to STR-2. Over the top of STR-2 a stream of almost exclusively CO_2 is obtained.

Table 15: Design parameters and dimensions of STR-2.

Name	Packing material	Stages	Pressure [bar]	Diameter [m]	Height [m]
STR-2	IMTP 75 mm	30	2.7	0.9	20

The CO_2-streams out from STR-1 and STR-2 are mixed, resulting in a CO_2-concentration of 96 mole-%. This stream is then elevated to a pressure of 150 bar in the compression section. As previously stated the PC-SAFT method is not accurate in the supercritical range and thus is the compression section modelled in a separate flowsheet, see Section 6.2.1 for a description.

The bottom product of STR-2 is feed to stage 5 of STR-3 which is a stripper equipped with both a partial condenser and a reboiler. STR-3 operates at 1.2 bar to enhance the desportion of both CO_2 and H_2S. The desorbed gases exit at the top and consists of 42 mole-% H_2S and the remaining part is almost exclusively CO_2. This stream is further processed in a Claus plant to obtain elemental sulfur which can be used to produce polysulfide cooking liquor. An almost pure methanol stream (total impurities lower than 5 ppmv) is obtained from the bottom of STR-3. This stream is recycled back to the inlet of the absorber. However, before it is fed to the top stage both pressure and temperature is adjusted to 60 bar and $-50\,^{\circ}C$. There will also be small losses of methanol in the gas streams leaving the system, a balance block is therefore added to adjust the make-up methanol injected to the recycle stream.

Table 16: Design parameters and dimensions of STR-3.

Name	Packing material	Stages	Pressure [bar]	Diameter [m]	Height [m]
STR-2	IMTP 75 mm	30	1.2	2.4	5

6.4.2 BLGMF-R-NC-case

If CCS is not applied to the BLGMF-R-scenario this will have almost no effect on the Rectisol process, since CO_2 still has to be removed from the syngas stream, see Section 4.3. The only difference is that the CO_2 stream is vented to the atmosphere instead of being compressed. Hence, the compression section is removed for this case. Otherwise the process is identical to the case with capture both regarding flowsheet layout and unit sizes. Thus, no additional modelling is needed for this case.

6.5 Auxiliary equipment modelling

The processes described in the previous sections have several basic unit operations in common such as pumps and valves. The same modelling approach has been used for these equipment throughout the simulations and the description in the following sections is therefore valid for all modelling cases. Information about the modelling blocks described in this section has been collected from Aspen Plus Help documentation.

6.5.1 Compressor

Compressors are modeled with the "Compr" block with the exception of the multistage compressor present in the cases with CO_2-sequestration, where instead the "MCompr" block is used. The calculation method is set to: "Polytropic using the ASME

method". To predict the power consumption with higher accuracy a polytropic efficiency for centrifugal compressors is estimated using Equation 1 which is dependent on volume flow, F, expressed in $\mathrm{m^3\,s^{-1}}$ (R. Smith, 2005). A mechanical efficiency for losses in e.g. bearings and seals is also specified, a value of 98 % is used for all compressors (Kurz et al., 2010).

$$\eta = 0.017 \ln(F) + 0.7 \tag{1}$$

6.5.2 Pump

The block "Pump" is used to model pressure increases. By specifying the outlet pressure as well as pump and driver efficiencies, Aspen Plus calculates the power requirement. For centrifugal pumps, the pump efficiency is dependent on volume flow rate, F expressed as $\mathrm{m^3\,h^{-1}}$ in Equation 2 (R. Smith, 2005). The driver efficiency compensates for losses in the electrical motor which converts electrical energy to mechanical energy. A value of 90 % is assumed for the driver efficiency and applies to all pumps (Evans, 2010).

$$\eta = -0.01(\ln F)^2 + 0.15 \ln(F) + 0.3 \tag{2}$$

6.5.3 Valve

Valves are modelled using the "Valve" block. The model assumes the flow is adiabatic and uses two-phase calculations to determine the outlet condition for the specified pressure.

6.5.4 Flash

For flashes, both vertical and horizontal, the "Flash2" block is used. This model performs rigorous two-phase calculation. The model assumes that sufficient vapour disengagement space is present, meaning that the gas stream leaving the flash does not contain any liquid and vice versa.

6.5.5 Mixer and Splitter

The "Mixer" block combines several streams into one and performs adiabatic phase equilibrium flash calculation to determine the outlet conditions. The "FSplit" block divides an ingoing stream into two or more outlet streams with same compositions and conditions as the inlet. The sizes of the streams are determined from a specified split fraction.

6.5.6 Heater and cooler

Both heaters and coolers are modelled using the "Heater" block. By specifying outlet temperature and pressure, "Heater" calculates the heating or cooling demand. Two-

phase flash calculations are carried out to determine the outlet conditions of the fluid.

6.5.7 Selector

The ”Selector” block does not have any real process equipment counterpart and is only used to choose which of the inlet streams connected to the block that is to be copied to the outlet.

7 Results and discussion

This chapter presents the results obtained from the simulations of the capture processes and how these result affect the overall material and energy balance of the pulp mill and consequently the cost of CO_2 capture.

7.1 Utility consumption of the capture processes

For each process simulated in Aspen Plus a utility demand for heating, cooling and electricity is obtained. Depending on whether heat has to be added or removed, and at which temperature levels, different utilities have to be used. Table 17 summarizes the utility consumption for the processes. The refrigeration duty in the table is the amount of cooling needed below 15 °C, for cooling at higher temperatures cooling water is used. The LP-steam is the amount of heat needed below 139 °C and the amount of MP-steam is the amount of heat needed between 139-186 °C. To minimize the utility demand of the processes pinch analysis is used. Details regarding pinch analysis and the resulting heat exchanger networks for the processes are found in Appendix B. All process equipment for each case is dimensioned, including pumps needed to overcome pressure drops, results are found in Appendix C. Table 17 presents the utility consumption for the processes after pinch analysis and dimensioning has been carried out.

Table 17: Utility consumption of the processes for both capture (CCS) and without capture (NC).

	RB-M		BLGCC-S		BLGMF-R	
Utility [MW]	**NC**	**CCS**	**NC**	**CCS**	**NC**	**CCS**
MP-Steam	0	0	12.9	12.9	0	0
LP-Steam	0	94.1	0	0	10.3	10.3
Cooling water	0	111.4	15.5	22.5	2.0	4.3
Refrigeration	0	0	0	0	11.9	11.9
Electricity	0	9.0	2.4	9.3	3.5	4.9

As explained in Appendix H, refrigeration duty is met by supplying electricity and cooling water to the refrigeration cycle. Hence, the actual utility demand of the process can be quantified as steam, cooling water and electricity. In Figure 18, 19 and 20 the actual utility demand for the capture case is compared to the corresponding case without capture for the three processes. It is important to consider that the MEA process is applied to the flue gases and thereby handles a gas flow which is about five times larger than for the Rectisol and Selexol process.

The RB-M-scenario shows large differences in utility demand between the capture case and the case without capture, see Figure 18. This is not surprising as the case without capture corresponds to the situation at the pulp mill today, hence no additional utilities are needed.

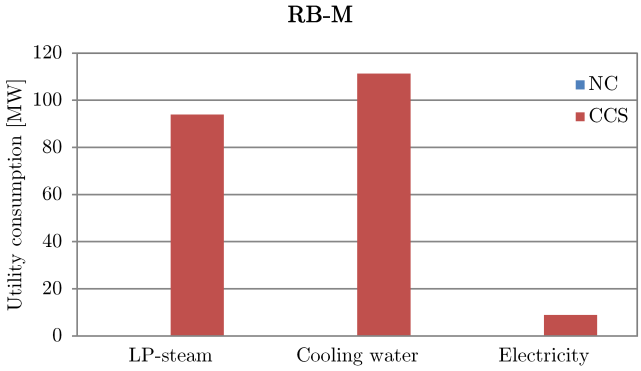

Figure 18: Utility consumption of the MEA process.

As illustrated in Figure 19, the BLGCC-S-scenario also has a considerable difference in both cooling water and electricity consumption. This is due to the removal of the top-cycle and the compression section in the case without capture. The steam demand is essentially unchanged as the reboiler duty in bottom-cycle is constant for both cases.

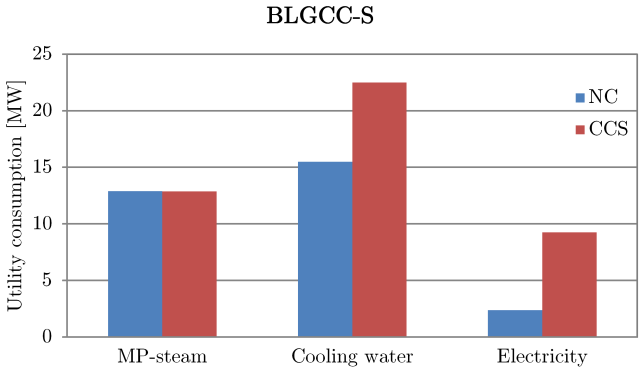

Figure 19: Utility consumption of the Selexol process.

For the BLGMF-R-scenario presented in Figure 20, the difference between the two cases is marginal. The difference stems from the removal of the compression section in the case without capture.

If the capture cases of the BLGCC-S- and BLGMF-R-scenarios are compared, it can be observed that the utility demands are essentially equal. The Selexol process has slightly lower electricity demand compared to the Rectisol process, but uses MP-steam instead of LP-steam. However, the use of MP-steam would outweigh the lower electricity demand. The reason is that usage of MP-steam implies a loss in electricity, since this steam cannot be expanded to LP-steam and produce electricity. Thus, if only utility demand is considered then the Rectisol process would be the preferred alternative also for the BLGCC-S-CCS-case, but by a very small margin. However, literature reports that the Selexol process is the economically

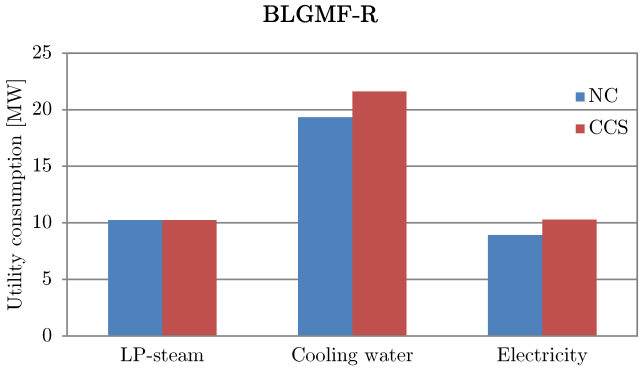

Figure 20: Utility consumption of the Rectisol process.

preferred alternative where applicable. One reason that the utility demand of the two processes is more alike than literature suggest could be that the simulation of the Selexol process overestimates the utility consumption due to unreasonable high reboiler temperature, see Section 6.3.1.

The difference in utility consumption between the capture case and the case without capture divided by the amount of CO_2 captured, is presented in Table 18. The table consequently presents the additional utility demand associated with capturing one kilo of CO_2. From this table it can be seen that the RB-M-scenario has the highest utility consumption per kilo CO_2 captured whereas the other two scenarios have seemingly low consumption, with the exception of the BLGCC-S-scenarios electricity demand.

Table 18: The additional utility consumption per kilo CO_2 captured for the three scenarios.

Utility [kJ/kgCO_2]	**RB-M**	**BLGCC-S**	**BLGMF-R**
LP-Steam	3760	0	0
Cooling water	4460	1130	370
Electricity	360	1110	220

7.2 Overall energy and mass balance

The previous section gives a good indication regarding which scenario that have the lowest cost of capturing CO_2. However, the results do not give the full picture as the utilities cannot be directly compared in terms of costs. This is due to the different assumptions the three scenarios are valid under. Electricity is e.g. sold and bought at different prices and the cost of steam differs depending on whether the pulp mill has a deficit or surplus of steam. To handle these differences an overall balance of the pulp mill, including the major in and outflows of energy and mass, has been constructed for all six cases, see Figure 21-26. For detailed information of the calculation procedure see Appendix D.

When the two cases presented in Figure 21 and 22 are compared it can be noticed that the capture case requires more solid wood fuel. The reason is that the capture process requires a considerable amount of LP-steam and to satisfy this demand more solid wood fuel has to be combusted to produce steam. The biofuel boiler produces HP-steam which is expanded to the needed LP-steam. Consequently the electricity production increases as well. This is a necessity as the capture case has larger electricity consumption. However, the increase in production is greater, resulting in a larger surplus that can be sold.

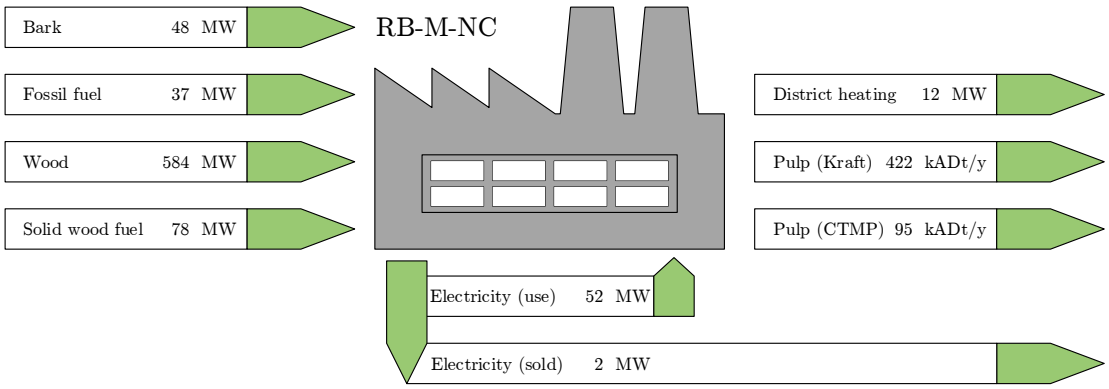

Figure 21: Overall balance displaying major in and out streams to the pulp process for the RB-M-NC-case. For better overview, pulp and CO_2 flows are presented on a yearly basis.

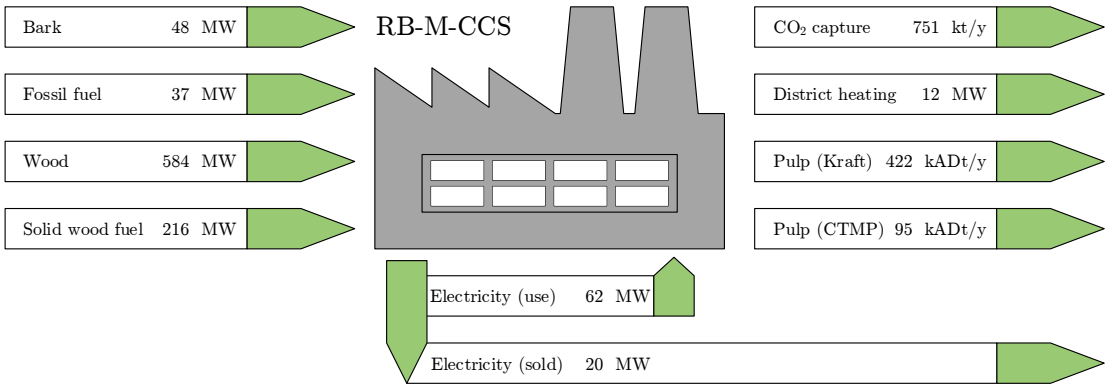

Figure 22: Overall balance displaying major in and out streams to the pulp process for the RB-M-CCS-case. For better overview, pulp and CO_2 flows are presented on a yearly basis.

The overall balance of the two BLGCC-S-cases, illustrated in Figure 23 and 24, differs from the balance of today's pulp mill i.e. the RB-M-NC-case. There is an increase in fossil fuel usage, since the BLGCC-S-scenario results in higher caustization load and thereby more fuel is needed in the lime kiln. Also the pulp production rate increases because of the use of polysulfide cooking liquors.

Regarding differences between the two BLGCC-S-cases, one can see that the capture process is electricity demanding and hence, the electricity surplus is decreased. The capture process changes the composition of the syngas entering the gas turbine and consequently the produced electricity is slightly lower. Another effect is that the flue gas flow is smaller and less heat can be extracted in the HRSG resulting in a slight increased need of solid wood fuel to satisfy the steam demand.

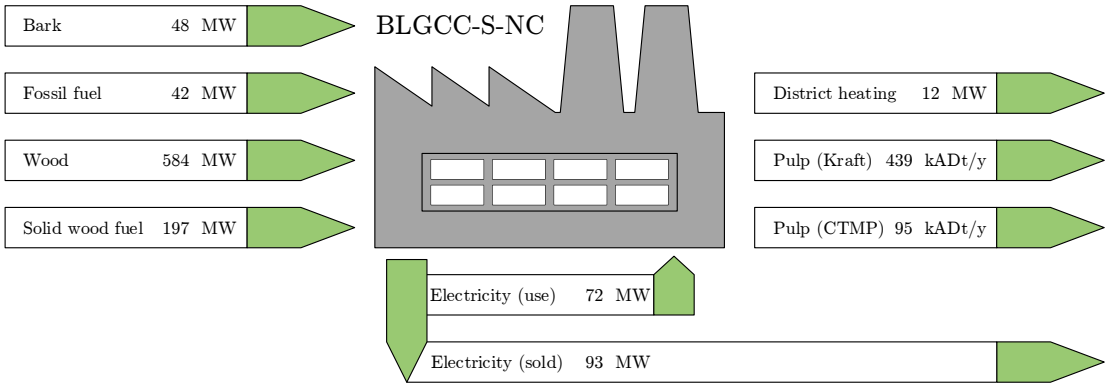

Figure 23: Overall balance displaying major in and out streams to the pulp process for the BLGCC-S-NC-case. For better overview, pulp and CO_2 flows are presented on a yearly basis.

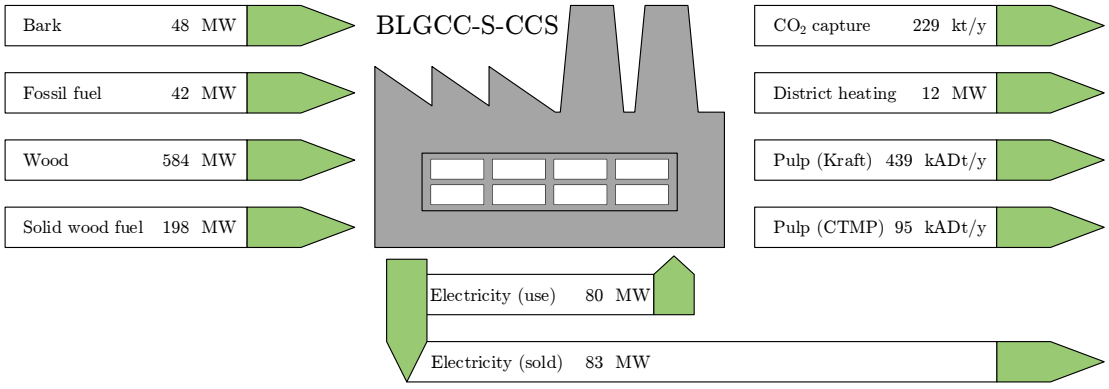

Figure 24: Overall balance displaying major in and out streams to the pulp process for the BLGCC-S-CCS-case. For better overview, pulp and CO_2 flows are presented on a yearly basis.

The BLGMF-R-cases, presented in Figure 25 and 26, have for the same reason as the BLGCC-S-cases an increased usage of fossil fuel as well as an increased pulp production rate. Another major difference for the BLGMF-R-cases compared to today's pulp mill, RB-M-NC-case, is a much higher need for solid wood fuel. The reason is that much of the energy contained in the black liquor is not used to satisfy the need for either heat or electricity but instead leaves the system in the form of DME. Hence, additional fuel and electricity has to be purchased from an external source to satisfy the demand.

If the two BLGMF-R-cases are compared, it becomes clear that they are identical with the exception that the capture case consumes marginally more electricity. That is the electricity needed for compressing the CO_2.

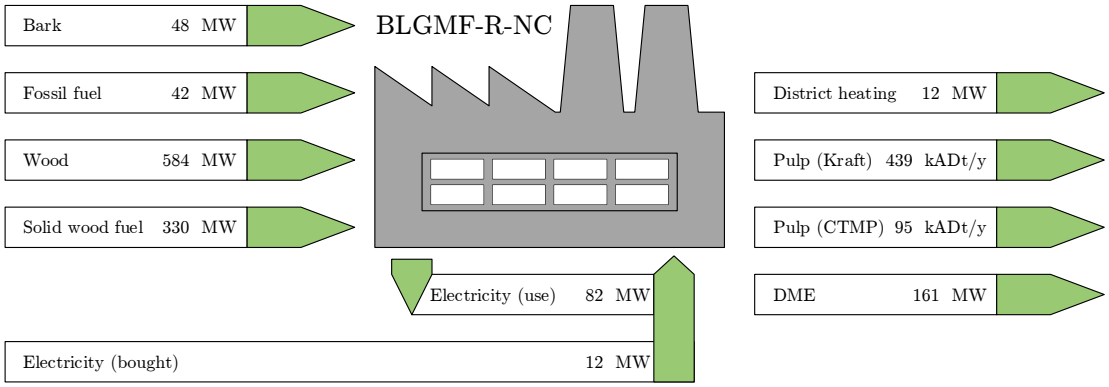

Figure 25: Overall balance displaying major in and out streams to the pulp process for the BLGMF-R-NC-case. For better overview, pulp and CO_2 flows are presented on a yearly basis.

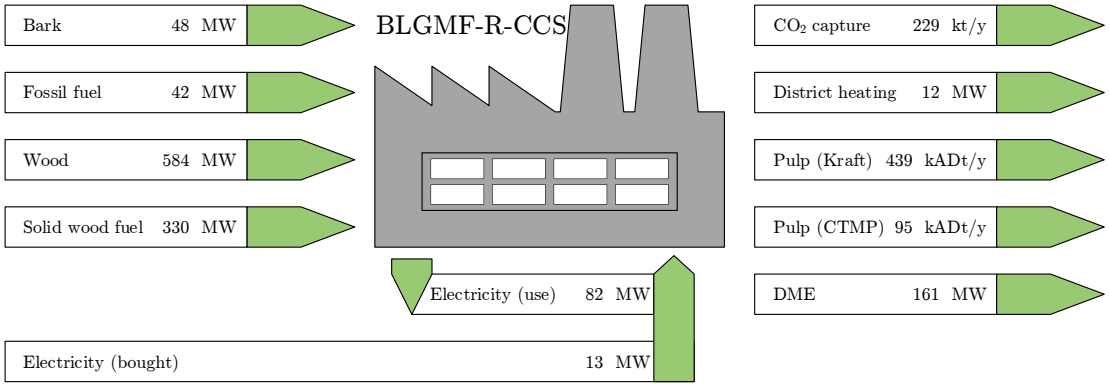

Figure 26: Overall balance displaying major in and out streams to the pulp process for the BLGMF-R-CCS-case. For better overview, pulp and CO_2 flows are presented on a yearly basis.

7.3 Potential of BECCS

From the information obtained in the calculations of the overall mass and energy balance, the total CO_2 emissions can be calculated. The pulp mills influence on the global CO_2 emissions for the RB-M-CCS-case is presented in Figure 27. The figure is divided into two categories. The first represent reduction of emissions and includes captured CO_2 but also substitution of electricity partially produced from fossil fuels. The substituted electricity is assumed to be a Nordic electricity mix, see Appendix D for more information regarding this assumption. The other category is the pulp mills gross emissions of CO_2 from various sources. If the emissions stem from fossil fuel it is coloured black and emissions originating from biofuels are coloured green. Biofuels are considered climate neutral since trees absorbs CO_2 as they grow. Hence, the global effect the pulp mill has on CO_2 emissions is the difference between the reduction of emissions and the emissions originating from fossil fuels. The RB-M-CCS-case has a net reduction of 715 $ktCO_2$/year, that corresponds to 1.39 tCO_2/ADtPulp.

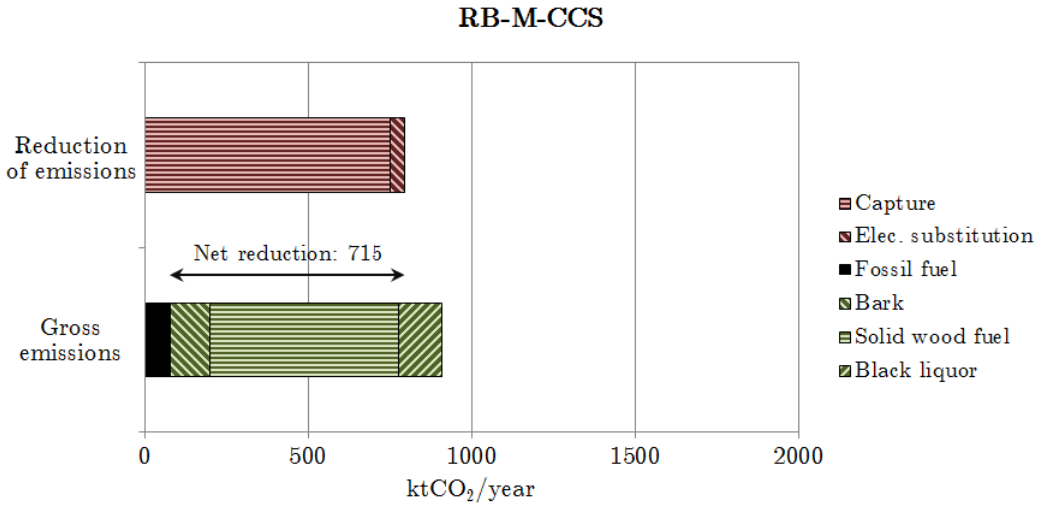

Figure 27: Reduction of emissions and gross emissions for the RB-M-CCS-case. The net reduction of global CO_2 emissions is illustrated by the arrow.

Figure 28 illustrates the effect the BLGCC-S-CCS-case has on global CO_2 emissions. This case has a lower capture rate compared to the RB-M-CCS-case, since the CO_2 is separated before the gas turbine in which additional CO_2 is formed and then vented to the atmosphere. The CO_2 is climate neutral since it originates from the black liquor. However, this highlights the drawback of the pre-combustion approach; that less CO_2 can potentially be captured. The lower capture rate is partially compensated for, by having a larger amount of substituted electricity from fossil fuel. The BLGCC-S-CCS-case has a lower potential effect of applying BECCS as the global net reduction is 318 $ktCO_2$/year, which corresponds to 0.60 tCO_2/ADtPulp.

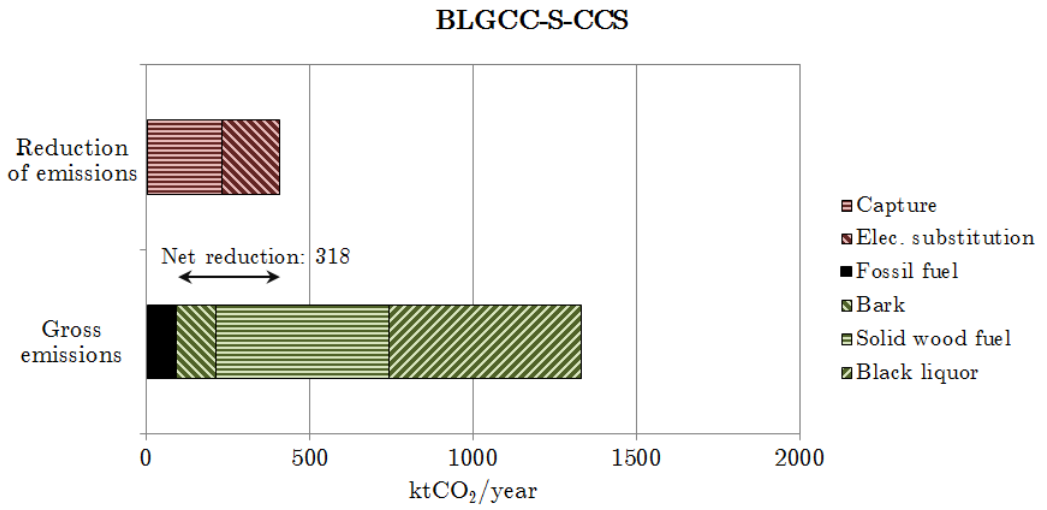

Figure 28: Reduction of emissions and gross emissions for the BLGCC-S-CCS-case. The net reduction of global CO_2 emissions is illustrated by the arrow.

The effect the BLGMF-R-CCS-case has on global CO_2 emissions is illustrated in Figure 29. This case captures the same amount of CO_2 as the BLGCC-S-CCS-case but instead of selling electricity, it is bought from the Nordic market which increases global CO_2 emissions. However, the produced DME is used in trucks which otherwise would have used diesel originating from fossil fuels, see Appendix D. Hence, this causes a large reduction of CO_2 emissions. Consequently the BLGMF-R-CCS-case reaches a better effect on global CO_2 emissions when applying BECCS than the BLGCC-S-CCS-case. The net reduction is is 393 $ktCO_2$/year, which corresponds to 0.76 tCO_2/ADtPulp.

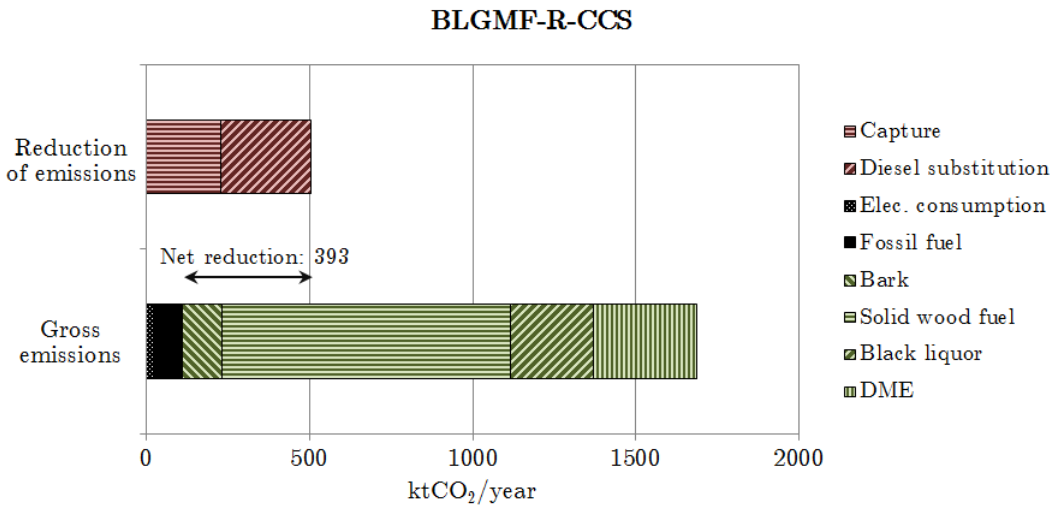

Figure 29: Reduction of emissions and gross emissions for the BLGMF-R-CCS-case. The net reduction of global CO_2 emissions is illustrated by the arrow.

7.4 Cost of carbon capture

By comparing the two overall balances for each scenario it is possible to quantify the cost of carbon capture in the form of additional amount of purchased solid wood fuel, cooling water and sold or bought electricity. The result of such a comparison is summarized in Table 19.

Table 19: The additional resource consumption per kilo CO_2 captured for the three scenarios.

Utility [kJ/kgCO_2]	**RB-M**	**BLGCC-S**	**BLGMF-R**
Solid wood fuel	5510	170	0
Cooling water	4460	1130	370
Electricity	-700	1360	220

A remark regarding electricity is that both the RB-M- and BLGCC-S-scenario have a surplus of electricity which is sold whereas the BLGMF-R-scenario has to purchase electricity to cover a deficit. Thus, the values in Table 19 should be interpreted as follows: applying carbon capture to the RB-M-scenario increases the sold electricity by 700 kJ/kgCO_2, the BLGCC-S-scenario decreases the sold electricity by 1360 kJ/kgCO_2 and in the BLGMF-R-scenario 220 kJ/kgCO_2 additional electricity has to be bought. It is important to distinguish between sold and bought electricity as they are priced differently. All resources listed in Table 19 can be priced and thereby, it is possible to calculate an operating cost for CO_2-capture. However, to calculate the total cost of CO_2-capture the investment cost of the capture processes has to be taken into account. Table 20 presents the investment cost for the six cases.

Table 20: Investment cost for the capture processes, provided by Skagestad & Eldrup (2014).

Investment cost [MSEK]	**RB-M**	**BLGCC-S**	**BLGMF-R**
CCS	659	656	380
NC	0	226	299

From the difference in investment cost between the case with capture and the case without capture, an annual payback cost is calculated. Table 21 shows the annual cost for carbon capture divided into different contributions. Costs for maintenance and salaries for operators and engineers were provided by Skagestad & Eldrup (2014).

The RB-M-scenario has the highest total annual cost, three times higher than the BLGCC-S-scenario. Each of the seven cost categories surpasses the other scenarios. The reason for this is that the MEA process handles a larger gas flow and hence will have both higher operating and investment cost. However, this also implies that the RB-M-scenario captures more CO_2. Consequently the specific cost of carbon capture is lower than for the BLGCC-S-scenario. It is hardly surprising that the BLGMF-R-scenario has the lowest capture cost since only the compression section is

Table 21: The cost of carbon capture for the three scenarios, divided into contribution of different categories. All costs are specified in MSEK/year.

Scenario	**RB-M**	**BLGCC-S**	**BLGMF-R**
Investment cost	60.0	39.1	7.4
Maintenance	23.2	15.2	2.9
Operators	13.2	0	0
Engineers	5.4	0	0
Solid wood fuel	229.8	2.2	0
Cooling water	63.9	4.9	1.6
Electricity	-72.0	42.4	8.2
Total cost [MSEK/year]	323.5	103.8	20.0
Specific cost [SEK/tCO_2]	431	453	88

added for the capture case. In Mars 2014 the price of a emission certificate was 5.0 €. If the capture cost for the of BLGMF-R-scenario, 88 SEK/tCO_2 corresponding to 9.7 €/tCO_2, is compared with the price of an emission certificate it can be concluded that carbon capture is not profitable. However, the BLGMF-R-scenario will not likely be implemented before several years have passed and by then the price level of emission certificates may have recovered. Hence, the pulp mill has the potential to be a profitable carbon capture and storage alternative in the future.

7.5 Sensitivity analysis

The largest contribution to the total annual cost in Table 21 is the electricity, with the exception of the solid wood fuel for the RB-M-scenario. However, the solid wood fuel price has held a steady level during the last few years and therefore, the electricity price was varied in a sensitivity analysis to evaluate its impact on the capture cost in the three scenarios (Swedish Energy Agency, 2014). Another reason is that the electricity price is harder to predict and even varies over the seasons of the year. Table 22 presents the electricity prices used in the sensitivity analysis. Both an increase and decrease of 30 % have been considered.

Table 22: Electricity price used in the sensitivity analysis.

Price [SEK/MWh]	**-30%**	**0%**	**+30%**
Sold	343	490	637
Bought	413	590	767

Figure 30 illustrates the result of the sensitivity analysis. A higher electricity price means a decreased cost for the RB-M-scenario, as the additional electricity sold generates a higher income. For the BLGCC-S-scenario, the penalty due to less

electricity sold is higher when the price goes up. Finally the BLGMF-R-scenario also experiences higher costs for an increased electricity price, since the purchased electricity is more expensive. For the case where electricity price decreases by 30 % the BLGCC-S-scenario actually has a lower capture cost than the RB-M-scenario. This shows that it cannot with certainty be determined which of the two scenarios that would have the highest capture cost, as the electricity price might vary within the 30 %-range. Pre-combustion capture with the BLGMF-R-scenario is undisputedly the most promising scenario regardless the price level of the electricity.

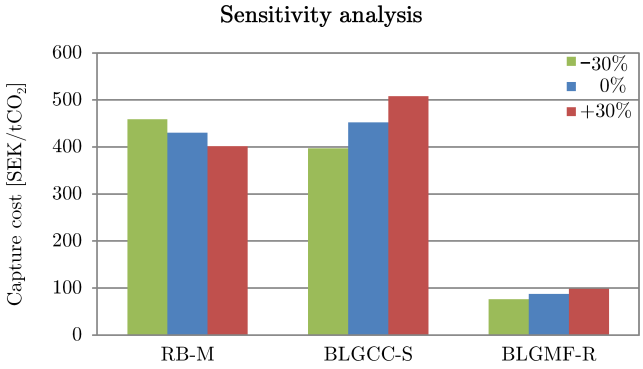

Figure 30: Sensitivity analysis with respect to the influence of the electricity price. The base case is compared to an increase and decrease by 30 %.

8 Conclusions

This thesis evaluates the possibility of applying carbon capture and storage onto a pulp mill. Three scenarios regarding the future development of the pulp mill is examined.

The first scenario assumes that the pulping process remains unaltered and hence uses the conventional recovery boiler to regenerate the cooking chemicals. For this scenario, post combustion capture using the MEA process was studied. The simulations resulted in a high utility consumption, especially regarding steam and cooling water. However, the overall balance showed that when producing the extra required stream, additional electricity was generated. Consequently more electricity could be sold and this reduced the cost of carbon capture. The cost of CO_2-capture was 431 SEK/tCO_2. The potential effect of applying BECCS was highest of the three scenarios with a net reduction of global CO_2 emissions by 715 ktCO_2/year.

In the second scenario black liquor gasification technology is used and the produced syngas is utilized for electricity production. The Selexol process was determined to be the most suitable capture process. The calculations resulted in rather low additional resource consumption, with the exception of electricity usage. Consequently the electricity consumption constitutes the major part of the CO_2-capture cost of 453 SEK/tCO_2. This was the most expensive of the three scenarios and also the potential effect of applying BECCS had the worst performance with a net reduction of global CO_2 emissions by only 318 ktCO_2/year.

Black liquor gasification technology is also used for the third scenario, but the syngas is instead utilized in DME production. The capture process used in this scenario is the Rectisol process. The additional resource consumption associated with CO_2-capture was shown to be the lowest of the three scenarios, resulting in a cost of only 88 SEK/tCO_2. The potential effect on global CO_2 emission for this scenario is a net reduction of 393 ktCO_2/year.

A sensitivity analysis was conducted to test the robustness of the results. The uncertainty of the electricity price greatly affects the results and thus this parameter was varied. The sensitivity analysis showed that for a decrease of the electricity price by 30 %, the scenario using the MEA process had a slightly higher capture cost than the scenario utilising the Selexol process. However, the scenario using the Rectisol process was superior regardless the pricing of electricity.

To conclude this thesis, the result implies that the pulp and paper industry could be a suitable future candidate to which BECCS can be applied. The cost penalty associated with carbon capture proved to be too high in the present day situation; with an over-abundance of low price emission certificates. However if the emission certificate market recovers, there would be an incentive for capturing CO_2 in the scenario utilizing the Rectisol process.

9 Future work

The RB-M-scenario only considers the flue gases originating from the recovery boiler, but since this scenario applies the post-combustion approach it would be possible to capture the flue gases from the biofuel boiler as well. This was not included in the thesis since sufficient process data regarding these flue gases was not available. To look into the consequences of this process alteration would be a suitable future work. This alteration would probably reduce the cost of carbon capture since the investment cost of a process usually does not increase linearly with increased capacity. It would also increase the potential net reduction in global CO_2 emissions.

To put the result in context, it would be interesting to look at it in the light of future energy market scenarios. These scenarios would have different price levels of e.g. emission certificates. It would thereby be possible to evaluate if the capture scenarios simulated in this thesis would be economically viable depending on the future development of the energy market.

10 References

Anderberg, K. (2010). *Evaluation of the efficiency of the Recovery boiler and Biofuel boiler at Smurfit Kappa Kraftliner in Piteå* (Tech. Rep.). Lund University, Lund.

Anderson, G. (1969). Successful recovery boiler combustion safeguard systems. *IEEE Transactions on Industry and General Applications*, *IGA-5*(2), 204–207.

Aspen Technology. (2010). *Aspen Physical Property System - Physical Property Methods* (Software documentation). Burlington: Aspen Technology.

Aspen Technology. (2012a). *Aspen Polymers Model of the CO2 Capture Process by DEPG* (Software documentation). Burlington: Aspen Technology.

Aspen Technology. (2012b). *Rate-Based Model of the CO2 Capture Process by MEA using Aspen Plus* (Software documentation). Burlington: Aspen Technology.

Aspen Technology. (2012c). *Rate-Based Model of the CO2 Capture Process by MEOH using Aspen Plus* (Software documentation). Burlington: Aspen Technology.

Bajpai, P. (2014). *Black Liquor Gasification* (1st ed.). London: Elsevier.

Bougie, F. & Iliuta, M. C. (2012). Sterically Hindered Amine-Based Absorbents for the Removal of CO2 from Gas Streams. *Journal of Chemical & Engineering Data*, *57*(3), 635–669.

Breckenridge, W., Holiday, A., Ong, J. O. Y. & Sharp, C. (2000). Use of SELEXOL® Process in Coke Gasification to Ammonia Project. In *Laurance reid gas conditioning conference.* Oklahoma, USA, February 27 - March 1.

Çöpür, Y. (2007). Refining of Polysulfide Pulps. *Journal of Applied Sciences*, *7*(2), 280–284.

Chemrec. (2011). *Technology.* Retrieved 2014, March 15, from `http://www.chemrec.se/Technology.aspx`

Consonni, S., Katofsky, R. E. & Larson, E. D. (2009). A gasification-based biorefinery for the pulp and paper industry. *Chemical Engineering Research and Design*, *87*(9), 1293–1317.

Consonni, S., Larson, E. D., Kreutz, T. G. & Berglin, N. (1998). Black Liquor Gasifier/Gas Turbine Cogeneration. *Journal of Engineering for gas turbines and power*, *120*(3), 442–449.

Dahlquist, E. (Ed.). (2013). *Technologies for Converting Biomass to Useful Energy: Combustion, Gasification, Pyrolysis, Torrefaction and Fermentation.* Boca Raton: CRC Press.

Davison, J. & Thambimuthu, K. (2005). Technologies for capture of carbon dioxide. *Greenhouse Gas Control Technologies*, *7*, 3–13.

Ek, M., Gellerstedt, G. & Henriksson, G. (Eds.). (2009a). *The Ljungberg Textbook (Volume 1): Wood Chemistry and Wood Biotechnology.* Walter de Gruyter & Company.

Ek, M., Gellerstedt, G. & Henriksson, G. (Eds.). (2009b). *The Ljungberg Textbook (Volume 2): Pulping Chemistry and Technology.* Walter de Gruyter & Company.

Ekbom, T., Berglin, N. & Lögdberg, S. (2005). *Black liquor gasification with motor fuel production–BLGMF II: A Techno-Economic Feasibility Study on Catalytic Fischer-Tropsch Synthesis for Synthetic Diesel Production in Comparison with Methanol and DME as Transport Fuels* (P21384-1). Stockholm: Nykomb Synergetics AB.

European Commission. (2013). *Quarterly Report on European Electricity Markets* (Second quarter). Brussel: European Commission.

European Council. (1996). *1939th Council Meeting - Environment - Brussels, 25 and 26 June 1996.* Retrieved 2014, March 29, from `http://europa.eu/rapid/press-release_PRES-96-188_en.htm?locale=en`

European Environment Agency. (2011). *The European Pollutant Release and Transfer Register.* Retrieved 2014, March 27, from `http://prtr.ec.europa.eu/IndustialActivity.aspx`

Evans, J. (2010). *Centrifugal Pump Efficiency - What, How, Why & When?* Retrieved 2014, May 9, from `http://pump-flo.com/pump-library/pump-library-archive/joe-evans,-phd/centrifugal-pump-efficiency-what,-how,-why-when.aspx`

Field, R. P. & Brasington, R. (2011a). Baseline Flowsheet Model for IGCC with Carbon Capture. *Industrial & Engineering Chemistry Research*, *50*(19), 11306–11312.

Field, R. P. & Brasington, R. (2011b). Baseline Flowsheet Model for IGCC with Carbon Capture (Documentation of Simulation Model GEE _ BIT _ SEL _ wCC _ NOSF). *Industrial & Engineering Chemistry Research*, *50*(19), 11306–11312.

Gadek, M., Kubica, R. & Jedrysik, E. (2013). Production of Methanol and Dimethyl ether from biomass derived syngas – a comparison of the different synthesis pathways by means of flowsheet simulation. In *23rd european symposium on computer aided process engineering.* Lappeenranta, Finland, June 9-12.

Gatti, M., Marechal, F., Martelli, E. & Consonni, S. (2013). Thermodynamic Analysis, Energy Integration and Flowsheet Improvement of a Methanol Absorption Acid Gas Removal Process. *Chemical Engineering Transactions*, *35*, 211–216.

Gebart, B. R., Westerlund, L., Nordin, A., Backman, R., Warnqvist, B., Richards, T., ... Landälv, I. (2005). Black liquor gasification - The fast lane to the biorefinery. In *Risoe international energy conference.* Risoe, Denmark, May 23-25.

Gebart, B. R., Wiinikka, H., Marklund, M., Carlsson, P., Grönberg, C., Weiland, F., ... Öhrman, O. (2011). Recent advances in the understanding of pressurized black liquor gasification. *Cellulose Chemistry and Technology*, *45*(7-8), 521–526.

Gibbins, J. & Chalmers, H. (2008). Carbon capture and storage. *Energy Policy*, *36*(12), 4317–4322.

Grace, T. M. (2008). Recovery Boiler Saftey and Audits. In *Tappi kraft recovery course.* St. Petersburg, USA, January 7-10.

Heat and Power Technology. (2013). *Guide-Lines for Tutorials on Cost-Effective and Energy Efficient Process Design - Case Study: MEK Production* (Course material in: Preliminary Plant Design). Göteborg: Chalmers University of Technology.

Hektor, E. (2008). *Post-combustion CO2 capture in kraft pulp and paper mills - Technical, economic and system aspects* (Ph.D. Thesis). Chalmers University of Technology, Göteborg.

IEA. (2007). *Tracking Industrial Energy Efficiency and CO2 Emissions - In Support of the G8 Plan of Action* (IEA Report). Paris: International Energy Agency.

IEA. (2013). *CO2 emissions from fuel combustion - Highlights, 2013 Edition* (IEA Statistics Report). Paris: International Energy Agency.

IPCC. (2005). *Carbon dioxide capture and storage* (IPCC Special Report). New York: Cambridge University Press.

IPCC. (2007). *Climate Change 2007, Mitigation of Climate Change* (Contribution of Working Group III to the Fourth Assessment Report of the IPCC). New York: Cambridge University Press.

Jilvero, H. (2014). *Personal communication, April 11.*

Ju, F., Chen, H., Ding, X., Yang, H., Wang, X., Zhang, S. & Dai, Z. (2009). Process simulation of single-step dimethyl ether production via biomass gasification. *Biotechnology advances*, *27*(5), 599–605.

Khartchenko, N. V. (1998). *Advanced Energy Systems.* Washington, DC: Taylor & Francis.

Korens, N., Simbeck, D. R. & Wilhelm, D. J. (2002). *Process screening analysis of alternative gas treating and sulfur removal for gasification* (Task Order No. 739656-00100). Mountain View: SFA Pacific, Inc.

Kothandaraman, A. (2010). *Carbon dioxide capture by chemical absorption: a solvent comparison study* (Ph.D. Thesis). Massachusetts Institute of Technology, Cambridge.

Kubek, D. I., Polla, E. & Wilcher, F. P. (2000). *Purification and recovery options for gasification* (Form No: 170-01448-0904). Des Plaines: UOP.

Kurz, R., Winkelmann, B. & Mokhatab, S. (2010). Efficiency and Operating Characteristics of Centrifugal and Reciprocating Compressors. *Pipeline and Gas Journal*, *237*(10).

Lindblom, M. & Landälv, I. (2007). Chemrec's Atmospheric & Pressurized BLG (Black Liquor Gasification) Technology – Status and Future Plans. In *2007 international chemical recovery conference.* Quebec City, Canada, May 29 - June 1.

Linde Process Plants Inc. (2012). *Sulfur Process Technology* (Brochure). Oklahoma: The Linde Group.

Lindström, M., Naithani, V., Jameel, H. & Kirkman, A. (2006). The Effect of Integrating Polysulfide Pulping and Black Liquor Gasification on Pulp Yield and Deliginification. In *2006 tappi engineering, pulping & environmental conference.* Atlanta, USA, November 6-8.

Marchionna, M., Patrini, R., Sanfilippo, D. & Migliavacca, G. (2008). Fundamental investigations on di-methyl ether (DME) as LPG substitute or make-up for domestic uses. *Fuel Processing Technology*, *89*(12), 1255–1261.

Maxwell, G. (2004). *Synthetic Nitrogen Products: A Practical Guide to the Products and Processes.* New York: Springer.

Moldenhauer, P., Rydén, M. & Lyngfelt, A. (2012). Testing of minerals and industrial by-products as oxygen carriers for chemical-looping combustion in a circulating fluidized-bed 300W laboratory reactor. *Fuel*, *93*, 351–363.

Mölndal Energi AB. (2012). *Elens Ursprung.* Retrieved 2014, May 29, from `http://www.molndalenergi.se/ELHANDEL/Elochmiljö/Elensursprung/tabid/494/language/sv-SE/Default.aspx`

Munder, B., Grob, S. & Fritz, P. M. (2010). Selection of Wash Systems for Sour Gas Removal. In *4th international freiberg conference on igcc & xtl technologies.* Dresden, Germany, May 3-5.

Ohno, Y., Yoshida, M., Shikada, T., Inokoshi, O., Ogawa, T. & Inoue, N. (2006). *New Direct Synthesis Technology for DME (Dimethyl Ether) and Its Application Technology* (JFE Technical Report No. 8). Tokyo: JFE Holdings, Inc.

Pettersson, K. (2011). *Black Liquor Gasification-Based Biorefineries – Determining Factors for Economic Performance and CO2 Emission Balances* (Ph.D. Thesis). Chalmers University of Technology, Göteborg.

Pettersson, K. (2014). *Personal communication, April 11.*

Pettersson, K. & Harvey, S. (2012). Comparison of black liquor gasification with other pulping biorefinery concepts – Systems analysis of economic performance and CO2 emissions. *Energy*, *37*(1), 136–153.

Salomonsson, P. (2013). *Production of DME from biomass and utilisation of fuel for transport and industrial use.* Retrieved 2014, March 22, from `http://www.biodme.eu/`

SCA Östrands Massafabrik. (2006). *Ny sodapanna och turbin vid Östrands massafabrik.* Retrieved 2014, April 13, from `http://www.sca.com/Global/SCA_Pulp/PDF/Brochures/new_recovery_boiler_and_turbine_se.pdf`

Sinnott, R. & Towler, G. (2009). *Chemical Engineering Design* (5th ed.). Oxford: Elsevier Ltd.

Skagestad, R. & Eldrup, N. H. (2014). *Personal communication, May 30.*

Smith, J. B., Schneider, S. H., Oppenheimer, M., Yohe, G. W., Hare, W., Mastrandrea, M. D., ... van Ypersele, J.-P. (2009). Assessing dangerous climate change through an update of the Intergovernmental Panel on Climate Change (IPCC) "reasons for concern". *Proceedings of the National Academy of Sciences of the United States of America*, *106*(11), 4133–4137.

Smith, R. (2005). *Chemical Process Design and Integration.* Chichester: John Wiley & Sons Ltd.

Stigsson, L. & Berglin, N. (1999). Black Liquor Gasification - Towards Improved Pulp and Energy Yields. In *The 6th international conference on new available technologies at spci '99.* Stockholm, Sweden, June 1-4.

Sun, L. & Smith, R. (2013). Rectisol wash process simulation and analysis. *Journal of Cleaner Production*, *39*, 321–328.

Swedish Energy Agency. (2012). *The Swedish-Norwegian Electricity Certificate Market* (Annual Report 2012). Stockholm: Swedish Energy Agency.

Swedish Energy Agency. (2013). *Utvecklingen påutsläppsrättsmarknaden 2013 - En beskrivning och analys av den globala utsläppshandeln* (ER 2013:29). Eskilstuna: Swedish Energy Agency.

Swedish Energy Agency. (2014). *Trädbränsle- och torvpriser Nr 1* (Statistiska meddelanden EN 0307 SM 1401). Eskilstuna: Swedish Energy Agency.

Swedish Environmental Protection Agency. (2013). *National Inventory Report Sweden 2013* (Inventory Report). Stockholm: Swedish Environmental Protection Agency.

The Climate Registry. (2013). *Climate Registry Default Emission Factors* (Default Emission Factor Updates). Los Angeles: The Climate Registry.

TRI. (2012). *Customized Deployments.* Retrieved 2014, March 3, from `http://www.tri-inc.net/TRI-inc/Deployments.html`

U.S. Environmental Protection Agency. (2003). *Wood Residue Combusion in Boilers.* Retrieved 2014, May 29, from `http://www.epa.gov/ttn/chief/ap42/ch01/index.html`

Vakkilainen, E. & Ahtila, P. (2011). Modern Method To Determine Recovery Boiler Efficiency. *O PAPEL*, *72*(12), 58–65.

Weiss, H. (1988). Rectisol wash for purification of partial oxidation gases. *Gas Separation & Purification*, *2*(4), 171–176.

A Output stream requirements and results

CO_2-outlet stream

Table 23: The requirements and the results of the simulations for the CO_2-stream ready for sequestration. Spices labelled with an "m" have their composition specified as mole-% and for "p" ppmw is used. A green colour indicates that the requirements are fulfilled and a red colour indicates the opposite.

Case	CO_2 [m]	CO [m]	H_2 [m]	CH_4 [m]	N_2 [m]	H_2O [p]	H_2S [p]	COS [p]	O_2 [p]	Solvent [p]
Requirements	>95	-	-	-	<4	-	<1500	-	<10	-
RB-M-CCS	99.2	0	0	0	0	2956	0	0	14	0
BLGCC-S-CCS	95.1	3.8	0.3	0.1	0.1	315	360	30	20	35
BLGMF-R-CSS	96.4	2.7	0.2	0.2	0	0	343	11	0	378

H_2S-outlet stream

Table 24: The requirements and the results of the simulations for the H_2S-stream entering the Claus process. Spices labelled with an "m" have their composition specified as mole-% and for "p" ppmv is used. A green colour indicates that the requirements are fulfilled and a red colour indicates the opposite.

Case	CO_2 [m]	CO [p]	H_2 [p]	CH_4 [p]	N_2 [m]	H_2O [m]	H_2S [m]	COS [p]	O_2 [m]	Solvent [p]
Requirements	-	-	-	-	-	-	>40	-	-	-
BLGCC-S-NC	24.1	3	1	1	22.8	2.4	50.5	146	0.2	3
BLGCC-S-CCS	24.3	0	0	0	23.1	2.4	50.0	156	0.2	0
BLGMF-R-NC	57.0	0	0	2	0	0	41.6	2598	0	1415
BLGMF-R-CCS	57.0	0	0	2	0	0	41.6	2598	0	1415

Flue gas-outlet for the RB-M-scenario

Table 25: The results of the simulations for the clean flue gas. No requirements are applied to this case, except that 85 % of the CO_2 should be captured, which is also true for the other capture scenarios. Spices labelled with an "m" have their composition specified as mole-% and for "p" ppmv is used.

Case	CO_2 [m]	CO [m]	H_2 [m]	CH_4 [m]	N_2 [m]	H_2O [m]	H_2S [m]	COS [m]	O_2 [m]	Solvent [p]
RB-M-CCS	3.7	0	0	0	74.4	16.0	0	0	5.9	4

Syngas-outlet for the BLGCC-S-scenario

Table 26: The requirements and the results of the simulations for the clean syngas. Spices labelled with an "m" have their composition specified as mole-% and for "p" ppmv is used. A green colour indicates that the requirements are fulfilled and a red colour indicates the opposite.

Case	CO_2 [m]	CO [m]	H_2 [m]	CH_4 [m]	N_2 [m]	H_2O [p]	H_2S [p]	COS [p]	O_2 [p]	Solvent [p]
Requirements	-	-	-	-	-	-	TotS: <20		-	-
BLGCC-S-NC	2.2	43.6	45.5	1.4	7.2	27	15	0.3	336	0.1
BLGCC-S-CCS	17.5	36.7	37.7	1.3	6.8	32	14	4	325	0.2

Syngas-outlet for the BLGMF-R-scenario

Table 27: The requirements and the results of the simulations for the clean syngas. Spices labelled with an "m" have their composition specified as mole-% and for "p" ppmv is used. A green colour indicates that the requirements are fulfilled and a red colour indicates the opposite.

Case	CO_2 [m]	CO [m]	H_2 [m]	CH_4 [m]	N_2 [m]	H_2O [m]	H_2S [p]	COS [p]	O_2 [p]	Solvent [p]
Requirements	<3	-	-	-	-	-	TotS: <0.1		-	-
BLGMF-R-NC	0.2	48.0	49.9	1.6	0.3	0	0.09	0.004	0	20
BLGMF-R-CCS	0.2	48.0	49.9	1.6	0.3	0	0.09	0.004	0	20

B Pinch analysis

Pinch analysis is a structured way of improving existing or creating new heat exchanger networks with an high degree of heat integration. Individual temperature differences are chosen for each type of stream. The following individual temperature differences are used in this work:

- 10 °C for gas streams.
- 5 °C for liquid streams.
- 5 °C for evaporating and condensing streams.

For these condition a pinch point is calculated. The pinch point is where the lowest allowed temperature difference is present. Over the pinch temperature there is a deficit of heat and hot utility is therefore needed. Below the pinch, cold utility is needed as there is an execs of heat. Hence, to minimize utility the three ”golden rules” of pinch analysis should be abided:

- Do not use external cooling above the pinch.
- Do not transfer heat through the pinch.
- Do not use external heating below the pinch.

If these rules are followed an maximum energy recovery heat exchanger network is obtained. However, this may not be the economically most advantages alternative since such an network often requires many units. To obtain an better design the network can be ”relaxed” i.e. the smallest heat exchangers are removed and are replaced with heaters and coolers. This increases utility consumption but gives lower capital cost. Hence, an optimum can be found. In this work no extensive cost analysis has been done to optimize the number of units. Instead, as a rule of thumb, heat exchangers smaller than 100 kW has been removed. The design of the heat exchanger networks for the capture processes are illustrated in the following pages.

RB-M-CCS-case

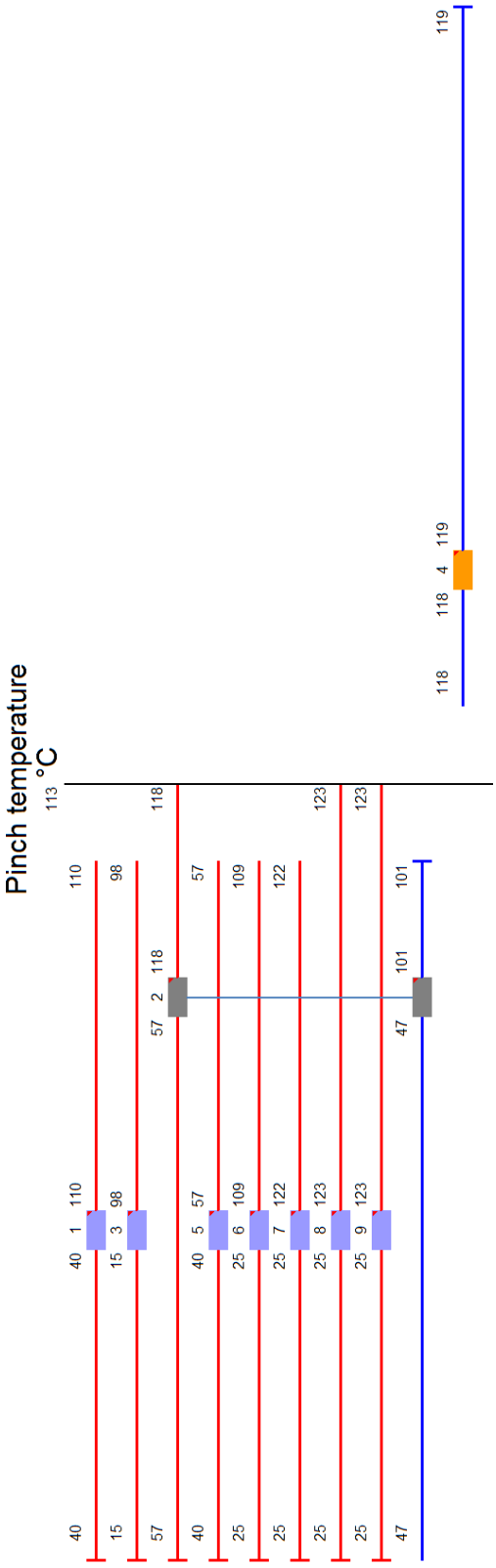

Figure 31: Heat exchanger network constructed in Pro-Pi2 for the RB-M-CCS-case. The numbering of the units match that found in Appendix C.

BLGCC-S-CCS-case

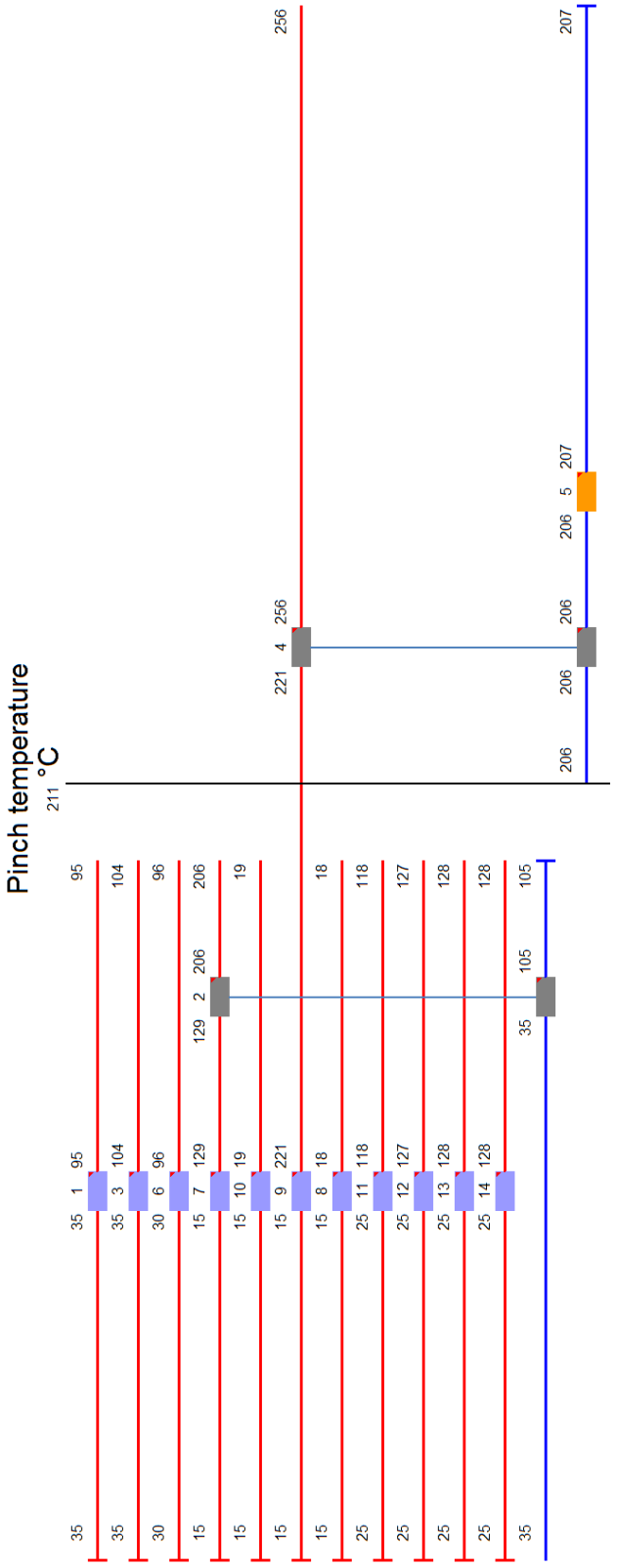

Figure 32: Heat exchanger network constructed in Pro-Pi2 for the BLGCC-S-CCS-case. The numbering of the units match that found in Appendix C.

BLGCC-S-NC-case

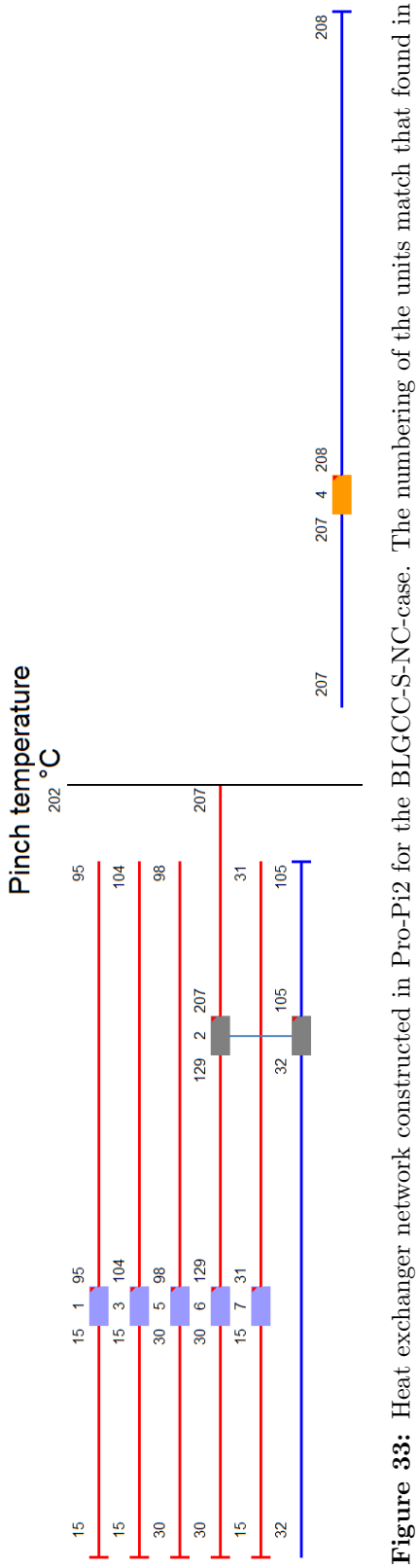

Figure 33: Heat exchanger network constructed in Pro-Pi2 for the BLGCC-S-NC-case. The numbering of the units match that found in Appendix C.

BLGMF-R-CCS-case

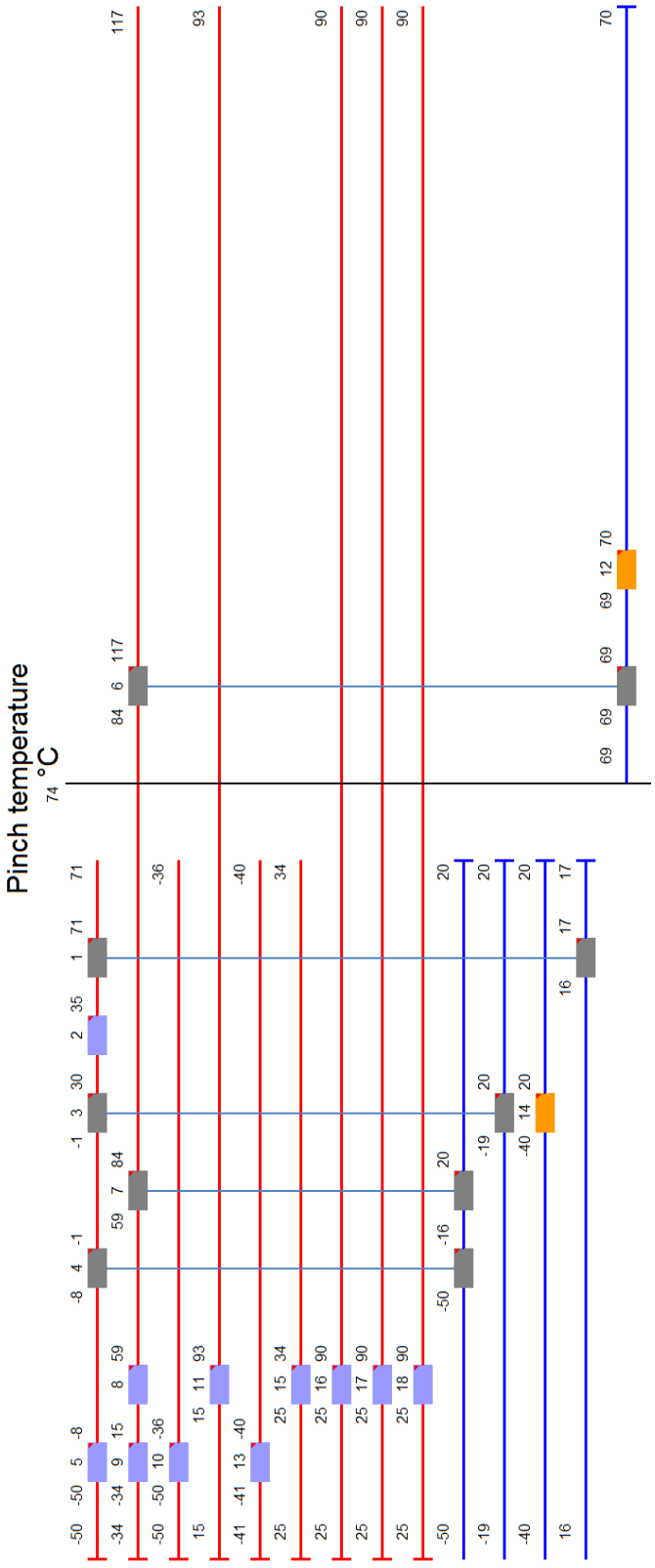

Figure 34: Heat exchanger network constructed in Pro-Pi2 for the BLGMF-R-CCS-case. The numbering of the units match that found in Appendix C.

BLGMF-R-NC-case

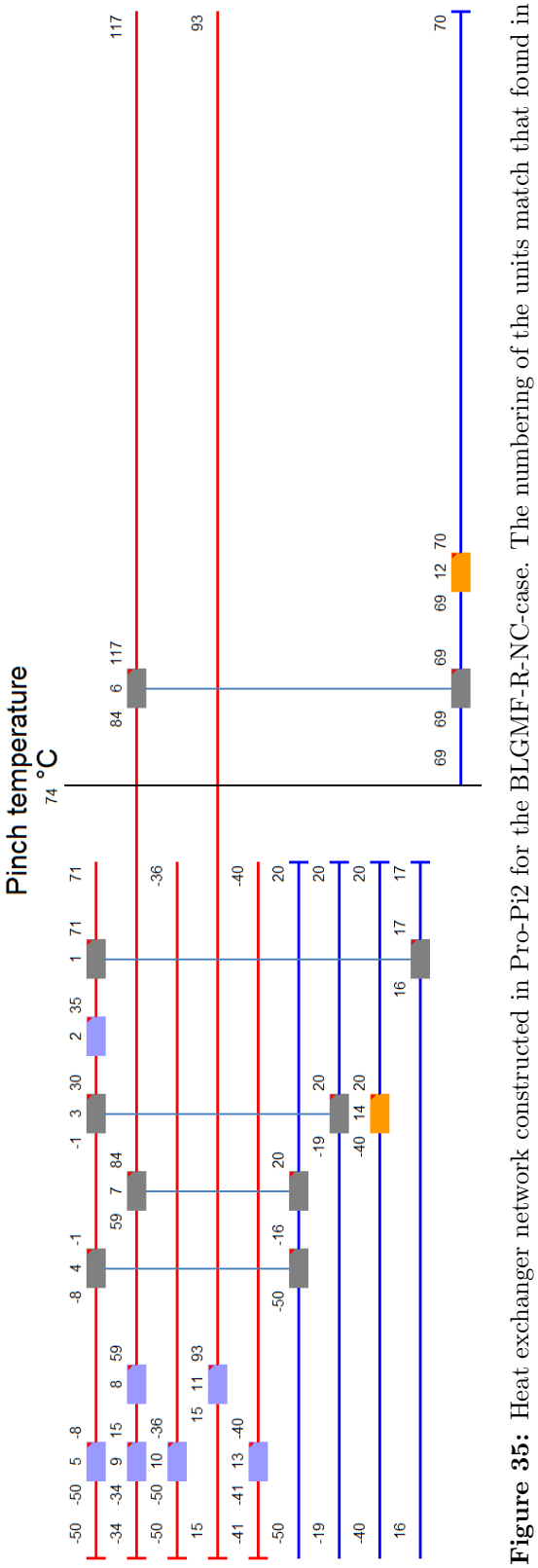

Figure 35: Heat exchanger network constructed in Pro-Pi2 for the BLGMF-R-NC-case. The numbering of the units match that found in Appendix C.

C Dimensioning

The complete flowsheet and component list for each case is presented on the following pages. In the component list the characteristic dimensions or properties of the equipment is shown, and they are obtained from the from the following sources:

- The height of the columns are chosen in the simulations in order to fulfils the 85 % capture rate of CO_2 and requirements on H_2S reduction. The packed height of the column is assumed to be 70 % of the total height (Jilvero, 2014). The diameter is also obtained from the simulations using the flooding approach. The diameter has been adjusted so that the largest fluxes are 70 % of those causing flooding.
- The Pinch analysis determined the capacity and the number of heat exchangers. The area was then calculated by assuming an overall heat transfer coefficient using data in Sinnott & Towler (2009).
- The sizes of both vertical and horizontal flashes were estimated by calculating the required vapour disengagement space for complete separation of vapour and liquid fractions. See Sinnott & Towler (2009) for further information about calculation procedure.
- The capacity of the compressors are obtained from Aspen Plus.
- The capacity of the pumps are calculated in Aspen Plus. However, the maintenance pumps capacity has been calculated by assuming they should overcome a elevation difference of the same hight as the highest column and the pressure drop caused by the first absorber in each case. See Sinnott & Towler (2009) for further information about calculation procedure.
- The Buffer tanks are dimensioned for a storage capacity of at least 10 % of the liquid holdup volume in the adjacent process equipment (Jilvero, 2014). Tanks for make-up chemical should have storage capacity of at least the amount needed for 10 days of production. The minimum tank size is 10 m^3 (Sinnott & Towler, 2009).

RB-M-CCS-case

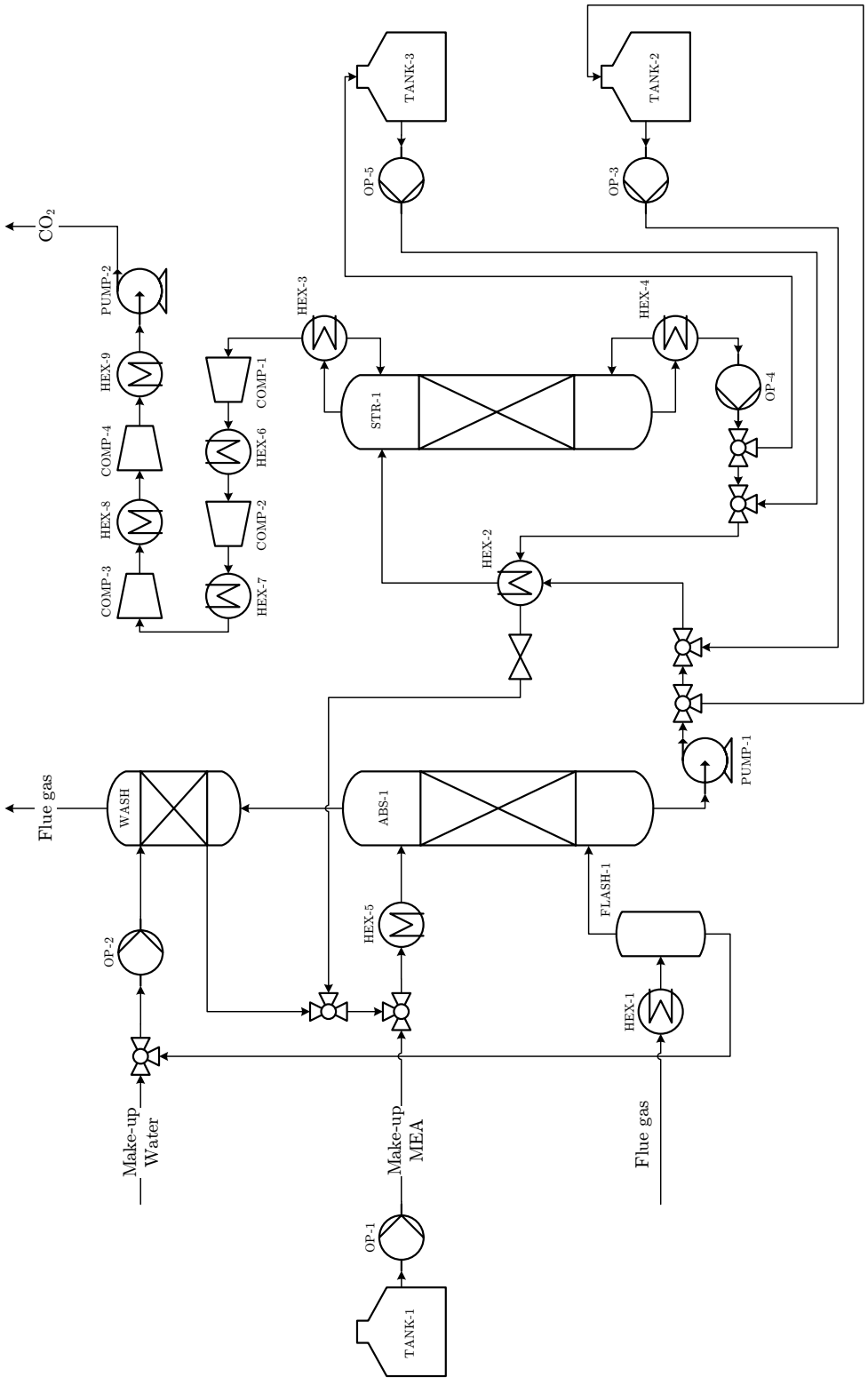

Figure 36: Detailed flowsheet of the MEA process for the RB-M-CCS-case. See Table 28 for sizes of the equipment.

Table 28: Equipment list presenting all units and characteristic dimensions for the RB-M-CCS-case. The total height of the columns is provided together with the packing height in parenthesis.

Column	Type	Pressure [bar]	Temperature [°C]	Heigth [m]	Diameter [m]
ABS-1	Sulzer Mellapak 250Y	1.0	40 - 66	21.4 (15.0)	9.82
STR-1	Sulzer Mellapak 250Y	1.8	15 - 118	21.4 (15.0)	6.35
WASH	Sulzer Mellapak 250Y	1.0	37 - 66	4.3 (3.0)	6.33

Heat exch.	Type	Pressure [bar]	Temperature [°C]	Capacity [kW]	Area [m]
HEX-1	Shell and Tube	1.0 - 1.0	10 - 110	38360	4002
HEX-2	Shell and Tube	1.8 - 1.8	47 - 118	99453	22173
HEX-3	Shell and Tube	1.0 - 1.8	10 - 98	30479	1519
HEX-4	Reboiler	1.8 - 3.5	118 - 139	94052	6586
HEX-5	Shell and Tube	1.0 - 1.0	10 - 57	28520	1176
HEX-6	Shell and Tube	1.0 - 4.6	10 - 109	1992	272
HEX-7	Shell and Tube	1.0 - 12.0	10 - 122	2296	288
HEX-8	Shell and Tube	1.0 - 31.0	10 - 123	2590	323
HEX-9	Shell and Tube	1.0 - 80.0	10 - 123	7149	893

Flash	Type	Pressure [bar]	Temperature [°C]	Heigth [m]	Diameter [m]
FLASH-1	Vertical	1.0	20 - 20	13.09	8.38

Compressor	Type	Pressure [bar]	Temperature [°C]	Capacity [kW]	-
COMP-1	Axial	1.8 - 4.6	15 - 109	2075	-
COMP-2	Axial	4.6 - 12.0	25 - 122	2112	-
COMP-3	Axial	12.0 - 31.0	25 - 123	2039	-
COMP-4	Axial	31.0 - 80.0	25 - 123	1832	-

Pump	Type	Pressure [bar]	Temperature [°C]	Capacity [kW]	-
PUMP-1	Centrifugal	1.0 - 3.5	47 - 47	136	-
PUMP-2	Centrifugal	80.0 - 150	25 - 40	369	-
OP-1	Centrifugal	1.0 - 2.7	20 - 20	91	-
OP-2	Centrifugal	1.0 - 2.7	37 - 37	91	-
OP-3	Centrifugal	1.8 - 3.5	47 - 47	91	-
OP-4	Centrifugal	1.8 - 3.5	118 - 118	91	-
OP-5	Centrifugal	1.8 - 3.5	118 - 118	91	-

Tank	Type	Pressure [bar]	Temperature [°C]	Volume [m^3]	-
TANK-1	Make-up MEA	1.0	20 - 20	10	-
TANK-2	Buffer tank	1.8	47 - 47	10	-
TANK-3	Buffer tank	1.8	118 - 118	10	-

BLGCC-S-CCS-case

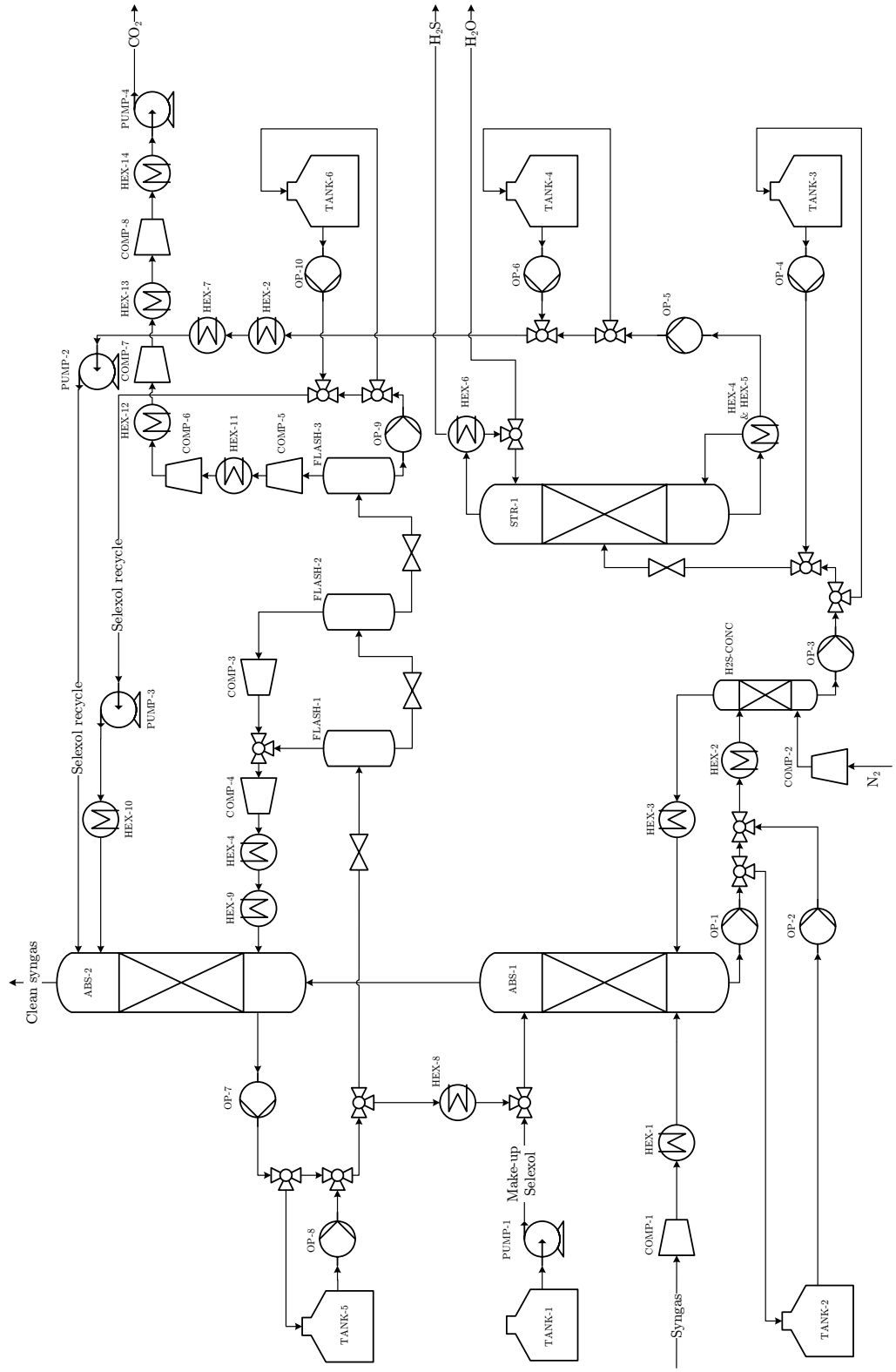

Figure 37: Detailed flowsheet of the Selexol process for the BLGCC-S-CCS-case. If an heat exchanger, e.g. HEX-4, is present at two places in the flowsheet it indicates that these streams are heat exchanged. See Table 29 for sizes of the equipment.

Table 29: Equipment list presenting all units and characteristic dimensions for the BLGCC-S-CCS-case. The total height of the columns is provided together with the packing height in parenthesis.

Column	Type	Pressure [bar]	Temperature [°C]	Heigth [m]	Diameter [m]
ABS-1	Norton IMTP: 2 IN	52.0	15 - 35	28.6 (20.0)	1.90
ABS-2	Norton IMTP: 2 IN	52.0	15 - 18	45.7 (32.0)	3.45
H2S-CONC	Norton IMTP: 2 IN	52.0	96 - 104	37.1 (26.0)	1.25
STR-1	Norton IMTP: 2 IN	2.0	30 - 206	7.1 (5.0)	1.70

Heat exch.	Type	Pressure [bar]	Temperature [°C]	Capacity [kW]	Area [m]
HEX-1	Shell and Tube	1.0 - 52.0	10 - 95	1695	211
HEX-2	Shell and Tube	2.0 - 52.0	35 - 206	8707	526
HEX-3	Shell and Tube	1.0 - 52.0	15 - 104	410	48
HEX-4	Reboiler	2.0 52.0	206 256	122	22
HEX-5	Reboiler	2.0 - 11.5	170 - 206	12886	1184
HEX-6	Shell and Tube	1.0 - 2.0	10 - 96	129	4
HEX-7	Shell and Tube	1.0 - 2.0	10 - 129	12784	863
HEX-8	Shell and Tube	1.0 - 52.0	10 - 18	276	166
HEX-9	Shell and Tube	1.0 - 52.0	10 - 221	708	77
HEX-10	Shell and Tube	1.0 - 52.0	10 - 19	3047	1600
HEX-11	Shell and Tube	1.0 - 4.1	10 - 118	544	70
HEX-12	Shell and Tube	1.0 - 11.0	10 - 127	620	76
HEX-13	Shell and Tube	1.0 - 29.0	10 - 128	689	84
HEX-14	Shell and Tube	1.0 - 80.0	10 - 128	1594	193

Flash	Type	Pressure [bar]	Temperature [°C]	Heigth [m]	Diameter [m]
FLASH-1	Horizontal	14.0	20 - 20	19.16	6.39
FLASH-2	Horizontal	6.2	20 - 20	19.15	6.38
FLASH-3	Horizontal	1.5	17 - 17	19.04	6.35

Compressor	Type	Pressure [bar]	Temperature [°C]	Capacity [kW]	-
COMP-1	Axial	31.5 - 52.0	30 - 95	1774	-
COMP-2	Axial	32.0 - 52.0	25 - 96	126	-
COMP-3	Axial	6.2 - 14.0	20 - 121	106	-
COMP-4	Axial	14.0 - 52.0	54 - 256	673	-
COMP-5	Axial	1.5 - 4.1	17 - 118	571	-
COMP-6	Axial	4.1 - 11.0	25 - 127	579	-
COMP-7	Axial	11.0 - 29.6	25 - 128	562	-
COMP-8	Axial	29.6 - 80.0	25 - 128	512	-

Pump	Type	Pressure [bar]	Temperature [°C]	Capacity [kW]	-
PUMP-1	Centrifugal	1.0 - 52.0	20 - 21	0.002	-
PUMP-2	Centrifugal	2.0 - 52.0	15 - 17	336	-
PUMP-3	Centrifugal	1.5 - 52.0	17 - 19	3264	-
PUMP-4	Centrifugal	80.0 - 150	25 - 48	133	-
OP-1	Centrifugal	52.0 - 54.6	35 - 35	20	-
OP-2	Centrifugal	52.0 - 54.6	35 - 35	20	-
OP-3	Centrifugal	52.0 - 54.6	97 - 97	20	-
OP-4	Centrifugal	52.0 - 54.6	97 - 97	20	-
OP-5	Centrifugal	1.5 - 4.1	206 - 206	20	-
OP-6	Centrifugal	1.5 - 4.1	206 - 206	20	-
OP-7	Centrifugal	52.0 - 55.1	18 - 18	229	-
OP-8	Centrifugal	52.0 - 55.1	18 - 18	229	-
OP-9	Centrifugal	1.5 - 4.1	17 - 17	20	-
OP-10	Centrifugal	1.5 - 4.1	17 - 17	20	-

Tank	Type	Pressure [bar]	Temperature [°C]	Volume [m^3]	-
TANK-1	Make-up DEPG	1.0	20 - 20	10	-
TANK-2	Buffer tank	52.0	35 - 35	10	-
TANK-3	Buffer tank	52.0	97 - 97	10	-
TANK-4	Buffer tank	2.0	206 - 206	10	-
TANK-5	Buffer tank	52.0	18 - 18	10	-
TANK-6	Buffer tank	1.5	17 - 17	30	-

BLGCC-S-NC-case

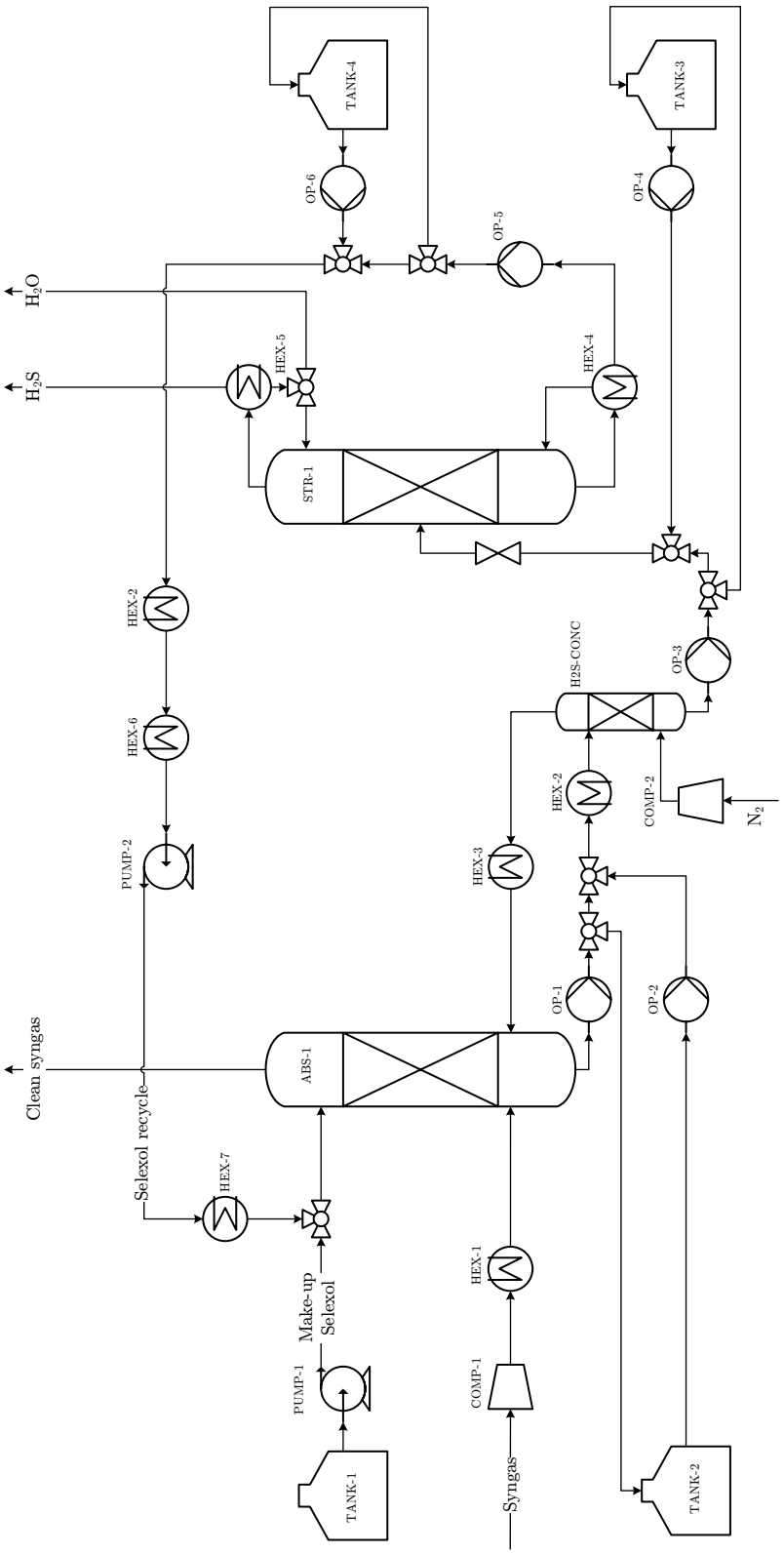

Figure 38: Detailed flowsheet of the Selexol process for the BLGCC-S-NC-case. If an heat exchanger, e.g. HEX-2, is present at two places in the flowsheet it indicates that these streams are heat exchanged. See Table 30 for sizes of the equipment.

Table 30: Equipment list presenting all units and characteristic dimensions for the BLGCC-S-NC-case. The total height of the columns is provided together with the packing height in parenthesis.

Column	Type	Pressure [bar]	Temperature [°C]	Heigth [m]	Diameter [m]
ABS-1	Norton IMTP: 2 IN	52.0	15 - 32	42.9 (30.0)	1.95
H2S-CONC	Norton IMTP: 2 IN	52.0	93 - 105	17.1 (12.0)	1.25
STR-1	Norton IMTP: 2 IN	2.0	30 - 207	7.1 (5.0)	1.72

Heat exch.	Type	Pressure [bar]	Temperature [°C]	Capacity [kW]	Area [m]
HEX-1	Shell and Tube	1.0 - 52.0	10 - 95	2257	491
HEX-2	Shell and Tube	2.0 - 52.0	32 - 207	8799	416
HEX-3	Shell and Tube	1.0 - 52.0	10 - 104	531	107
HEX-4	Reboiler	2.0 11.5	170 206	12893	1185
HEX-5	Shell and Tube	1.0 - 2.0	10 - 98	195	6
HEX-6	Shell and Tube	1.0 - 2.0	10 - 129	11071	482
HEX-7	Shell and Tube	1.0 - 52.0	10 - 31	1437	358

Compressor	Type	Pressure [bar]	Temperature [°C]	Capacity [kW]	-
COMP-1	Axial	31.5 - 52.0	30 - 95	1774	-
COMP-2	Axial	32.0 - 52.0	25 - 96	141	-

Pump	Type	Pressure [bar]	Temperature [°C]	Capacity [kW]	-
PUMP-1	Centrifugal	1.0 - 52.0	20 - 21	0.01	-
PUMP-2	Centrifugal	2.0 - 52.0	30 - 31	355	-
OP-1	Centrifugal	52.0 - 54.8	32 - 32	20	-
OP-2	Centrifugal	52.0 - 54.8	32 - 32	20	-
OP-3	Centrifugal	52.0 - 54.8	97 - 97	20	-
OP-4	Centrifugal	52.0 - 54.8	97 - 97	20	-
OP-5	Centrifugal	2.0 - 4.8	207 - 207	20	-
OP-6	Centrifugal	2.0 - 4.8	207 - 207	20	-

Tank	Type	Pressure [bar]	Temperature [°C]	Volume [m^3]	-
TANK-1	Make-up DEPG	1.0	20 - 20	10	-
TANK-2	Buffer tank	52.0	32 - 32	10	-
TANK-3	Buffer tank	52.0	97 - 97	10	-
TANK-4	Buffer tank	2.0	207 - 207	10	-

BLGMF-R-CCS-case

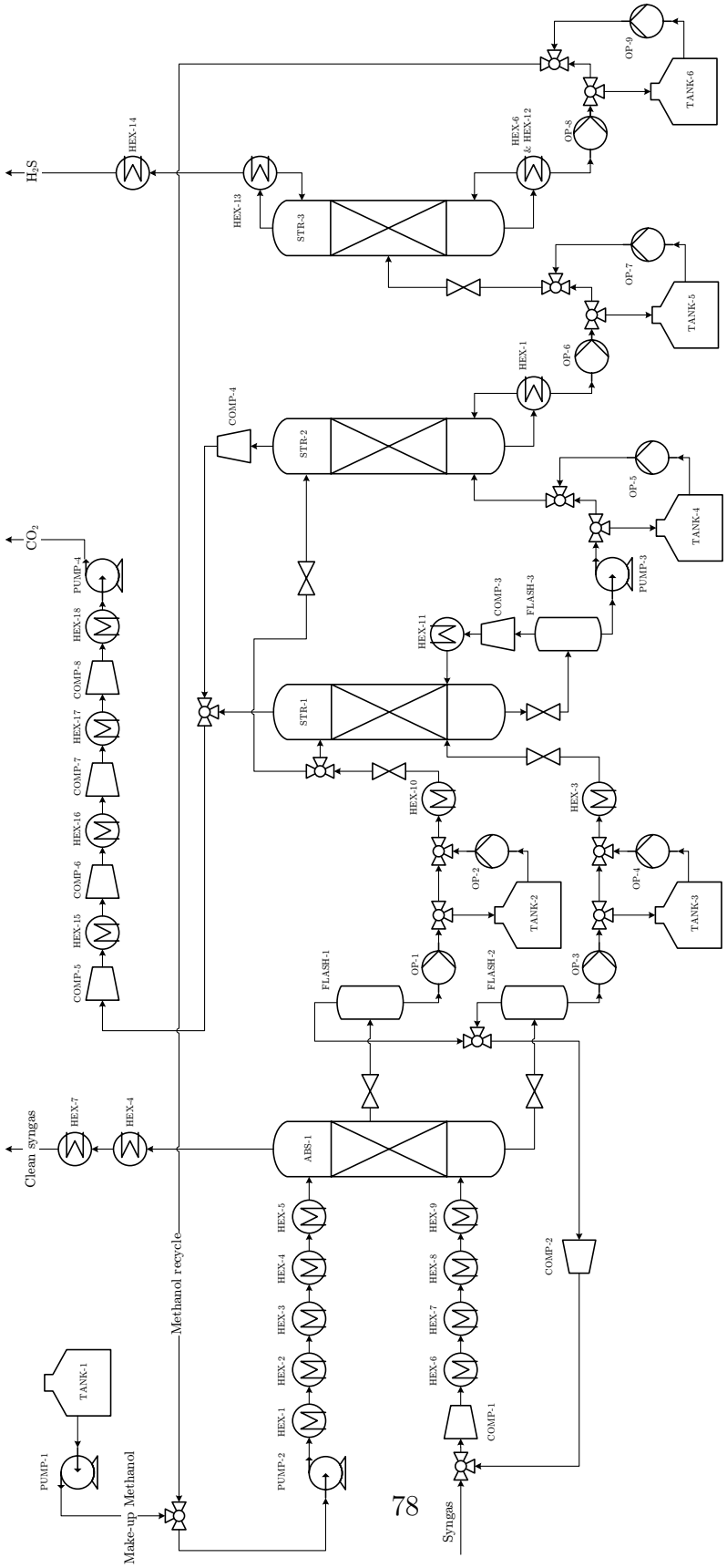

Figure 39: Detailed flowsheet of the Rectisol process for the BLGMF-R-CCS-case. If an heat exchanger, e.g. HEX-4, is present at two places in the flowsheet it indicates that these streams are heat exchanged. See Table 31 for sizes of the equipment.

Table 31: Equipment list presenting all units and characteristic dimensions for the BLGMF-R-CCS-case. The total height of the columns is provided together with the packing height in parenthesis.

Column	Type	Pressure [bar]	Temperature [°C]	Heigth [m]	Diameter [m]
ABS-1	Norton IMTP: 3 IN	60.0	-50 - -17	31.0 (21.7)	1.45
STR-1	Norton IMTP: 3 IN	6.0	-50 - 15	21.4 (15.0)	1.47
STR-2	Norton IMTP: 3 IN	2.7	-50 - 16	28.6 (20.0)	0.93
STR-3	Norton IMTP: 3 IN	1.2	-40 - 69	7.1 (5.0)	2.41

Heat exch.	Type	Pressure [bar]	Temperature [°C]	Capacity [kW]	Area [m]
HEX-1	Reboiler	2.7 - 60.0	16 - 71	3429	149
HEX-2	Shell and Tube	1.0 - 60.0	10 - 35	508	37
HEX-3	Shell and Tube	14.0 - 60.0	-19 - 30	2993	647
HEX-4	Shell and Tube	60.0 - 60.0	-50 - -1	694	208
HEX-5	Shell and Tube	2.0 - 60.0	-55 - -8	3996	314
HEX-6	Reboiler	1.2 - 60.0	69 - 117	1001	138
HEX-7	Shell and Tube	60.0 - 60.0	-16 - 84	742	126
HEX-8	Shell and Tube	1.0 - 60.0	10 - 59	1304	428
HEX-9	Shell and Tube	2.0 - 60.0	-55 - 15	1464	169
HEX-10	Shell and Tube	2.0 - 14.0	-55 - -36	595	83
HEX-11	Shell and Tube	1.0 - 6.0	10 - 93	228	50
HEX-12	Reboiler	1.2 - 3.5	69 - 139	10176	190
HEX-13	Shell and Tube	1.2 - 2.0	-55 - -40	5200	480
HEX-14	Shell and Tube	1.2 - 3.5	-50 - 139	84	3
HEX-15	Shell and Tube	1.0 - 11.5	10 - 35	50	17
HEX-16	Shell and Tube	1.0 - 21.9	10 - 90	408	64
HEX-17	Shell and Tube	1.0 - 41.9	10 - 90	479	76
HEX-18	Shell and Tube	1.0 - 80.0	10 - 90	1334	210

Flash	Type	Pressure [bar]	Temperature [°C]	Heigth [m]	Diameter [m]
FLASH-1	Horizontal	14.0	-36 - -36	6.78	2.26
FLASH-2	Horizontal	14.0	-19 - -19	7.55	2.52
FLASH-3	Horizontal	2.0	-15 - -15	8.60	2.87

Compressor	Type	Pressure [bar]	Temperature [°C]	Capacity [kW]	-
COMP-1	Axial	31.5 - 60.0	31 - 117	2442	-
COMP-2	Axial	14.0 - 31.5	-23 - 69	96	-
COMP-3	Axial	2.0 - 6.0	-15 - 93	304	-
COMP-4	Axial	2.7 - 6.0	-44 - 30	51	-
COMP-5	Axial	6.0 - 11.5	-24 - 34	286	-
COMP-6	Axial	11.5 - 21.9	25 - 90	339	-
COMP-7	Axial	21.9 - 41.9	25 - 90	322	-
COMP-8	Axial	41.9 - 80.0	25 - 90	283	-

Pump	Type	Pressure [bar]	Temperature [°C]	Capacity [kW]	-
PUMP-1	Centrifugal	1.0 - 1.2	20 - 20	0.0001	-
PUMP-2	Centrifugal	1.2 - 62.4	69 - 71	439	-
PUMP-3	Centrifugal	2.0 - 5.1	-15 - -15	21	-
PUMP-4	Centrifugal	80.0 - 150	25 - 45	123	-
OP-1	Centrifugal	14.0 - 16.4	-36 - -36	16	-
OP-2	Centrifugal	14.0 - 16.4	-36 - -36	16	-
OP-3	Centrifugal	14.0 - 16.4	-19 - -19	16	-
OP-4	Centrifugal	14.0 - 16.4	-19 - -19	16	-
OP-5	Centrifugal	2.7 - 5.1	-15 - -15	16	-
OP-6	Centrifugal	2.7 - 5.1	16 - 16	16	-
OP-7	Centrifugal	2.7 - 5.1	16 - 16	16	-
OP-8	Centrifugal	1.2 - 3.6	69 - 69	16	-
OP-9	Centrifugal	1.2 - 3.6	69 - 69	16	-

Tank	Type	Pressure [bar]	Temperature [°C]	Volume [m^3]	-
TANK-1	Make-up MEOH	1.0	20 - 20	10	-
TANK-2	Buffer tank	14.0	-36 - -36	10	-
TANK-3	Buffer tank	14.0	-19 - -19	10	-
TANK-4	Buffer tank	2.7	-15 - -15	10	-
TANK-5	Buffer tank	2.7	-15 - -15	10	-
TANK-6	Buffer tank	1.2	69 - 69	10	-

BLGMF-R-NC-case

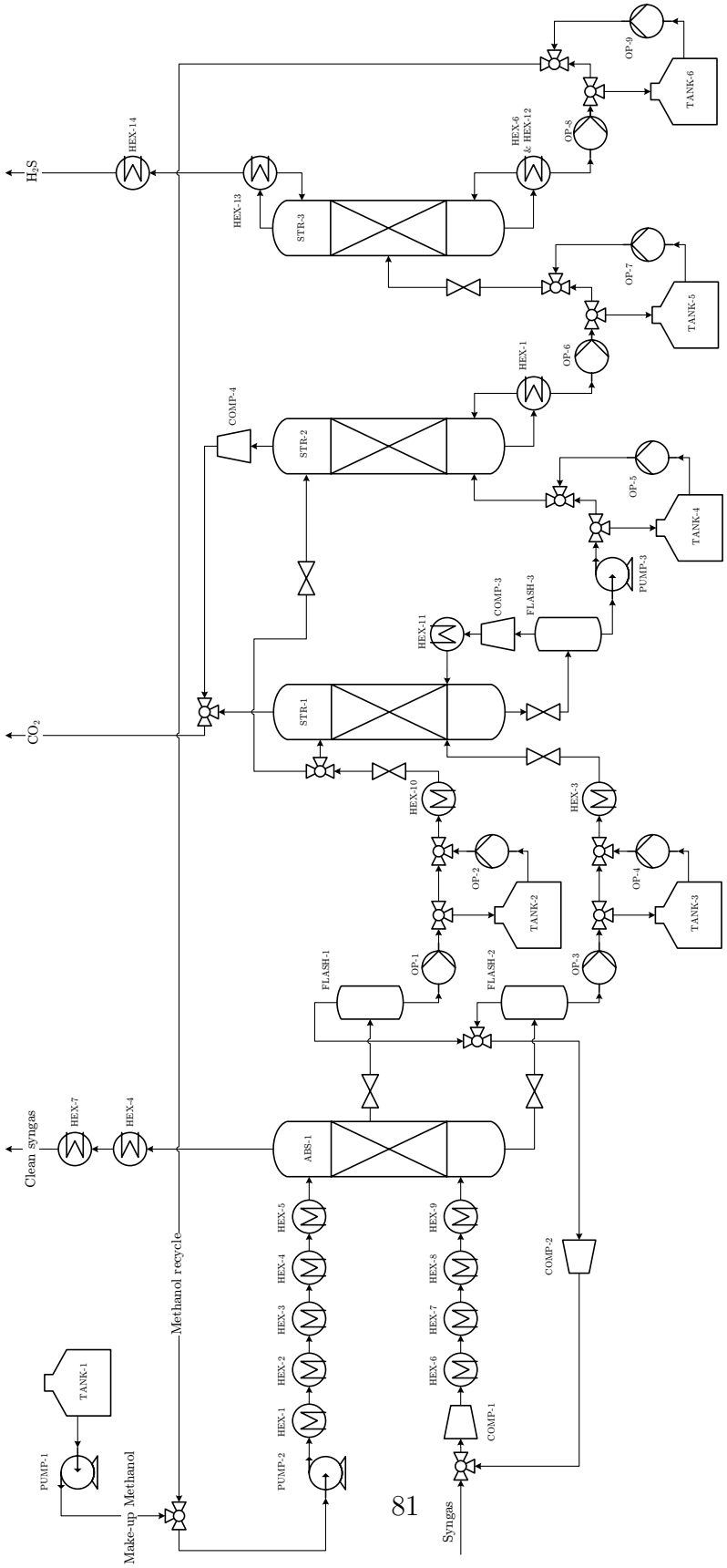

Figure 40: Detailed flowsheet of the Rectisol process for the BLGMF-R-NC-case. If an heat exchanger, e.g. HEX-4, is present at two places in the flowsheet it indicates that these streams are heat exchanged. See Table 32 for sizes of the equipment.

Table 32: Equipment list presenting all units and characteristic dimensions for the BLGMF-R-NC-case. The total height of the columns is provided together with the packing height in parenthesis.

Column	Type	Pressure [bar]	Temperature [°C]	Heigth [m]	Diameter [m]
ABS-1	Norton IMTP: 3 IN	60.0	-50 - -17	31.0 (21.7)	1.45
STR-1	Norton IMTP: 3 IN	6.0	-50 - 15	21.4 (15.0)	1.47
STR-2	Norton IMTP: 3 IN	2.7	-50 - 16	28.6 (20.0)	0.93
STR-3	Norton IMTP: 3 IN	1.2	-40 - 69	7.1 (5.0)	2.41

Heat exch.	Type	Pressure [bar]	Temperature [°C]	Capacity [kW]	Area [m]
HEX-1	Reboiler	2.7 - 60.0	16 - 71	3429	149
HEX-2	Shell and Tube	1.0 - 60.0	10 - 35	508	37
HEX-3	Shell and Tube	14.0 - 60.0	-19 - 30	2993	647
HEX-4	Shell and Tube	60.0 - 60.0	-50 - -1	694	208
HEX-5	Shell and Tube	2.0 - 60.0	-55 - -8	3996	314
HEX-6	Reboiler	1.2 - 60.0	69 - 117	1001	138
HEX-7	Shell and Tube	60.0 - 60.0	-16 - 84	742	126
HEX-8	Shell and Tube	1.0 - 60.0	10 - 59	1304	428
HEX-9	Shell and Tube	2.0 - 60.0	-55 - 15	1464	169
HEX-10	Shell and Tube	2.0 - 14.0	-55 - -36	595	83
HEX-11	Shell and Tube	1.0 - 6.0	10 - 93	228	50
HEX-12	Reboiler	1.2 - 3.5	69 - 139	10176	190
HEX-13	Shell and Tube	1.2 - 2.0	-55 - -40	5200	480
HEX-14	Shell and Tube	1.2 - 3.5	-50 - 139	84	3

Flash	Type	Pressure [bar]	Temperature [°C]	Heigth [m]	Diameter [m]
FLASH-1	Horizontal	14.0	-36 - -36	6.78	2.26
FLASH-2	Horizontal	14.0	-19 - -19	7.55	2.52
FLASH-3	Horizontal	2.0	-15 - -15	8.60	2.87

Compressor	Type	Pressure [bar]	Temperature [°C]	Capacity [kW]	-
COMP-1	Axial	31.5 - 60.0	31 - 117	2442	-
COMP-2	Axial	14.0 - 31.5	-23 - 69	96	-
COMP-3	Axial	2.0 - 6.0	-15 - 93	304	-
COMP-4	Axial	2.7 - 6.0	-44 - 30	51	-

Pump	Type	Pressure [bar]	Temperature [°C]	Capacity [kW]	-
PUMP-1	Centrifugal	1.0 - 1.2	20 - 20	0.0001	-
PUMP-2	Centrifugal	1.2 - 62.4	69 - 71	439	-
PUMP-3	Centrifugal	2.0 - 5.1	-15 - -15	21	-
OP-1	Centrifugal	14.0 - 16.4	-36 - -36	16	-
OP-2	Centrifugal	14.0 - 16.4	-36 - -36	16	-
OP-3	Centrifugal	14.0 - 16.4	-19 - -19	16	-
OP-4	Centrifugal	14.0 - 16.4	-19 - -19	16	-
OP-5	Centrifugal	2.7 - 5.1	-15 - -15	16	-
OP-6	Centrifugal	2.7 - 5.1	16 - 16	16	-
OP-7	Centrifugal	2.7 - 5.1	16 - 16	16	-
OP-8	Centrifugal	1.2 - 3.6	69 - 69	16	-
OP-9	Centrifugal	1.2 - 3.6	69 - 69	16	-

Tank	Type	Pressure [bar]	Temperature [°C]	Volume [m^3]	-
TANK-1	Make-up MEOH	1.0	20 - 20	10	-
TANK-2	Buffer tank	14.0	-36 - -36	10	-
TANK-3	Buffer tank	14.0	-19 - -19	10	-
TANK-4	Buffer tank	2.7	-15 - -15	10	-
TANK-5	Buffer tank	2.7	-15 - -15	10	-
TANK-6	Buffer tank	1.2	69 - 69	10	-

D Overall energy and mass balance

The calculations of the overall energy and mass balance has used the work of Pettersson (2014) as a starting point. Pettersson has in turn based her calculation on public data published by Skogsindustrins miljödatabas in 2010. From this data Pettersson calculated various energy flows for e.g. bark and black liquor. The pulp production in 2010 were 409 kADt/year but in 2014 the pulp production rate has increased to 422 kADt/year. Hence, the values provided by Pettersson (2014) has been linearly scaled to match the new production rate. By doing this calculation the overall balance for the RB-M-NC-case is obtained.

For the RB-M-CCS-case knowledge of the steam cycle is needed. The ratio between LP-steam and MP-steam use is assumed to be 2.7 for the pulp mill without capture (Pettersson & Harvey, 2012). The utility demand results from the MEA process simulations are added to the steam use of the pulp mill without capture. To balance the energy demand of the pulp mill the steam cycle is simulated. These simulations determines the solid wood fuel need and also the electricity production of the pulp mill.

For the BLGCC-S-scenario the simulations was carried out using the black liquor mass flow obtained from SCA. However, by comparison with the black liquor mass flow reported by Pettersson (2014) it was concluded that the data provided by SCA was extracted when the pulp mill was running at part load. Hence, the results from the simulations was linearly scaled to the correct sizes. The BLGCC-S-scenario includes a number of additional processes, see Figure 9, their utility demand is obtained from the following sources and scaled to match the black liquor mass flow. The utility consumption of the gasifier, gas cooler and the air separation unit has been extracted from Consonni et al. (2009). The steam demand for the Claus and SCOT processes are extracted from Consonni et al. (2009) as well but, the electricity consumption is taken from Field & Brasington (2011a). The gas turbine and the HRSG are modelled and the produced utilities are incorporated in the overall balance. To balance the energy demand the steam cycle is modelled.

In the BLGMF-R-scenario, the sources mentioned in the previous paragraph is used as well. For the DME synthesis and separation, process data is extracted from Gadek et al. (2013) and Ohno et al. (2006). Following the same principle as the other scenarios, the steam cycle is modelled to balance the energy demand.

For all cases the district heating is assumed to be constant. The reason is that the heat used for the generation of district heating originates from the pulping process and this is unaltered for every case. Only the recovery of the cooking chemicals is changed, hence it is reasonable to assume the district heating is constant.

Other parameters needed for the calculations are obtained from the following sources:

- The pulp mill is assumed to operate 355 days/year with an availability of 98 % which means the operating time is 8350 h/year. (Ekbom et al., 2005)

- The biofuel boiler is assumed to have an efficiency of 90 %. (Pettersson, 2014)
- When applying black liquor gasification the causticization load increases and consequently so does the fuel need in the lime kiln. A 25 % increase in fossil fuel usage in the lime kiln is assumed. (Ekbom et al., 2005)
- Polysulfide cooking is assumed to increase the pulp yield by 4 %. (Çöpür, 2007)
- The fossil fuel used in the pulp mill is assumed to be Fuel Oil No. 6 with an emission factor of 71.2 tCO_2/TJ. (The Climate Registry, 2013)
- Bark combusted in the biofuel boiler is assumed to originate from spruce and pine. The emission factor is 83.9 tCO_2/TJ. (U.S. Environmental Protection Agency, 2003)
- The emission factor for solid wood fuel is assumed to be 88.9 tCO_2/TJ. (The Climate Registry, 2013)
- The substituted electricity when the pulp mills sells their electricity surplus is assumed to be a Nordic electricity mix which emits 258 g/kWh. (Mölndal Energi AB, 2012)
- In the scenario where DME is produced it substitutes diesel which emits 160 gCO_2eqv/km. (Salomonsson, 2013)
- Electricity is estimated to be sold at 490 SEK/MWh, this price includes profit from electricity certificates. (Swedish Energy Agency (2012); European Commission (2013))
- Electricity is estimated to be bought at 590 SEK/MWh. (European Commission, 2013)
- The price of cooling water is assumed to be 0.4 SEK/m^3, which corresponds to 69 SEK/MWh if the water is utilized between 10-15 °C. (Heat and Power Technology, 2013)
- The cost of solid wood fuel is about 200 SEK/MWh, under the assumption that wood chips from branches and treetops are used. (Swedish Energy Agency, 2014)

E Modelling of gas turbine

The flowsheet of the gas turbine is shown in Figure 41. The model is based on the work of Field & Brasington (2011b). Information about the property method and components used in the simulations is from Aspen Plus help documentation.

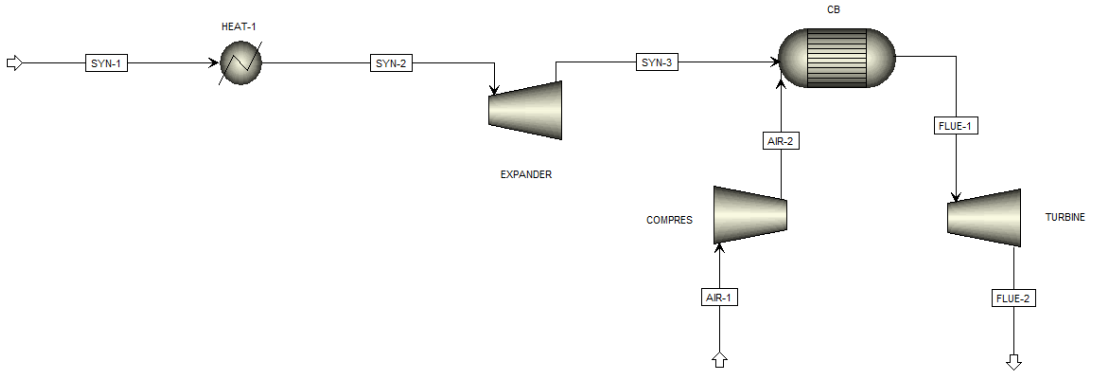

Figure 41: Aspen Plus flowsheet of the gas turbine used for the BLGCC-S-scenario.

The PR-BM (Peng Robinson cubic equation of state with the Boston-Mathias alpha function) is used as property method, since this mehtod is recommended for gas-processing of light gases such as CO_2 and H_2.

The syngas exiting the Selexol process is first heated (HEAT-1) to 240 °C and then expanded from 52 bar to 31.7 bar. The EXPANDER is modelled using the "Compr" block with the turbine setting checked. A isentropic efficiency of 0.8 and a mechanical efficiency of 0.98 is used. The syngas enters the combustion chamber together with compressed air at 16.2 bar. A "Compr" block with an isentropic efficiency of 0.865 and a mechanical efficiency of 0.98 is used to compress the air. The combustion chamber is modelled using a "RGibbs" block. This block models chemical equilibrium by minimizing Gibbs free energy and taking atom balance constraints into account. A pressure drop over the combustion chamber of 0.58 bar is assumed. The amount of air injected to the combustion chamber is adjusted so that the outlet temperature is 1300 °C. Higher inlet temperatures to the turbine would be possible if advanced material or thermal barrier coatings are used (Khartchenko, 1998). The turbine is modelled using the "Compr" block and the outlet pressure is specified to 1.05 bar. A isentropic efficiency and mechanical efficiency of 0.898 respectively 0.988, has been used.

F Modelling of HRSG

The flowsheet of the HRSG (heat recovery steam generator) is shown in Figure 42. The model is based on the guidelines found in Khartchenko (1998) regarding the design of a dual pressure HRSG. Information about the property method and components used in the simulations is from Aspen Plus help documentation. The PR-BM (Peng Robinson cubic equation of state with the Boston-Mathias alpha function) is used as property method.

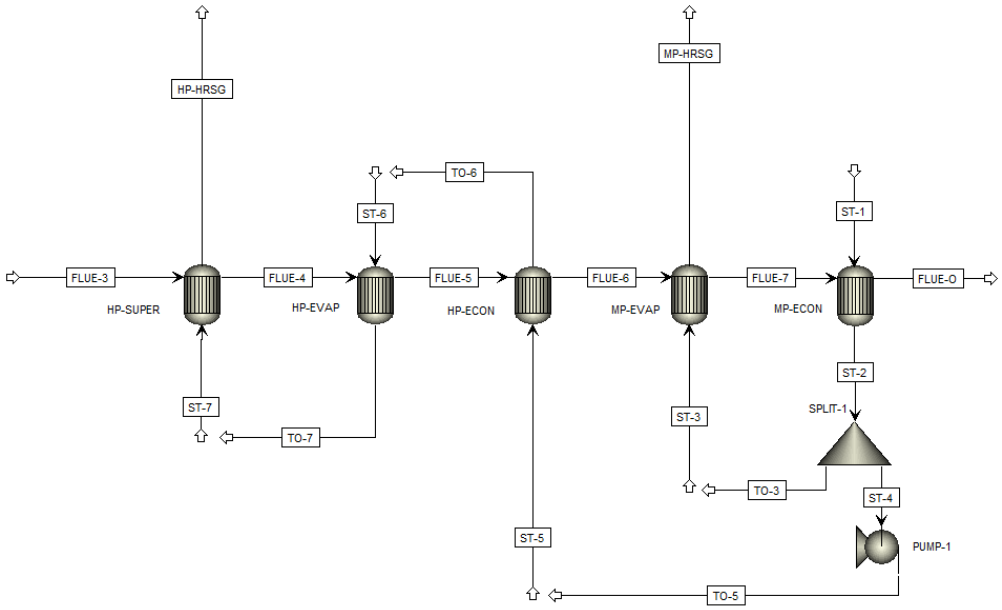

Figure 42: Aspen Plus flowsheet of the HRSG used for the BLGCC-S-scenario.

The flue gas exiting the gas turbine flows through a number of heat exchangers and leaves at a temperature of 154 °C. All heat exchangers are modelled using the "HeatX" block which is set to counter-current and shortcut calculation. The heat supplied by the flue gases is used to generate HP- and MP-steam. Feed-water of 140 °C and 11.5 bar enters the MP-ECON unit where it is preheated to the saturation temperature of 186 °C. This stream is then split into two, where 9 % enters the MP-EVAP where MP-steam is produced. The rest is pumped to a pressure of 105 bar and is heated to the saturation temperature of 314 °C in HP-ECON. After being evaporated in HP-EVAP the steam is superheated to a temperature of 514 °C in HP-SUPER. As can be seen in Figure 42 the steam streams have been manually divided to ease convergence. The properties of the streams is copied by a "Transfer" block in these cases.

The temperature-heat flux diagrams of the HRSG for the two BLGCC-S-cases are found in Figure 43 and 44. They are almost identical with the exception that the BLGCC-S-NC-case have slightly higher flue gas temperatures, because of a higher flue gas flow, and thereby generates a small additional amount of MP-steam.

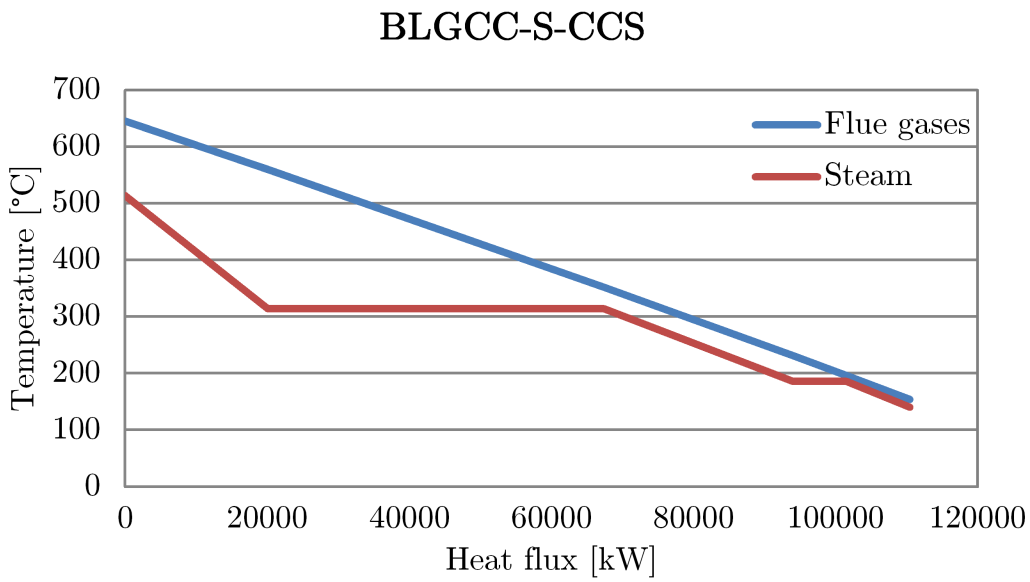

Figure 43: The temperature-heat flux diagram of the HRSG for the BLGCC-S-CCS-case.

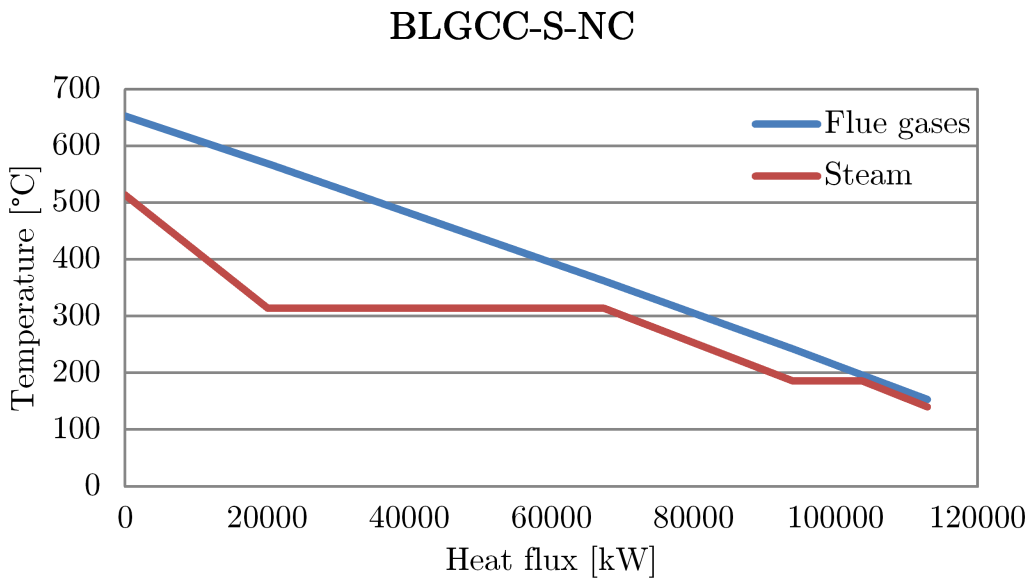

Figure 44: The temperature-heat flux diagram of the HRSG for the BLGCC-S-NC-case.

G Modelling of steam cycle

The steam cycle is modelled in Aspen Plus to balance the energy demand of the pulp mill. Figure 45 presents the Aspen Plus flowsheet of the steam cycle. Information about the property method and components used in the simulations is from Aspen Plus help documentation. The PR-BM (Peng Robinson cubic equation of state with the Boston-Mathias alpha function) is used as property method.

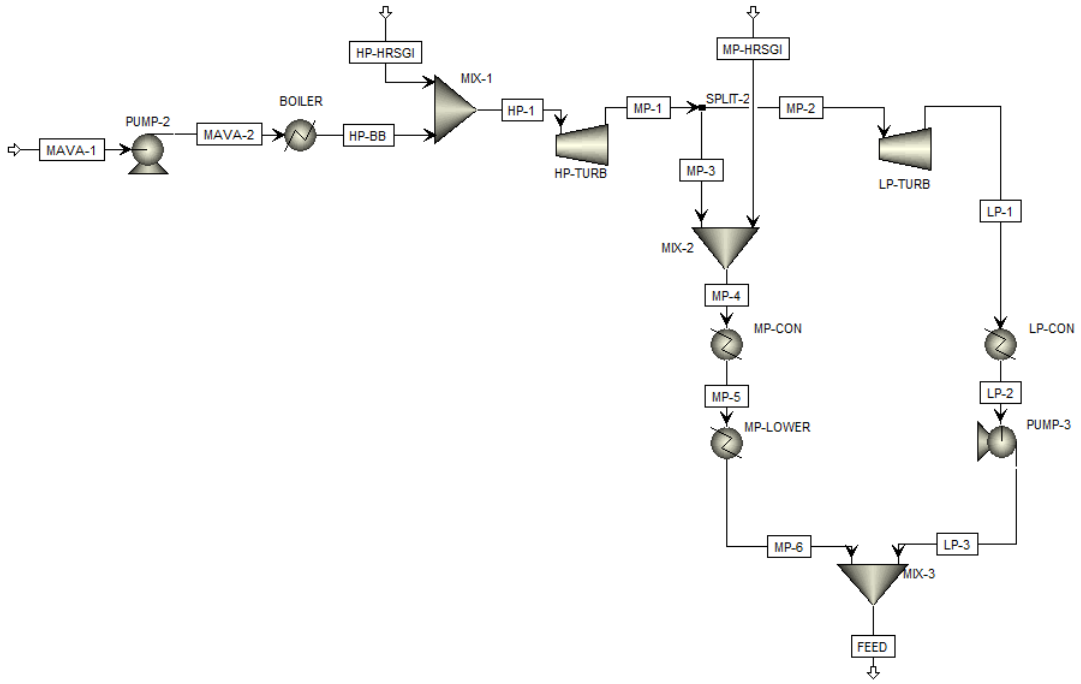

Figure 45: Aspen Plus flowsheet of the steam cycle.

The pressure levels in the steam cycle is identical to those present in SCAs pulp mill (SCA Östrands Massafabrik, 2006). The following three levels are used:

- LP-steam at 3.5 bar and 139 °C
- MP-steam at 11.5 bar and 186 °C
- HP-steam at 105 bar and 314 °C

For the BLGCC-S-scenario the two streams exciting the HRSG, "HP-HRSGI" and "MP-HRSGI", enters the steam cycle at their respective pressure level. For the two other scenarios these streams are non-existent. Feed-water is pumped to 105 bar and then enters the unit named BOILER, where HP-steam is generated. This is the boifuel boiler of the plant and it is modelled as a "Heater" block. The HP-steam is expanded in a high pressure turbine, HP-TURB, which is modelled by a "Compr" block set to turbine calculations. A isentropic efficiency and mechanical efficiency

of 0.871 respectively 0.98, is used. MP-steam exits the high pressure turbine and is divided into two streams. One stream goes to the cooler MP-CON which represents the MP-steam need of the pulp mill. It then passes a second unit in which the temperature is lowered to the LP-steam temperature. The heat released is used to cover a part of the LP-steam demand. The other stream enters a second turbine, LP-TURB, which expands the MP-steam to LP-steam. A isentropic efficiency of 0.871 and a mechanical efficiency of 0.98 is used. The LP-steam then passes a cooler, LP-CON, which represent the LP-steam need of the pulp mill. The condensate from LP-CON is pumped to 11.5 bar and then rejoined with the MP-steam condensate in a deaerator. The loop is now closed as this mixture is used as feed-water for both the biofuel boiler and the HRSG.

Two design specifications are used in the simulations. The fist one adjusts the split fraction in SPLIT-2 so that enough MP-steam enters MP-CON to satisfy the demand. The other design specification adjusts the amount of heat added in the BOILER unit so that the LP-steam demand is satisfied. From the heat added in the BOILER unit it is possible to calculate the amount of solid wood fuel that is needed.

H Refrigeration cycle

Where temperatures below 15 °C is needed, cooling water cannot be used to provide cooling. Instead a refrigeration cycle has to be utilised. A simple refrigeration cycle is shown in Figure 46.

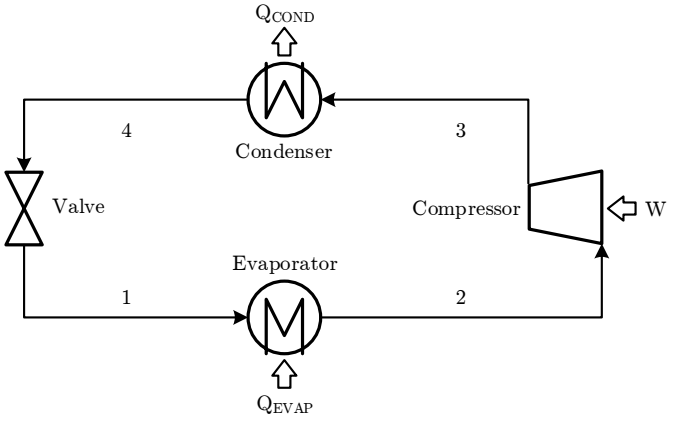

Figure 46: Schematic representation of a simple refrigeration cycle. Adapted from R. Smith (2005).

The refrigeration cycle is basically a heat pump which extracts heat from a low temperature and rejects it at a higher temperature. A refrigerant fluid is used as a medium for this transport. The refrigerant is evaporated (1-2) at a low temperature and thereby provides cooling to the process stream. By compressing (2-3) the refrigerant the condensation temperature increases. Thereby, cooling water can be used as a heat sink in the condenser (3-4). The refrigerant is thereafter throttled (4-1) by a valve to complete the cycle. The temperature-entropy and the pressure-enthalpy diagrams for the refrigeration cycle are illustrated in Figure 47.

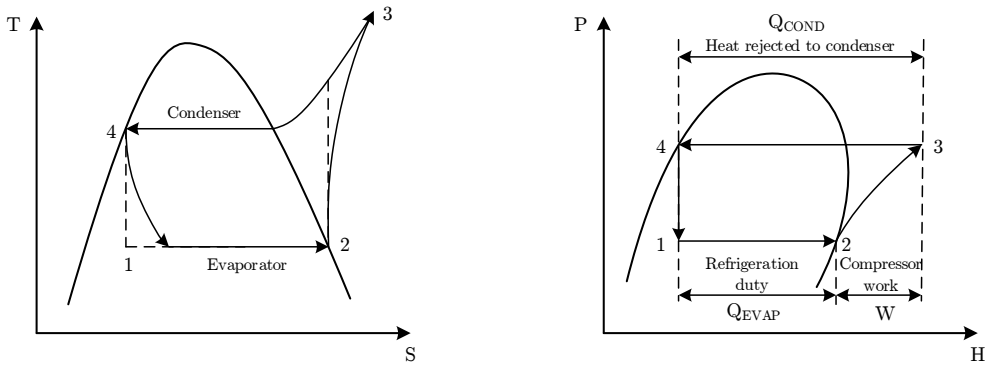

(a) Temperature-entropy diagram **(b)** Pressure-enthalpy diagram

Figure 47: Diagrams showing the characteristics of a simple refrigeration cycle. The numbering corresponded to that found in Figure 46. Adapted from R. Smith (2005).

From the simulations the refrigeration duty is obtained and to calculate both the compressor work and the cooling water duty, the coefficient of performance can be used. The ideal coefficient of performance is defined in Equation 3.

$$COP_{\text{Ideal}} = \frac{Q_{\text{EVAP}}}{W} = \frac{T_{\text{EVAP}}}{T_{\text{COND}} - T_{\text{EVAP}}} \tag{3}$$

The actual performance of a simple refrigeration cycle is typically 0.6 of the ideal performance (R. Smith, 2005). Simple refrigeration cycles can be used to provide cooling down to $-40\,^{\circ}\text{C}$. However, the Rectisol process requires cooling as low as $-50\,^{\circ}\text{C}$. Hence, more complex cycles are needed such as multistage compression cycles or cascade cycles. These are more efficient than simple cycles and therefore a value of 0.75 is used instead. By multiplying the coefficient of performance by 0.75 and rearranging Equation 3, the required compressor work can be calculated.

$$W = \frac{Q_{\text{EVAP}}(T_{\text{COND}} - T_{\text{EVAP}})}{0.75 T_{\text{EVAP}}} \tag{4}$$

As seen in Figure 47, the heat rejected at the condenser to the cooling water is equal to the sum of the compressor work and the refrigeration duty.

$$Q_{\text{COND}} = W + Q_{\text{EVAP}} \tag{5}$$